



UNIVERSITÀ  
DEGLI STUDI  
DI PADOVA

Administrative Office: Università degli Studi di Padova  
Department of Pharmaceutical and Pharmacological Sciences

---

Doctoral School in Molecular Sciences  
*Curriculum in Pharmaceutical Sciences*  
Cycle XXVI

**NOVEL POLYSACCHARIDE ANTI-TUMOUR DRUG DELIVERY SYSTEM FOR  
ACTIVE TARGETING AND CONTROLLED RELEASE TO BREAST CANCER  
BONE METASTASES**

**School Director:** Prof. Antonino Polimeno

**Curriculum Coordinator:** Prof. Alessandro Dolmella

**Supervisor:** Prof. Paolo Caliceti

**PhD Candidate:** Gwénaëlle Bonzi



# CONTENTS

---

Table of figures.....	5
Abbreviations and Symbols.....	9
Abstract.....	11
Riassunto.....	13

---

1. Introduction.....	19
1.1 Anti-tumour therapy - state of the art .....	19
1.2 The tumour microenvironment .....	23
1.2.1 Tumour vascular architecture .....	23
1.2.2 Lack of lymphatic drainage .....	24
1.2.3 pH decrease.....	24
1.2.4 Tumour hypoxia .....	24
1.3 Breast cancer and bone metastasis .....	25
1.4 Polymer therapeutics .....	29
1.4.1 Models of polymer bioconjugates .....	29
1.4.2 Characteristics of polymeric carriers.....	30
1.4.3 Examples of molecular models clinically used.....	33
1.5 Passive and active tumour targeting.....	35
1.5.1 Passive targeting .....	36
1.5.2 Active targeting .....	37
1.5.3 Intracellular trafficking .....	38
1.5.4 Targeting to bone .....	39
1.6 Drug release from polymer-drug conjugates .....	41
1.6.1 Carboxylic esters .....	41
1.6.2 Carbonate esters .....	42
1.6.3 Carbamate esters .....	42
1.6.4 Hydrazones.....	42
1.6.5 Amide.....	42
1.6.6 Peptidyl spacers.....	42
1.7 Examples of drug release triggered by small proteases.....	43
1.8 Material involved in the project – Design of Pullulan-paclitaxel alendronate with Cathepsin K sensitive spacer.....	45
1.8.1 Pullulan .....	47
1.8.2 Polyethylene glycol .....	49
1.8.3 Paclitaxel.....	51
1.8.4 Bisphosphonates and Alendronate.....	53

1.8.5	Cathepsin K.....	57
2.	Materials and methods.....	61
1.9	Reagents.....	61
1.10	Cell culture.....	62
1.11	Instruments.....	63
1.12	Methods.....	65
1.12.1	Analytical methods.....	65
1.12.2	Synthesis.....	69
1.12.3	Cell culture.....	78
3.	Results.....	83
1.13	Synthesis of Pullulan-Paclitaxel-Alendronate – Pull-PTX-ALN.....	83
1.13.1	Carrier function: Periodate oxidation of pullulan.....	83
1.13.2	Enzyme triggered release function: Synthesis of the FmocGlyGlyProNle peptide.....	87
1.13.3	Anti-tumour function: Synthesis of NH <sub>2</sub> T <sub>φ</sub> PTX paclitaxel prodrug.....	92
1.13.4	Targeting function: Synthesis of NH <sub>2</sub> -PEG-Alendronate.....	100
1.13.5	Polymer therapeutics: Synthesis of Pullulan-Paclitaxel-Alendronate (Pull-PTX-ALN).....	103
1.14	Properties of Pull-PTX-ALN.....	107
1.14.1	Solubility of Pull-PTX-ALN.....	107
1.14.2	Identification of the polymer-drug conjugate composition.....	107
1.14.3	Molecular size and surface charge of conjugates.....	109
1.14.4	Stability of polymeric structures in buffer solutions at different pH over time.....	111
1.14.5	Stability of polymeric structures in buffer solutions at different T°C.....	112
1.14.6	Critical micellar concentration.....	112
1.14.7	Transmission electron microscopy (TEM).....	114
1.15	Pull-PTX-ALN: In-Vitro assays.....	115
1.15.1	Hydroxyapatite binding assay.....	115
1.15.2	Drug release in-vitro assay.....	116
1.15.3	Red Blood Cell Lysis Assay.....	118
1.16	Cell Studies.....	119
1.16.1	Evaluation of the anti-tumour properties of Pull-PTX-ALN.....	119
1.16.2	Inhibition of angiogenic cascade.....	123
4.	Discussion.....	129
5.	Conclusion.....	145
6.	References.....	149

# TABLE OF FIGURES

---

Figure 1-1 Tumour hypoxia – The unique physiology of solid tumours <sup>1</sup> .....	25
Figure 1-2 Tumour metastases <sup>14</sup> .....	25
Figure 1-3 Breast tumour metastases to bone .....	27
Figure 1-4 Factors that promote differentiation and function of osteoclasts and osteoblasts <sup>15</sup> .....	28
Figure 1-5 Tumour-targeted nanomedicines: principles and practice <sup>13</sup> .....	29
Figure 1-6 OPAXIO .....	31
Figure 1-7 PK1 and PK2 HPMA copolymers for drug delivery .....	32
Figure 1-8 Abraxane model .....	33
Figure 1-9 Doxil model .....	34
Table 1-1 Current clinical trial on nano-systems for drug delivery <sup>17</sup> .....	34
Figure 1-10 The EPR effect – inspired from Eldon et. al Oct 2007 <sup>19</sup> .....	36
Figure 1-11 Passive and active targeting approaches of nanomedicines in cancer therapy <sup>24</sup> .....	38
Figure 1-12 Tetracycline .....	39
Figure 1-13 Model of polymeric carrier .....	45
Figure 1-14 Pullulan .....	47
Figure 1-15 Synthesis of polyethylene glycol. ....	49
Figure 1-16 Paclitaxel .....	51
Figure 1-17 Sodium alendronate .....	54
Figure 1-18 Comparison inorganic pyrophosphate and bisphosphonate .....	54
Figure 1-19 Bisphosphonate structures and approximate relative potencies for osteoclast inhibition. ....	55
Figure 1-20 General features of bisphosphonates .....	56
Figure 1-21 Osteoclast morphology .....	57
Scheme 2-1 Titration of aldehydes by hydroxylamine .....	65
Scheme 2-2 Titration of primary amine group containing compounds by Snyder colorimetric assay .....	66
Graph 2-1 Primary amine calibration curve by Snyder test – Reference compound: NH <sub>2</sub> gly-glyOH .....	66
Graph 2-2 Alendronate calibration curve by spectrophotometry .....	67
Graph 2-3 Paclitaxel calibration curve by HPLC .....	68
Graph 2-4 Pullulan calibration curve by GPC .....	69

Figure 3-1 Kinetics of oxidation of pullulan by periodate oxidation – 30% target (■) and 100% target (◆).....	83
Scheme 3-1 Periodate oxidation of pullulan .....	84
Figure 3-2 <sup>1</sup> H NMR Spectra in D <sub>2</sub> O of native Pullulan- Top (–) and Pull <sub>ox30</sub> -Bottom (–).....	85
Figure 3-3 FT-IR spectra on KBr plate of native Pullulan (A) and Pull <sub>ox30</sub> (B) .....	86
Scheme 3-2 Titration of aldehyde groups in oxidised pullulan .....	86
Scheme 3-3 Spontaneous hemiacetal formation occurring in a maltotriose unit. ....	87
Figure 3-4 GPC chromatogram of aldehyde pullulan Pull <sub>ox30</sub> .....	87
Scheme 3-4 Solid Phase Peptide Synthesis general principle.....	88
Scheme 3-5 Mechanism of Fmoc protected amine deprotection by piperidine.....	89
Table 3-1 <sup>1</sup> HNMR chemical shifts (δ) and proton number for FmocGlyGlyProNle.....	92
Figure 3-7 Molecules designed for the synthesis of a Cathepsin K sensitive PTX prodrug. First design S1-PTX or NH <sub>2</sub> TPTX (A), second design S1-S2-PTX or NH <sub>2</sub> T <sub>φ</sub> PTX (B) .....	93
Scheme 3-6 Synthesis of the NH <sub>2</sub> T <sub>φ</sub> PTX paclitaxel prodrug.....	94
Figure 3-8 Mass spectrometry (ESI-TOF, positive mode) of FmocT <sub>φ</sub> OH .....	95
Figure 3-9 Products of degradation of p-nitrophenyl-chloroformate (a, b, c).....	96
Figure 3-10 Mass spectrometry (ESI-TOF, positive mode) of FmocT <sub>φ</sub> NO <sub>2</sub> .....	97
Figure 3-12 Mass spectrometry (ESI-TOF, positive mode) of NH <sub>2</sub> T <sub>φ</sub> PTX.....	99
Figure 3-13 HPLC chromatograms of NH <sub>2</sub> T <sub>φ</sub> PTX (A) and free PTX (B).....	100
Figure 3-14 Molecules designed for the synthesis of a Cathepsin K sensitive ALN prodrug. First strategy S1-ALN (A), second strategy PEG-ALN (B).....	101
Scheme 3-7 Synthesis of NH <sub>2</sub> -PEG-Alendronate.....	101
Scheme 3-8 General mechanism of deprotection of tBoc protected amine by TFA .....	102
Figure 3-15 <sup>1</sup> H NMR spectra in DMSO of protected and deprotected PEGylated alendronate .....	102
Scheme 3-9 Synthesis of Pull-PTX-ALN .....	104
Figure 3-16 GPC traces of Pull-PTX-ALN against Pullulan standards.....	105
Figure 3-17 FT-IR spectra of Pull-PTX*ALN (A) and native Pullulan (B) .....	106
Figure 3-18 HPLC chromatograms of native Pullulan (A) free PTX (B) and Pull-PTX-ALN (B) .....	106
Figure 3-19 Solubility of the free drug paclitaxel (left) and PullIPTXALN (right) in ultrapure water at room temperature .....	107
Figure 3-21 UV-VIS spectra in MeOH of Pull-PTX-ALN (–) and PTX (---) .....	108
Table 3-2 Composition of Pull-PTX-ALN in comparison with non-modified pullulan.....	109
Figure 3-22 Size analysis by DLS of Pull-PTX-ALN in PBS, pH5.5 (A) at 25°C in water (B) at 25°C and in PBS, pH 7.4 (C) at 25°C .....	109
Figure 3-23 Comparison of the size by DLS of native pullulan (–) and the Pull-PTX-ALN (–) conjugate in water at 25°C .....	110
Figure 3-24 ζ- potential of Pull-PTX-ALN in water at 25°C.....	110

Figure 3-25 Size-time course profiles of Pull-PTX-ALN at 25°C at pH5.5(◆), 6.0 (■)and 7.4(▲).....	111
Figure 3-26 Polydispersity-time course profiles of Pull-PTX-ALN at 25°C at pH5.5(◆), 6.0(■) and 7.4(▲).....	111
Figure 3-27 Size-temperature of Pull-PTX-ALN at 25°C and 37°C and at pH5.5, 6.0 and 7.4 .....	112
Figure 3-28 Determination of CMC using a pyrene probe – Spectra at increasing concentration of polymer drug conjugate Pull-PTX-ALN.....	113
Figure 3-29 critical micellar concentration of the Pull-PTX-ALN.....	113
Figure 3-30 TEM images of Pull-PTX-ALN micelles in water .....	114
Figure 3-31 Binding kinetics of ALN, (◆)Pull-PTX-ALN(■), Pull-PTX (▲) to the bone mineral hydroxyapatite at the temperature of 37°C and pH 7.4 .....	115
Figure 3-32 Binding kinetics of ALN, (◆)Pull-PTX-ALN(■), Pull-PTX (▲) to the bone mineral hydroxyapatite at the temperature of 37°C and pH 5.5 .....	116
Figure 3-33 HPLC traces of the drug release assay using Cathepsin K as trigger for the release of paclitaxel .....	117
Figure 3-34 Kinetics of the drug release assay using Cathepsin K as trigger for the release of paclitaxel .....	118
Figure 3-35 Biocompatibility of PTX, Pull-PTX-ALN, Dextran and PEI in RBC.....	119
Figure 3-39 Cell toxicity assay in human sarcoma SAOS-2 cells were incubated with free PTX, free ALN, Pullulan, Pull-PTX, Pull-ALN and Pull-PTX-ALN at equivalent concentration of PTX and ALN for 72 h. Data represent the mean ±SD (standard deviation). The X-axis is presented as a logarithmic scale.....	121
Figure 3-40 Wound healing assay on MDA-MB231 BM cells incubated with free PTX, free ALN, Pullulan, Pull-PTX, Pull-ALN and Pull-PTX-ALN at equivalent concentration of PTX and for 24 h. (scale bar represents 100 μm). .....	122
Figure 3-41 % migrated cells in a wound healing assay performed on MDA-MB231 BM cells incubated with free PTX, free ALN, a combination of PTX and ALN, Pullulan, Pull-PTX, Pull-ALN and Pull-PTX-ALN at equivalent concentration of PTX and ALN for 24h-123	
Figure 3-42 Cell toxicity assay in human umbilical vein endothelial cell (HUVEC). HUVEC were incubated with free PTX, free ALN, Pullulan, Pull-PTX, Pull-ALN and Pull-PTX-ALN at equivalent concentration of PTX and ALN for 72 h. Data represent the mean ±SD (standard deviation). The X-axis is presented at as logarithmic scale .....	124
Figure 3-43 Capillary like-tube formation assay : representative images of capillary-like tube structures of HUVEC seeded on Matrigel following treatment (scale bar represents 100 μm).....	125
Figure 3-44 Capillary like-tube formation assay: Quantitative analysis of the mean length of the tubes. Data represents mean ± SD. *p<0.05.....	125
Scheme 4-1 Proposed mechanism for Cathepsin K triggered drug release .....	140





# ABBREVIATIONS AND SYMBOLS

---

<b>° C</b>	Degree Celsius
<b>4T1</b>	Murine mammary adenocarcinoma cell line
<b>A</b>	Absorbance
<b>ACN</b>	Acetonitrile
<b>ALN</b>	Alendronate
<b>BPs</b>	Bisphosphonates
<b>CDCl<sub>3</sub></b>	Deuterated chloroform
<b>CMC</b>	Critical Micellar Concentration
<b>D<sub>2</sub>O</b>	Deuterated water
<b>Da</b>	Dalton
<b>DCC</b>	Dicyclohexylcarbodiimide
<b>DLS</b>	Dynamic Light Scattering
<b>DMAP</b>	N,N'-dimethylaminopyridine
<b>DMEM</b>	Dulbecco's Modified Eagle's Medium
<b>DMF</b>	N,N'-Dimethylformaldehyde
<b>DMSO</b>	Dimethylsulfoxide
<b>PEG</b>	PolyEthylene Glycol
<b>EPR</b>	Enhanced Permeability and Retention Effect
<b>FDA</b>	Food and Drug Administration
<b>FBS</b>	Foetal bovine Serum
<b>tBocPEG-NHS</b>	tBoc protected polyethylene glycol NHS activated
<b>HAp</b>	Hydroxyapatite
<b>HOBT</b>	1-Hydroxybenzotriazole
<b>HPLC</b>	High Performance Liquid Chromatography
<b>HPMA</b>	Poly-hydroxypropylmethacrylamide
<b>HUVEC</b>	Human umbilical vein endothelial cells
<b>IC<sub>50</sub></b>	50% Inhibition Concentration
<b>IR</b>	Infrared spectroscopy
<b>MDA-MB-231</b>	Human mammary adenocarcinoma cell line
<b>MeOH</b>	Methanol
<b>mQ</b>	Deionized water and filtered through Millipore filter ®
<b>MTT</b>	3 - (4,5-Dimethylthiazole-2-yl) -2,5-diphenyltetrazolium bromide
<b>Mw</b>	Molecular weight
<b>NHS</b>	N-hydroxysuccinimide
<b>NMR</b>	Nuclear magnetic resonance spectroscopy

### ***Abbreviations and Symbols (Continued)***

<b>PBS</b>	Phosphate Buffer Saline
<b>PEG</b>	Polyethylene glycol
<b>ppm</b>	Parts per million
<b>PTX</b>	Paclitaxel
<b>RI</b>	Refractive Index
<b>RP-HPLC</b>	Reverse Phase High Performance Liquid Chromatography
<b>SAOS-2</b>	Osteosarcoma cells
<b>SEC or GPC</b>	Size Exclusion Chromatography or Gel-Permeation Chromatography
<b>TEA</b>	Triethylamine
<b>TFA</b>	Trifluoroacetic acid
<b>TMS</b>	Tetramethylsilane
<b>TNBS</b>	2,4,6-trinitrobenzenesulfonic acid
<b>tR</b>	Retention time
<b>UV</b>	Ultraviolet
<b>UV-Vis</b>	Ultraviolet-Visible Spectrophotometry

# ABSTRACT

---

In the late stage of the disease, breast cancer patients often develop bone metastases, a major cause of cancer-related death among women worldwide.

The common treatment currently used clinically includes the anti-neoplastic agent paclitaxel combined with the bisphosphonate alendronate.

Paclitaxel is an anti-neoplastic drug which cytotoxic effect is mainly attributed to its ability to promote the assembly of microtubules as well as prevent the depolymerisation of these microtubules. Stabilization of the microtubule networks stops mitotic functions that, in sequence, blocks cell division. Paclitaxel is approved for treatment of ovarian, breast, and non-small cell lung cancers at late stage. However, the anti-tumour drug is highly hydrophobic and consequently is poorly soluble in water. Additionally, the formulation of paclitaxel currently used clinically, known as Taxol, contains the anti-neoplastic drug dissolved in a mixture of Cremophor EL and ethanol in order to increase its solubility. Nevertheless, administration of Cremophor EL results in serious dose-limiting toxicities such as hypersensitivity responses and neuropathy. Furthermore, the chemotherapeutic agent suffers from poor selectivity towards tumours, leading to damage of normal healthy cells. As a result, much effort has been made into the development of novel formulations of paclitaxel using biocompatible and biodegradable polymeric systems.

Additionally, bone metastases are of considerable concern for patients with advanced breast cancer. Patients may tackle supplemental challenges to the cancer itself as their skeletal health declines and contributes to a manifest decrease in their quality of life and survival. Several bisphosphonates have been assessed in patients with bone metastases from breast primary tumour, including alendronate, in order to reduce bone resorption and tumour progression.

The present project aims at developing a new nano-drug delivery system for site target, and controlled release of anti-tumour drug. The model developed is a polymer-drug conjugate where the anti-tumour drug Paclitaxel and alendronate, are attached to a natural polymeric carrier, Pullulan, through a spacer.

The polymer-drug conjugate designed for controlled release under specific physiological conditions uses two main mechanisms for the release, including an enzymatic hydrolysis and non-enzymatic hydrolysis. The choice of spacers between the polymer and the drug was made so that the drug release only occurs once the system reaches the bone metastasis, using an enzymatic hydrolysis first. When polymer-drug conjugates are elaborated for tumour delivery, the linkage between the drug and the polymer must be necessarily stable under physiological conditions until the tumour target is reached. The drug is then cleaved rapidly to be activated.

The colloidal carrier was designed to improve the biopharmaceutical and therapeutic properties of the anti tumoural drug paclitaxel, increasing the paclitaxel solubility in water and targeting the tumour itself. The alendronate bisphosphonate was chosen as a targeting agent to confer a high affinity of the conjugate toward the apatite structure of bone metastases by exploiting the strong bone seeking properties of bisphosphonates, together with the micro-environment of bone metastases, in order to ensure a selective release and accumulation of the anti-tumour drug at the desired site of action; the bone metastases.

First, preliminary studies investigated the influence of the time of oxidation of pullulan onto its architecture (molecular weight and polydispersivity). Pullulan was modified by periodate oxidation to obtain a highly reactive polysaccharide towards amines. Given the results of the preliminary studies, it was chosen to prepare a 30% oxidised pullulan. The Cathepsin K sensitive spacer Gly-Gly-Pro-Nle was then synthesised by solid phase peptide synthesis (SPPS) using the Fmoc strategy.

Paclitaxel was coupled to the enzyme sensitive spacer and a self-immolative spacer via a six step synthesis to form a prodrug. Consecutively, the bone targeting agent alendronate was PEGylated via an activated carboxylic acid with N-hydroxysuccinimide.

Finally, both “prodrugs” were successively anchored to the polysaccharide backbone through Schiff base formation and reductive amination. Once the polymer-drug conjugate, named Pull-PTX-ALN, was fully synthesised, physico-chemical characteristics of the colloid were investigated.

All synthesised conjugates were characterised in terms of PTX and ALN contents, purity and stability under physiological conditions. These conjugates showed release of the anti-neoplastic drug only in presence of Cathepsin K at pH 5.5, confirming that, the type of bond chosen allows for the drug release under precise physiological conditions, in the bone metastases environment only.

The polymer-drug conjugate bearing PTX and ALN also presented a high affinity for hydroxyapatite in vitro, proving the potential of alendronate as targeting agent. Cytotoxic activity was similar to free drug or in combination with alendronate in 4T1 cells (murine mammary adenocarcinoma cell line), MDA-MB-231 BM (human mammary adenocarcinoma from Bone Metastases cell line) and SAOS-2 (osteosarcoma cell line).

Anti-angiogenic properties of alendronate in combination with paclitaxel were also assessed, as well as polymer conjugates challenging the materials with HUVEC (Human Umbilical Vein Endothelial Cells). PTX and ALN together in their free form or conjugated onto Pullulan backbone presented a similar inhibition of proliferation and migration of HUVEC. Additionally, a reduction of capillary-like tube formation, by approximately 40-50%, was observed after 8hour incubation with the primary cell line.

# RIASSUNTO

---

Nell'ultima fase della malattia, i pazienti che hanno il cancro al seno spesso sviluppano metastasi ossee, una delle principali cause di morte legata al cancro tra le donne nel mondo.

Il trattamento comune attualmente utilizzato clinicamente include l'agente anti-neoplastico paclitaxel (PTX) e il bisfosfonato alendronato (ALN).

Il paclitaxel è un farmaco anti-neoplastico a quale l'effetto citotossico è attribuito principalmente alla sua capacità di impedire la depolimerizzazione dei microtubuli. La stabilizzazione dei microtubuli mitotici interrompe le funzioni che, in sequenza, blocca la divisione cellulare. Il paclitaxel è approvato per il trattamento del cancro dell'ovaio, della mammella, e del cancro ai polmoni in fase avanzata. Tuttavia, il farmaco anti-tumore è altamente idrofobico e, di conseguenza, è scarsamente solubile in acqua. Inoltre, la formulazione di paclitaxel attualmente utilizzata in ambito clinico, nota come Taxolo, contiene il farmaco anti-neoplastico disciolto in una miscela di Cremophor EL ed etanolo per aumentarne la solubilità. Tuttavia, la somministrazione di Cremophor EL causa grave dose-limitante tossicità, come ipersensibilità e neuropatia. Infine, l'agente chemioterapeutico soffre di scarsa selettività verso i tumori, e risulta in danneggiare le cellule normale e sane. Come risultato, molti sforzi sono stati compiuti per lo sviluppo di nuova formulazione di paclitaxel mediante polimerici biocompatibili e biodegradabili.

Inoltre, metastasi ossee sono fonte di notevole preoccupazione per i pazienti con carcinoma della mammella in fase avanzata. I pazienti possono affrontare sfide supplementari al cancro come il declino della loro salute del scheletro, e contribuisce a una manifesta diminuzione della qualità di vita e sopravvivenza. Alcuni bisfosfonati sono stati valutati in pazienti con metastasi ossee da tumore primario della mammella, e più particolarmente l'alendronato, al fine di ridurre riassorbimento osseo e progressione del tumore.

Il presente progetto mira allo sviluppo di un nuovo nano-sistema di veicolazione di farmaco al sito target, ed il rilascio controllato di farmaco anti-tumore. Il modello sviluppato è un coniugato polimero-farmaco dove il farmaco anti-tumore Paclitaxel - utilizzato per trattare il cancro della mammella - e l'alendronato, sono collegati ad un supporto polimerico naturale, il Pullulano, attraverso un distanziatore.

Il coniugato polimero-farmaco, progettato per il rilascio controllato in particolare condizione fisiologiche, utilizza due meccanismi principali per il rilascio, compreso un idrolisi enzimatica e un idrolisi non-enzimatica. La scelta del distanziatore tra il polimero e il farmaco è stata fatta in modo che il rilascio del farmaco si verifica solo una volta che il sistema raggiunge le metastasi ossee, rilascio utilizzando una idrolisi enzimatica prima. Quando i coniugati polimero-farmaco sono elaborati per tumore, il legame tra il farmaco

e il polimero deve essere necessariamente stabile in condizioni fisiologiche fino a quando raggiunge il bersaglio tumorale. Il veicolo colloidale è stato progettato per migliorare la biofarmaceutica e le proprietà terapeutiche del farmaco anti-tumore paclitaxel, aumentando la solubilità in acqua e l'individuazione del tumore stesso. Il bisfosfonato alendronato è stato scelto come agente di mira a conferire una elevata affinità del coniugato verso la struttura di apatite di metastasi ossee, sfruttando la forte proprietà di grande affinità per l'osso dei bisfosfonati, insieme con il micro-ambiente di metastasi ossee, al fine di garantire un rilascio selettivo e l'accumulo dei farmaci anti-tumori nel punto di azione desiderato; le metastasi ossee.

Primo, gli studi preliminari sono stati eseguiti studiando l'influenza del tempo di ossidazione del Pullulano sulla sua architettura (peso molecolare e polydispersivity). Il Pullulano è stato modificato per ossidazione con periodato in vista di ottenere un polisaccaride altamente reattivo verso le ammine. Dagli risultati di studi preliminari, si è scelto di preparare un Pullulano ossidato a 30%. Il distanziatore GlyGlyProNle sensibile alla Catepsina K è stato poi sintetizzato mediante il metodo sintesi di peptidi in fase solida (SPPS) usando la strategia Fmoc.

Paclitaxel è stato accoppiato con il distanziatore sensibile all'enzima, ed con un distanziatore auto-immolabile tramite una sintesi in sei passi, per formare un profarmaco. Consecutivamente, il targeting delle ossa è stato eseguito con l'alendronato, PEGilato tramite un acido carbossilico attivato con N-idrossisuccinimide.

Infine, i due "profarmaci" sono stati successivamente ancorati al backbone del polisaccaride via formazione di base di Schiff e amminazione riduttiva. Una volta che il coniugato polimero-farmaco, chiamato Pull-PTX-ALN, è stato completamente sintetizzato, caratteristiche chimico-fisiche del colloide sono state investigate.

Tutti gli coniugati sintetizzati sono stati caratterizzati in termini di contenuto in PTX e ALN, purezza e stabilità in condizioni fisiologiche. Questi coniugati hanno mostrato il rilascio del farmaco anti-neoplastici solo in presenza di catepsina K a pH 5,5, confermando che il tipo di legame scelto consente il rilascio del farmaco sotto precise condizioni fisiologiche, solo nel ambiente delle metastasi ossee.

Il coniugato polimero-farmaco, veiculando PTX e ALN, anche presenta un'alta affinità per l'idrossiapatite in vitro, dimostrando il potenziale del alendronato come agente di mira. L'attività citotossica era simile al farmaco libero o in combinazione con alendronato in linea cellulare 4T1 (linea cellulare adenocarcinoma mammario in murine), MDA-MB-231 BM (linea cellulare del adenocarcinoma mammario umano da metastasi ossee) e SAOS-2 (linea cellulare di osteosarcoma).

Le proprietà anti-angiogeniche dell'alendronato in combinazione con paclitaxel sono state valutate con HUVEC (cellule umane endoteliali di vena ombelicale), anche per i coniugati polimero-farmaco. Il PTX e ALN insieme, nella loro forma libera, e coniugati al Pullulano, hanno presentato un'inibizione notevole della proliferazione e della migrazione delle

cellule HUVEC. Inoltre, una riduzione della formazione di tubi capillari di circa 40-50 %, è stata osservata dopo 8 ore di incubazione con la linea cellulare.





# INTRODUCTION

---



# 1. Introduction

## 1.1 Anti-tumour therapy - state of the art

Tumours result from the uncontrolled proliferation of cells as a result of mutations of many genes, called oncogenes, which control the cell growth (growth factors genes and their receptors, intracellular transducers for nuclear transcription factors). The extra proliferation of tumour cells result in the formation of an extra cellular matrix, connective tissue, which provides structural support. The extra cellular matrix can be divided into two parts; the basement membrane which anchors the cells, and the interstitial matrix which forms the bulk. When mutations become more significant, the cells may take the ability to degrade the basal lamina, to escape the surveillance of the immune system and start to make contact with cells of different tissue types. The tumour then becomes invasive and can spread throughout the lymphatic system and circulatory system, also away from the first site of incidence. This process is formerly defined as tumour metastasis and defines the malignancy of the tumour.

After cardiovascular diseases, cancer is the second leading cause of death in industrialised countries. Consequently, many efforts are made in the search for the development of effective anticancer therapies.

Paul Ehrlich created the term chemotherapy in 1914 while searching for a substance to cure syphilis with his collaborator Sahachiro Hata<sup>2</sup>.

Contemporary chemotherapy finds its roots in the battlefields during the First World War when military doctors noted that after exposure to the chemical agent called *mustard gas*, soldiers died due to their bone marrow destruction, the marrow became abnormal and the cells in charge of producing blood cells greatly decreases (bone marrow aplasia).

After these recurrent events, specialists began to investigate what was the cause of bone marrow destruction and found out that Nitrogen mustard works by physically modifying the DNA in cells. In 1942, the substance was used in USA hospitals to treat lymphoma patients with success.

Nowadays, chemotherapy is used in treating half the patients who develop cancer. Most chemotherapy drugs kill cancer cells completely, or stop their duplication and spread, by inhibiting metabolic functions of the cancer cell.

Most chemotherapeutic agents discovered during the first twenty years of research are highly cytotoxic. Their objective is targeted to damage DNA or to inhibit the cell replication, causing the non-selective death both of tumour cells and normal cells in

phase of replication. The lack of specificity of action of chemotherapeutic drugs is at the origin of their considerable toxicity that limits their use in anti-tumour therapy.

Only in recent years, research started to have a basic understanding of oncogenes, gene suppressors. The identification of new targets for chemotherapy such as the mechanism of apoptosis, the signals of transduction, and the tumour vascularization and angiogenesis led to the development of new diagnosis, prognosis and, above all, new kinds of cancer therapies for targeted treatment of neoplasms. The modern therapeutic approach uses different mechanism/methods under development including:

- The destruction of the cells by radiation;
- The use of cytotoxic substances, often in association with one another;
- Potentiation of the patient immune defences (adjuvant therapy),
- Surgical removal of the cancerous tissue;
- Gene therapy which is designed to induce the patient's own immune system to fight the tumour;
- Pharmacological prevention of metastasis of the primary tumour (anti angiogenetic);
- Hormone therapy which can be provided or blocked for inhibiting the growth of some cancers.

Radiotherapy is beneficial to treat localised tumours and its effectiveness can be increased by combining it with radio sensitizer drugs. Chemotherapy, due to its systemic action, is more indicated for tumours at a metastatic stage.

Different methods can be combined with each other, therefore evolving various therapeutic strategies such as:

- Adjuvant therapy (post-operative treatment) used when solid tumours are localised. It generally proceeds in two steps, first a surgical excision of the tumour mass is performed, followed by chemotherapy treatment and radiotherapy, to eliminate any micro metastases and therefore to prevent relapses;
- Neo-adjuvant therapy (pre-surgery treatment) is practiced to decrease the tumour volume, to support subsequent interventions by radiotherapy or surgery, that are typically needed for solid tumours, as chemotherapeutic agents often fail to reach the tumour heart.

The aim of chemotherapy is either to target the complete healing of patients or to prolong their life or alleviate the symptoms. The advancement in anti-tumour therapy research over the last forty years has progressed rapidly, passing by alkylating agents, antimetabolites to natural products, and more recently interests in gene therapies, vaccines and other drugs that act on the immune system have increased. This has led to

considerable development, especially in the treatment of malignant and fatal neoplasms as the testicular carcinoma, lymphoma, and in particular the Hodgkin's lymphoma, and leukaemia. However, the tumour remission remains often difficult to achieve, especially in the case of solid tumours such as those of colon, prostate, breast and lung, which are today, the most widespread. The development of new therapeutic systems is divided into four main directions:

- The combinatorial chemistry and screening of substances to develop low molecular weight natural or semi-natural molecules with anti-proliferative activity<sup>3</sup>;
- The use of biochemistry and molecular biology methods to identify new target sites for chemotherapy, such as receptors, antigens, angiogenic factors and chemical mediators<sup>4</sup>;
- Development of gene therapies and antisense nucleotides<sup>5</sup>;
- Investigation of systems directing and releasing the drug to make the therapy more selective towards tumours.

The groups of chemotherapeutic agents currently on the market or in development include inhibitors of cell replication and DNA synthesis (cross-linking agents, alkylating agents, DNA-intercalating antimetabolites, and precursors), topoisomerase inhibitors and antibiotics-anti-tumour substances, substances stabilizing or destabilizing microtubules, enzyme inhibitors receptor antagonists.

Some new drugs do not interfere directly with DNA; among these agents, there are monoclonal antibodies and inhibitors of the tyrosine kinase (Gleevec), which aim to hit specific targets present on some types of tumour cells. Other drugs modulate the characteristics of tumour cells without binding to them, within this category of adjuvants, fall hormones.

With the discovery of new anticancer agents, the chances of a cure have already increased. However, due to their low selectivity for cancer cells, there are still major issues encountered and to be resolved. These drugs are often very powerful; nonetheless, most of anticancer drugs enter non-specifically into all types of cells, both healthy and sick, causing serious side effects that often cause a drastic worsening in the patient's life and in the most severe cases even death.

In addition, the reduced specificity infers the use of these drugs in high doses, with consequent impact including serious toxic effects. A further limitation of chemotherapy treatments is the occurrence of resistance to the drug due to significant heterogeneity of neoplastic cells and selective pressure. Furthermore, sometimes resistance is seen towards other anti-tumour drugs, thus negating the possibility of intervention. Finally the same chemotherapeutic agents can become in their turn mutagenic and carcinogenic, due to modifications that are within the body. Initially, the patient may responds well to a

treatment, but at times, as a result of a recurrence of the tumour, the same drug or even other with different structure can be becomes inefficient.

Many experts believe that a sufficient number of anticancer agents are known, but an effective cancer therapy can be only reached by obtaining suitable drug delivery systems, able to act solely into target site. Finding a molecule that is selectively toxic to tumour cells is much difficult, because these cells have essentially the same biological events as healthy cells and the differences in biochemical and molecular mechanisms are minimal<sup>6</sup>. Consequently, the diffusion of the drug in various organs can cause cellular and tissue damage.

The normal cells most affected by anticancer drugs are those with a rapid proliferation, such as those of hair bulbs, red blood cells, white blood cells and the cells of the intestinal epithelium. The side effects that occur most often are linked to the cytostatic action on the bone marrow cells and include myeloid suppression, leukopenia, neutropenia, thrombocytopenia, anaemia and damage to the immune system, involving the patient's exposure to pathologies induced by microorganisms. Other issues might be ulcerations of mouth and intestine mucous membranes with predisposition to bacterial sepsis of the intestinal tract (in case of immunosuppression); pulmonary fibrosis; venous occlusion of the liver; neurotoxicity and ototoxicity, alopecia, nausea, vomiting, diarrhoea or constipation; cardio toxicity, hepatotoxicity and nephrotoxicity. Other side effects may include erythema, loss of appetite with consequent malnutrition and weight loss. In some cases, memory loss and dizziness, dehydration or water retention, xerostomia and haemorrhage are observed.

Support therapy is often use to address these problems and may provide transfusion of platelets, or whole blood, or even bone marrow transplantation, administration of allopurinol in order to prevent the hyperuricemia, growth factors, hematopoietic to counteract the loss of red blood cells and neutrophils, broad spectrum antibiotics to prevent bacterial infections, and powerful antiemetics<sup>7</sup> as antagonists 5-HT<sub>3</sub> inhibitors<sup>8</sup> or substance P<sup>9</sup> as aprepitant as well as derivatives of THC (tetrahydrocannabinol), as the Marinol<sup>10</sup>.

Another limitation of chemotherapy is that every treatment allows to remove only a fraction of cells (fractional kill), for which continual administrations and numerous chemotherapy cycles are necessary to prevent the tumour regrowth and continues reduction of its size. The development of effective therapeutic procedures is, however, complicated by the tumour physico-pathological trends and the diverse evolution trends, by the different pathological severity and by individual variability.

The main challenges in the research for new cancer therapies are to reduce the systemic toxicity, increase the selectivity, improve compliance, reduce the frequency of administration, decrease the dose and increase the absorption; these are the primary objectives in the development of efficient anticancer systems.

## 1.2 The tumour microenvironment

Currently, the identification of tumours genetic constitution, enzymatic activity and growth is better known; yet, no actual treatment is able to exploit these characteristics.

Nonetheless, tumour tissues are a lot different from the healthy tissues and these distinctions could be advantageous for target therapy thus, an understanding of the pathophysiology of cancer is required to target drug in the systemic circulation.

### 1.2.1 Tumour vascular architecture

Tumours develop from a single neoplastic cell. The uncontrolled proliferation of the cells produce a mass of about 150-200 nm. At the beginning, the tumour cells beneficiates of the blood supply from the vasculature of healthy tissues. As it increases in size, the cell mass needs another supply for supply of oxygen, nutrients and metabolites to ensure its growth. The cell mass then starts to produce its own vascular system, producing new blood vessels through the mechanism of angiogenesis.

Angiogenesis in tumour tissue is particularly active and extended<sup>11</sup>; the production of a new vascular system is disordered in all possible directions, at all junctures. The central part of the tumour remains in hypoxia, devoid of nutrients, which lead to poor penetration of blood supply inside the solid tumour.

As a result, a dense network of vascularization jars with incomplete endothelium, and with ample fenestrations is formed, thus, the tumour tissues are particularly permeable, causing intra-tumour dissimilarities.

Healthy tumour cells have a regular lining of endothelial cells which form tight junction with neighbouring endothelial cells, from 2 to 6nm.

Tumour vasculature is significantly different from those present in healthy tissues in terms of cellular composition of the endothelial wall, basement membrane shape and of dimensions of the fenestrations, which may reach 100-780nm wide due to the discontinuous endothelial lining. New vessel walls are devoid of pericytes, which are the regulators of maturation and differentiation of capillaries. The blood vessel permeability is extremely high, not only due to the increased width of intercellular junctions and the incompleteness of the basal membrane, but also for the presence of numerous factors of permeabilisation such as an elevated level of growth factors (VEGF, bFGF, bradykinin and nitric oxide) leading to vasodilatation, extravasation of large molecule and retention in tumours.

### 1.2.2 Lack of lymphatic drainage

Lymphatic vessels are formed as termination capillaries delimited by a single layer of endothelium. The lymph fluid is drained by a series of lymphatic vessels and lymph nodes and flocked in the venous circulation. Their greater permeability than blood vessel allows them to transport macromolecules in normal tissues such as proteins from the interstitial spaces back into the blood circulation.

Solid tumours are exempted of effective lymphatic drainage system. Fluid is not seeped efficiently, resulting in a backpressure increase and thus, restricts the blood escape from vessels. The higher backpressure encourages outward flow of fluid from the tumour tissue, therefore limiting the convective extravasation of macromolecules, despite leaky vasculature.

This can lead to the collapse of the capillaries in the cancerous tissue with the formation of hypoxic and anoxic regions and the consequent start of necrotic foci within the neoplastic tissue itself.

### 1.2.3 pH decrease

Tumour uses preferentially glycolysis as route of energy, producing lactate. The poor vasculature and the lack of lymphatic drainage in solid tumour increase the concentration of metabolites by-products including lactic acid and carbonic acid in the tumour interstices, inducing a decrease of pH.

Healthy tissues and tumour having different pH, it can be exploited to design site-specific cancer drugs. Tumour acidity influences drug uptake into tumour cells. For example, a weak acid drug can be dissociated; therefore it becomes relatively lipophilic at an acid pH at the tumour site and can easily cross the cell membrane<sup>12</sup>.

### 1.2.4 Tumour hypoxia

The high density of tumour cells deprives certain region of oxygen, phenomenon known as hypoxia. Malignant progression is often connected to hypoxia, increased tumour invasion, angiogenesis and an increased risk of metastasis formation. Hypoxia might also induce increased resistance to apoptosis and as a result, indirectly contributes to treatment resistance.

Hypoxia is an issue in radiotherapy as oxygen radicals are produced following radiation under well-oxygenated conditions, contributing to DNA damage<sup>1, 13</sup>.



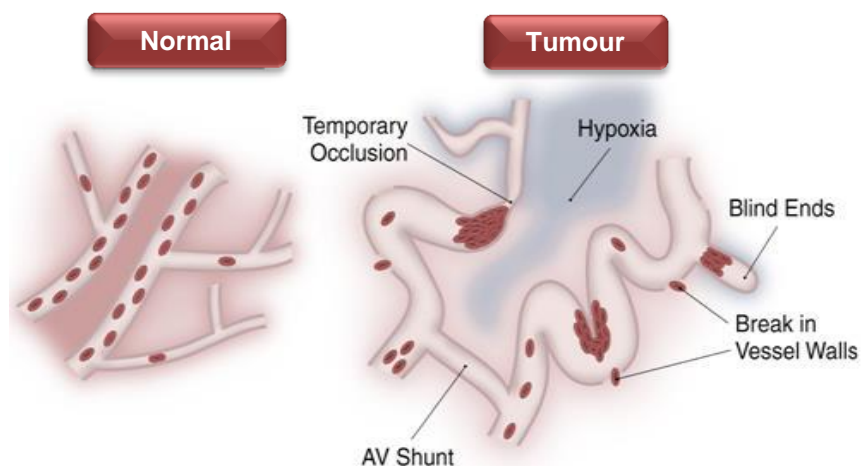


**Figure 1-1 Tumour hypoxia – The unique physiology of solid tumours<sup>1</sup>**

Effects of chemotherapy may also be inhibited through the same mechanism. In the presence of oxygen, some drugs, doxorubicin for example, can produce reactive oxygen species such as super-oxides that can damage DNA<sup>12b</sup>.

### 1.3 Breast cancer and bone metastasis

Cellular movement is a key component in tumour progression. Neovascularisation and angiogenesis are the results of endothelial cell movement; it also is the factor contributing to tumour cell movement, leading to cancer progression and metastasis.

Metastasis is defined as the delocalisation and propagation of tumour cells from primary site to distant tissues or organs. Metastases are directly connected to breast cancer-related mortality and occur in 25 to 50% of patient diagnosed with the disease. Only 25% of patients reached the average of 5 year survival rate.

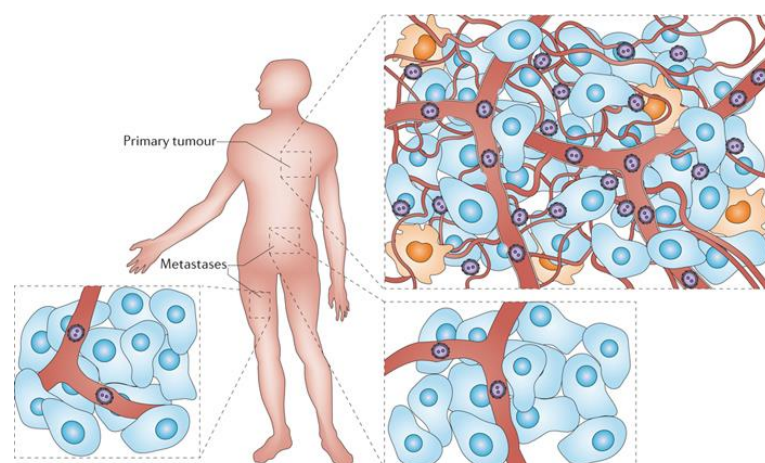


**Figure 1-2 Tumour metastases<sup>14</sup>**

The metastasis process is understood as an inefficient process, a cascade progression consisting of multiple barriers to cancer cell propagation, for instance:

- The invasion through the extracellular matrix and stromal cells in the local tumour microenvironment;
- The intravasation into the lamina of blood vessels;
- The survival and persistence into circulation;
- The extravasation into the parenchyma of a distant tissue;
- The survival and proliferation in a foreign microenvironment.

The most common site for breast cancer dissemination is the bone, with 65 to 80% of patients in late stage disease diagnosed with skeletal metastasis.

Breast tumour progression to bone is often related to oestrogen receptors in the primary mass, in contrast with tumours which metastases develop in visceral organs and brain.

The dissemination into bone is generally a sign of an irredeemable disease and the median survival is between 2 to 3 years.

Bone metastatic lesions are seldom a direct cause of death in cancer patients; however they contribute to a noteworthy degree of morbidity.

Complications include chronic bone pain, pathological fractures, hypercalcaemia, and spinal cord or nerve root compression.

The initial significant event in breast cancer bone metastasis is the tumour cell seeding within the bone.

The process thought to be involved in seeding is the adhesion of breast cancer cells to the bone marrow endothelium, mechanism similar to the physiological mechanism used by hematopoietic cells (HSCs) migrating to bone. In recent years, there has been an increase interest in defining which disseminated tumour cells first self-establish once they reach the bone marrow.

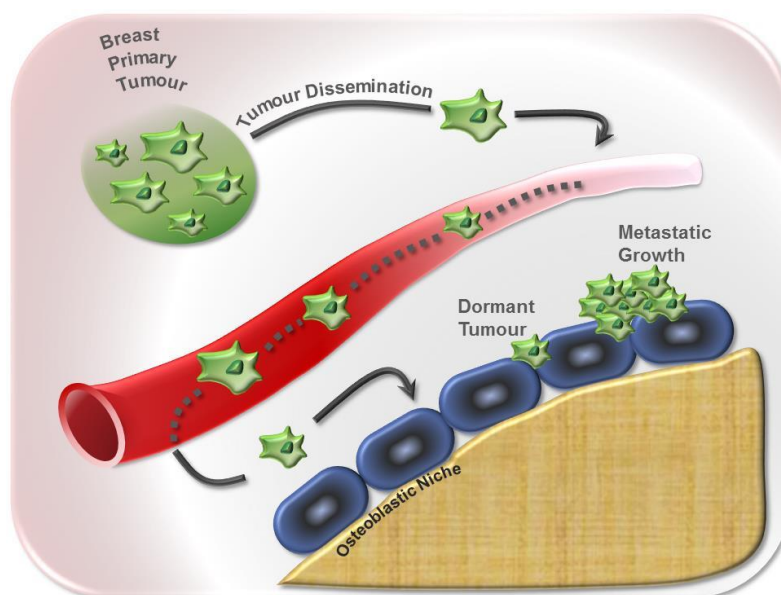


**Figure 1-3 Breast tumour metastases to bone**

Bone is a multifunctional organ which micro-environment consists of a mineralised organic matrix and a variety of bone resident cells namely chondrocytes, osteoblasts, osteocytes, osteoclasts, endothelial cells, monocytes, macrophages, lymphocytes and haemopoietic cells. The cell environment produces a range of biological regulators which control the local bone metabolism.

The entrance of tumour cells within the bone internal environment disturbs the finely organised homeostasis, releasing tumour derived growth factors and cytokine.

Mineralisation of the bone matrix is achieved through the activity of osteoblasts while osteoclasts are responsible for bone resorption. Sustain of bone architecture and mass are accountable to these two major cells in the bone micro-environment.

The bone-forming cells osteoblasts originate from mesenchymal stem cells and are recruited to bone formation sites where they actively synthesise and secrete an organic bone matrix called osteoid. This matrix is essentially composed of type I collagen and other protein of non-collagenous origins. Once the matrix formed, osteoid undergoes fast mineralisation with hydroxyapatite. Osteoblasts not only synthesise bone matrix but they also have a role of producing many regulatory elements such as prostaglandins, cytokines and growth factors, and maintaining a high alkaline phosphatase activity. These elements are thought to stimulate both bone formation and resorption.

In contrast, osteoclasts are large specialised multinucleated cells of hematopoietic origin that adhere to the bone surface and actively demineralise and degrade the bone matrix. They are formed from the fusion of mononuclear progenitor cells that arrive via vasculature. Following the production and release by osteoclasts of lysosomal enzymes,

hydrogen protons and free radical into a restricted space next to the bone (resorptive compartment), the bone matrix mineral dissolves and degrades.

Distinctive resorptive cavities called Howship's lacunae are produced by osteoclasts in contact with mineralised surfaces. Bone modelling and remodelling process is therefore influenced by the regulatory control of systemic and local factors in bone cells.

A significant signalling system effective both in bone and immune cell communication is the RANKL-RANK-OPG association (Figure 1-4).

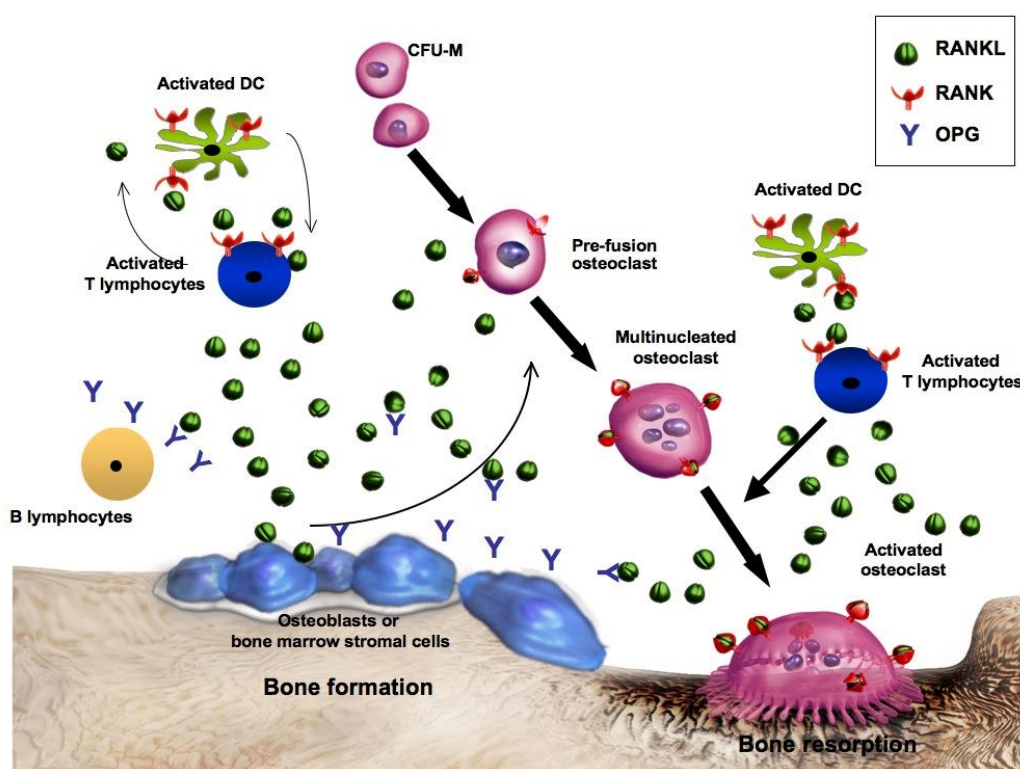


**Figure 1-4 Factors that promote differentiation and function of osteoclasts and osteoblasts<sup>15</sup>**

RANKL protein is secreted or expressed on osteoblast surfaces and activates T cells. RANKL is a member of the tumour necrosis factor (TNF) cytokine family and is ligand or osteoprotegerin (OPG). It plays a key role in giving the necessary signal to pre-osteoclast to differentiate and activate. OPG is produced by dendritic cells and is a soluble decoy receptor for RANKL that competitively inhibits RANKL binding to RANK. On the other hand, RANK is expressed on osteoclasts or pre-osteoclasts, and dendritic cells, both resulting from myeloid stem cells.

## 1.4 Polymer therapeutics

In recent years, the field of polymer therapeutics represents a sphere of major interest in drug formulation and is main subject of research in private and public institutions. They allow controlled release and drug delivery to a target site. They include covalently attached drug onto a polymer backbone and self-assembled polymer or polymer complexes.

Conventional drugs are often of micro molecular size and consequently free and easily diffused throughout the biological system. Many substances are potentially active and efficient as drugs but suffer from the serious drawbacks of being too rapidly excreted or metabolised or having grave side effects<sup>2</sup>. Additionally, drug release relies on the physico-chemical properties of the drug itself, targeting an organ or a tissue can then turn out to be difficult. On the other hand, polymer therapeutics diffuses slowly and the attachment of pharmaceutical moieties leads to polymer-drug with specific pharmaceutical properties and behaviour<sup>3</sup>. They are very attractive as they possess a prolonged drug activity, and improve drug release and latency.

### 1.4.1 Models of polymer bioconjugates

The area of polymer therapeutics can be mainly divided in five categories. The first category includes polymer as drugs where the polymer is not a carrier but is a drug itself. The four next categories are all macromolecular carriers which can themselves be divided into two subtypes: the drug can be either entrapped into a polymer matrix through physical bond (an example would be Van-der-Waals bonds) or through chemical covalent bonds. Polymer-drug conjugate and polymer-protein conjugates, polyplexes and finally self-assembled polymeric micelles are the four other categories of polymer therapeutics.

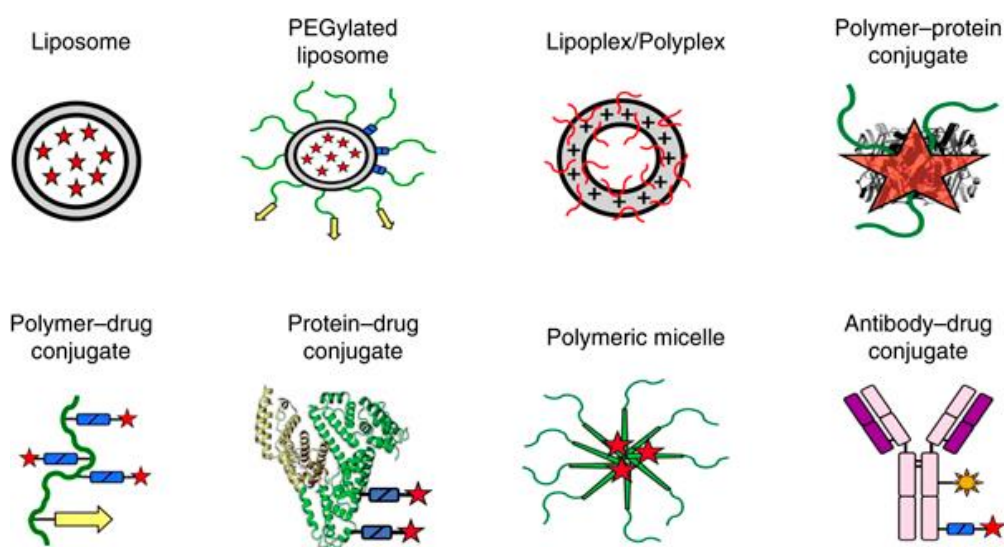


**Figure 1-5 Tumour-targeted nanomedicines: principles and practice<sup>13</sup>**

In the case of macromolecular carriers, the polymer plays a protective role of the drug to avoid its rapid elimination or metabolism. Generally temporarily lost when onto its macromolecular carrier, the activity of the drug can be restored by cleavage from the polymer. The latter can be achieved via hydrolysis or enzymatic degradation of a cleavable bond such as an ester, anhydride, orthoester or acetal. In most cases, the drug is attached away from the main polymer chain and pendant groups, using a spacer moiety which allows better hydrolysis or the use of specific enzymes.

The control of the polymer molecular weight allows to decide the mode of excretion (kidney or liver), whether it should pass the blood stream barrier or whether it should accumulate in a particular site (type I : tissue or organ, type II : certain cells or type III : intracellular compartments) and implicate the notion of target.

#### 1.4.2 Characteristics of polymeric carriers

Polymers used as drug carriers must be eliminated from the body. They should be either degraded in the case of biodegradable polymers or excreted in the case of non-degradable polymers.

Polymeric carriers can be natural polymers, sometimes partially chemically modified, and synthetic polymers.

- Biodegradable polymeric carriers are macromolecules which bonds in the backbone can undergo hydrolytic or enzymatic cleavage. Degradations products such as saccharides and amino acids are then formed and may be eliminated following the biological pathway in the body; this is the case of the natural polymers collagen and hyaluronic acid for example. Some acetylated residues may also be obtained by lysosome degradation of the polysaccharide chitosan. Another example is dextran which is degraded in presence of dextranase. Synthetic polymers may degrade in a similar fashion, namely poly(L-glutamic acid) and poly(aspartic acid). These two polymers are extremely prone to be degraded by lysosomal enzymes, generating amino acids as products of degradation.
- Semi-degradable polymers are macromolecules which chain backbone is attached to a degradable linker. At the target site, the active drug is release by cleavage of the degradable linker, simultaneously degrading the polymer backbone into some blocks able to be excreted by the kidney. Monomer units may be bound to acid labile linkers such as ketal or acetal bonds followed by polymerisation. In such way, the polymer is able to degrade under acidic conditions in the intracellular environment.



- Non-degradable polymers can be used in drug delivery, for example polyethylene glycol (PEG) and poly(hydroxypropylmethacrylate) copolymer (HPMA). However, their elimination might be hampered if their molecular weight is higher than the kidney threshold. The poor lymphatic drainage in tumour already leads to slow elimination. A high molecular weight increases the accumulation of the polymer in the tumour upon repeated administration and might cause adverse clinical effects. Sometimes, accumulation might be observed also in clearance organs such as kidney, liver, or spleen resulting in iatrogenic illnesses.

The most popular polymers used as carrier in polymer therapeutics are synthetic or natural or semi-synthetic, namely PEG, PGA, HPMA copolymer, Dextran and Chitosan respectively:

- PEG, widespread in the market, stands for linear polyethylene glycol and can bear one or two functional groups at its ends, useful for the attachment with drugs or other functional groups. PEG was the first polymer used as a carrier as it has the advantage of being biocompatible. It is also soluble either in water or organic solvents. These features make it a good candidate for PEG-protein conjugation as well as carrier, or spacer. It will be discussed later in the section 1.8.2.
- PGA or poly(glutamic acid) contains glutamic acid monomer units and can be easily degraded in the physiological environment, thanks to cysteine proteases which encourage its lysosomal degradation. As well as being water-soluble, non-toxic and biodegradable, PGA is a versatile polymer thank to its 9 carboxylic groups present on the backbone on which multiple drug attachment can be done. PGA is an attractive carrier for polymer therapeutic and the actual most advanced polymer-drug conjugate in the channel for market approval (Phase III trials) derived from PGA, namely OPAXIO, which is a PGA conjugated to the anti-tumour drug Paclitaxel against ovarian cancer and non-small lung cancer (Figure 1-6).

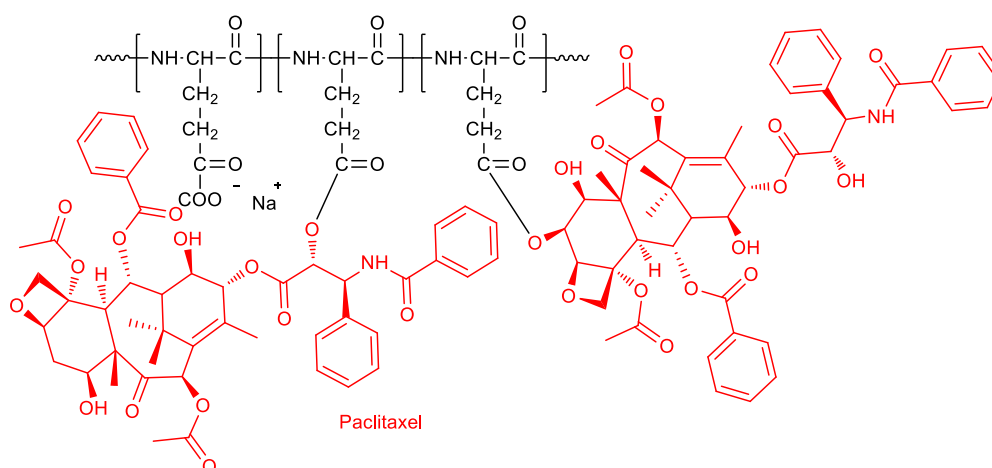
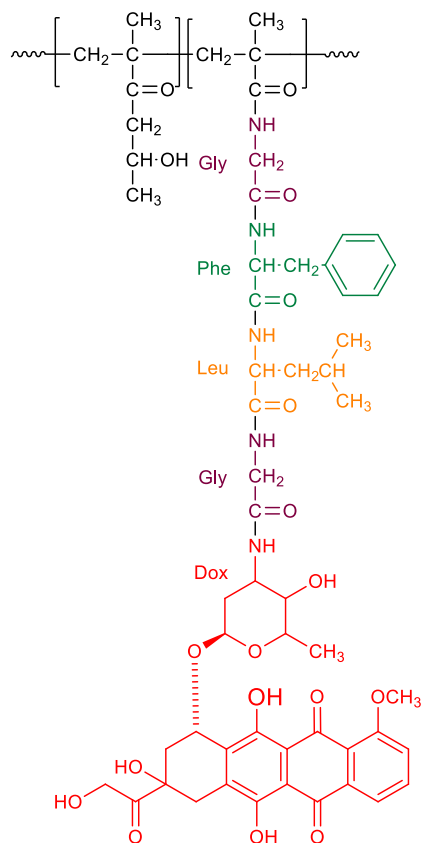
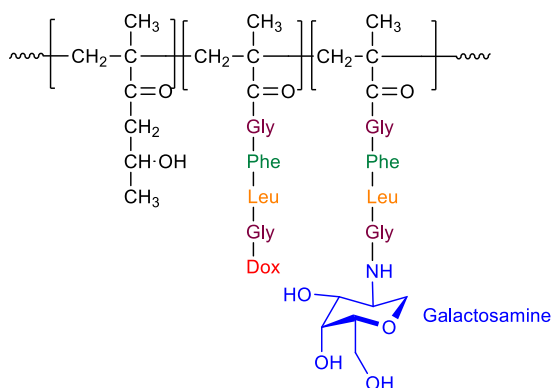


**Figure 1-6 OPAXIO**

- HPMA copolymer or poly(hydroxypropylmethacrylate) copolymer have been of major interest in the last thirty years, often investigated for the development of new polymer-drug conjugate for cancer therapy, often modified for target specific drug delivery of anti tumoural drugs. The key event which led to this amplified interest has been the clinical trial performed in 1994 on PK1 and PK2, HPMA copolymers carrying doxorubicin (DOX) on their backbone, linked through a degradable peptidyl linker (Figure 1-7). HPMA has the advantage of being non-immunogenic, neutral and bio-compatible.



PK1



PK2

**Figure 1-7 PK1 and PK2 HPMA copolymers for drug delivery**



- Dextran belongs to the family of polysaccharides. From bacterial origins, it contains glucose monomer units bound via  $\alpha$ -1,6 linkages. The presence of several primary alcohol groups on its backbone allows direct conjugation of drugs, spacers, or proteins. The natural polymer is able to dissolve in water and organic solvents and is biocompatible and biodegradable in the gastro-intestinal tract and blood. The polysaccharide has been clinically approved as blood expander.
- Chitosan also belongs to the polysaccharide family, derivatised from deacetylation of chitin. The poly(D-glucosamine) contains numerous amines, available for chemical conjugation. The polymer is biodegradable and biocompatible. Polymer-drug conjugates based on chitosan and camptothecin have already been tested clinically<sup>16</sup>. Chitosan can also be used for oral delivery of drugs due to its strong muco-adhesive property and for gene therapy.

#### 1.4.3 Examples of molecular models clinically used

Abraxane, which is an albumin-bound paclitaxel, was the first passively tumour targeting polymer therapeutic approved by Food and Drug Administration (FDA) in 1995.



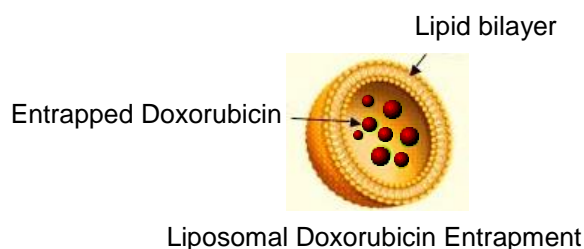
**Figure 1-8 Abraxane model**

Cremophor-formulated version of paclitaxel has gone through a large phase III trial in which over 400 women with metastatic breast had an improved response and less side effects than standard free drug,

Besides these paclitaxel based drugs, a variety of polymer therapeutics has been assessed clinically. Oncaspar, for example, is a PEG polymer conjugated to the protein L-asparaginase in order to decrease allergic reactions and frequency of administration and has been used for treating patients with acute lymphoblastic leukaemia for over 10 years.

Doxil is a PEGylated (polyethylene glycol coated) liposome-encapsulated form of doxorubicin (Figure 1-9), ordinarily used in the treatment of an extensive range of cancers, including haematological malignancies, various types of carcinoma, and soft tissue sarcomas. Doxil was the first FDA-approved nano-drug (1995). The free drug doxorubicin is very potent but severe side effects, such as cardiotoxicity and myelo-

suppression, have restricted its use. Doxil has shown considerably enhanced safety and efficiency, compared with conventional doxorubicin



Liposomal Doxorubicin Entrapment

**Figure 1-9 Doxil model**

Another example of drug delivery system, not yet approved by FDA but promising in clinical trials is Aurimune. Aurimune (CYT-6091) entails a recombinant human tumour necrosis factor alpha (TNF), a known tumour-killing agent, bound to the surface of PEGylated colloidal gold nanoparticles. The gold PEGylated surface prevents the therapeutic payload from immune detection and allows its safe travel through the bloodstream. Patients taking an intravenous injection of Aurimune have been able to tolerate 20 times higher dose than the usual dose of conventional TNF- $\alpha$ .

The following table summarizes the current clinical trials investigating nano-medicines (Table 1-1).

**Table 1-1 Current clinical trial on nano-systems for drug delivery<sup>17</sup>**

Nano-systems	Commercial Name	Cancer type	Clinical Phase
Liposomal doxorubicin	Myocet, Caelyx (Doxil)	Breast, ovarian, KS	Approved
Liposomal daunorubicin	Daunoxome	Kaposi sarcoma	Approved
Liposomal vincristine	Onco-TCS	Non-hodgkin lymphoma	Approved
Liposomal cisplatin	SPI-77	Lung	Phase II
Liposomal lurtotecan	OSI-221	Ovarian	Phase II
Cationic liposomal c-Raf AON	LErafAON	Various	Phase I/II
Cationic liposomal E1A pDNA	PLD-E1A	Breast, ovarian	Phase I/II
Thermosensitive liposomal doxorubicin	ThermoDox	Breast, liver	Phase I
Albumin-paclitaxel	Abraxane	Breast	Approved
Albumin-methotrexate	MTX-HSA	Kidney	Phase II
Dextran-doxorubicin	DOX-OXD	Various	Phase I
PEG-L-asparaginase	Oncaspar	Leukaemia	Approved
PEG-IFN $\alpha$ 2a/IFN $\alpha$ 2b	PegAsys/ PegIntron	Melanoma, leukaemia	Phase I/II
PHPMA-doxorubicin	PK1	Breast, lung, colon	Phase II

<b>Table 1- (continued)</b>	<b>Commercial Name</b>	<b>Cancer type</b>	<b>Clinical Phase</b>
<b>Galactosamine-targeted PK1</b>	PK2	Liver	Phase I/II
<b>PGA-paclitaxel</b>	Xyotax	Lung, ovarian	Phase III
<b>Paclitaxel-containing polymeric micelles</b>	Genexol-PM	Breast, lung	Phase II
<b>Cisplatin-containing polymeric micelles</b>	Nanoplatin	Various	Phase I
<b>Doxorubicin-containing polymeric micelles</b>	NK911	Various	Phase I
<b>SN38-containing polymeric micelles</b>	LE-SN38	Colon, colorectal	Phase I
<b><sup>90</sup>Yttrium-Ibritumomab tiuxetan (<math>\alpha</math>-CD20)</b>	Zevalin	Non-hodgkin lymphoma	Approved
<b>DTA-IL2 fusion protein (<math>\alpha</math>-CD25)</b>	Ontak	T-cell lymphoma	Approved
<b>Ozogamycin-gemtuzumab (<math>\alpha</math>-CD33)</b>	Mylotarg	Leukaemia	Approved
<b>Doxorubicin-cBR96 (<math>\alpha</math>-CD174)</b>	SGN-15	Lung, prostate, breast	Phase II

## 1.5 Passive and active tumour targeting

One of the major causes for the toxicity of antineoplastic chemotherapeutic agents is their poor selectivity for tumours cells. Their low molecular weight contributes to the large distribution volume. Low molecular weight drugs enter the cells mainly by a diffusion mechanism. By acting without distinction even on healthy cells, it gives rise to a whole series of side effects. Creating a drug which is able to act only on the tumour is today's challenge. The conjugation of low molecular weight drugs to high molecular weight carrier substantially influences the mechanism of entry into the cell. The drug can be brought to the tumour by two main mechanisms, the EPR effect also known as passive and the active targeting<sup>18</sup>.

More efficient targeting may be obtained by conjugation of polymer-dugs with specific target molecules, characteristic of tumours of specific to an organ or tissue.

### 1.5.1 Passive targeting

Substances of low molecular weight generally diffuse in healthy and diseased tissues without distinction. On the contrary, macromolecular drugs like albumin accumulate passively in the tumour mass. This phenomenon was observed for the first time by H. Maeda in 1986. Their studies demonstrated that solid tumours produce a large amount of various vascular permeability factors, resulting from the faulty architecture of their blood vessels. This amplified permeability ensures sufficient supply of nutrients and oxygen for the tumour to grow rapidly. The reduced drainage of the lymphatic system associated with the high interstitial fluid pressure in the tumour tissues (enhanced retention) reduces the clearance of the macromolecule and therefore increases passively its accumulation in tumour tissues. This phenomenon results in a greater extravasation of a drug in the tumour tissues and permanence in the site of action. The distinctive pathophysiological feature of tumour vasculature, easing the transport of molecules in the tumour tissue, was then namely introduced as the Enhanced Permeability and Retention (EPR) effect<sup>18</sup>.

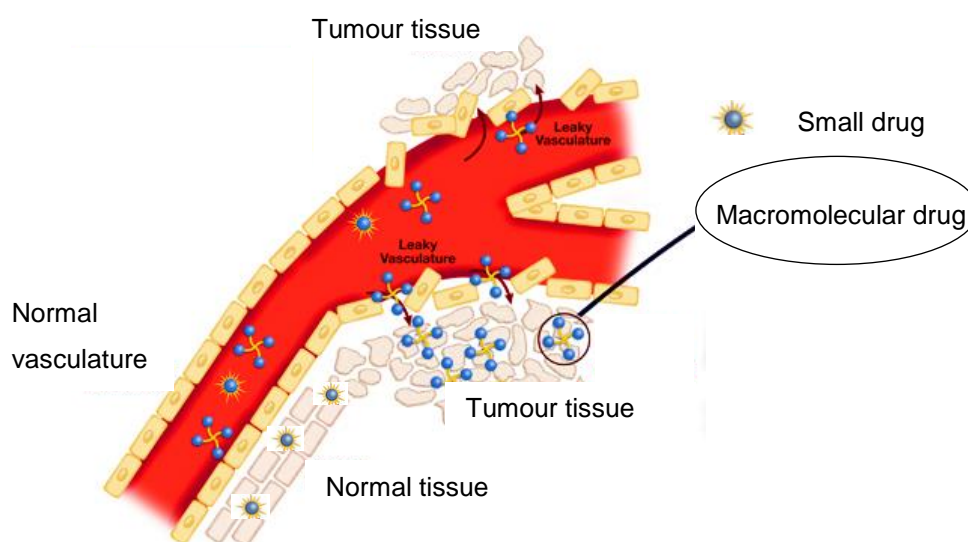


**Figure 1-10 The EPR effect – inspired from Eldon et. al Oct 2007<sup>19</sup>**

The EPR effect depends on molecular size. Molecules should be larger than 40kDa, value of renal threshold for polymers to ensure a slower clearance, hence a prolonged circulation time<sup>20</sup>. Molecules can then gradually permeate the tumour and stay for a reasonably long time in the tumour.

Not only molecular size is important but also surface charge. Positive charge polymer-drug conjugate might bind rapidly to vascular endothelial luminal cell surface which is known to carry a negative charge. The plasma half-life decreases and consequently the tumour drug accumulation decreases too. Weakly negative or near-neutral particles are therefore more likely to have longer plasma half-life.

Finally, a third aspect that might be taken into account for the EPR effect, is the hydrophobicity. A highly hydrophobic molecule has a greater affinity for cell membranes and a much faster endocytosis up-take. However, attention should be paid as highly hydrophobic polymers might cause haemolysis of red blood cells.

### 1.5.2 Active targeting

The active targeting of drugs represents one of the most interesting approaches to obtain effective therapeutic systems. Targeting is obtained by insertion onto the macromolecular structure, of molecules able to recognise antigen or specific cell population receptor.

Antibodies and antibody fragments, vitamins, peptides, folate and transferrin are some targeting ligands which have been evaluated in cancer therapy.

The targeting ligand must be subtly chosen according to its specificity, stability, availability and to the selective display of its corresponding pair on the target cells.

Other factors should also be considered such as conjugation chemistry, density and accessibility of the ligand in order to design an efficient targeting vector.

Active targeting complements passive accumulation into tumours and therefore offers an improved result due to specific interactions with target cells

Many studies have been focusing on folic acid, galactose<sup>21</sup> and small peptides for active targeting. The high affinity of these ligands for biological receptors, mainly the membrane, allows a selective bio-distribution of the macromolecular system and in some cases promotes the cell internalisation.

Attractive results have been obtained, employing ligands that are internalised through the endocytosis pathway after recognition with the actual membrane receptor, such as the folic acid<sup>17c, 22</sup>. Folate receptor is a well-known tumour marker. It binds to the folic acid vitamin and folate-drug conjugate. This high affinity allows the transport of these bound molecules into the cells via receptor-mediated endocytosis. This way the entire supramolecular drug penetrates in the cell, carrying a drug. Such systems, besides favouring the localised drug build-up in the target tissue and reducing the distribution and systemic toxicity, also often consent to escape the intrinsic resistance acquired or multidrug-resistance.

Another receptor highly present in cancer cells is the transferrin receptor. Transferrin is a serum glycoprotein which transports iron through the blood and into cells by binding to transferrin receptor<sup>23</sup>.

### 1.5.3 Intracellular trafficking

As soon as the drug delivery carrier has reached tumour tissues, successive drug release may occur in the extracellular space, or following internalisation of the carrier. Some drugs with intracellular action are unable to cross cell membranes and necessitate to be assisted in getting to their target. Mechanisms or combination of mechanisms involved in cellular uptake diverge accordingly with the cell type (phagocytic or non-phagocytic cells), the physicochemical properties of the internalised entity and the mode of activation (receptor mediated endocytosis).

Non-targeted polymer-drug conjugates reach the tumour tissue target passively through the EPR effect. Subsequently, they release the drug in the vicinity of the cell or in contact with the cell membrane.

Furthermore, intracellular targeting is feasible through the use of ligands. Ligand targeted polymer therapeutics may bind to epitopes on cell surface, endocytosis may occur following binding to receptors which stimulate internalisation, or it may not be specific (Figure 1-11). Once internalised, the colloid either escapes into the cytoplasm or discharges the drug in vesicular organelles in response to environmental stimuli such as enzymes, pH, temperature or reductive conditions.

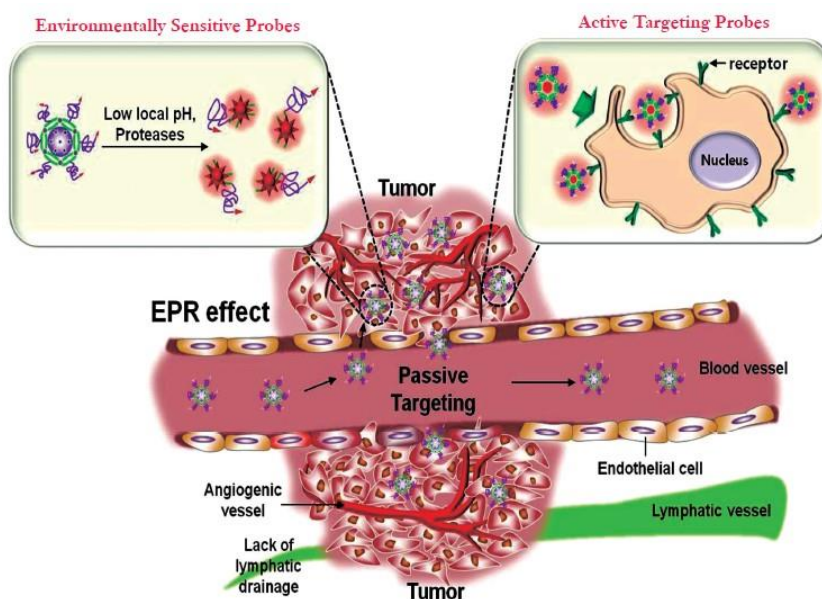


**Figure 1-11 Passive and active targeting approaches of nanomedicines in cancer therapy<sup>24</sup>**

Desired subcellular localisation has already been achieved successfully by the use of lysosome degradable linkers, nuclear localisation and acid or reduction responsive polymer-drug conjugates, exploiting the endosome maturation.

### 1.5.4 Targeting to bone

One of the main bone features which differs the most from other tissues is the presence of bone calcium/phosphate-based mineral, hydroxyapatite (HAp)  $\text{Ca}_{10}(\text{PO}_4)_6(\text{OH})_2$ , which introduces other ions and salts in its structure. The mineral component is the main constituent of bone (per mass basis) and is the essential element responsible for the mechanical support function. As osseous tissues mainly consist of this mineral, they also have a very low blood flow rate.

In order to get bone targeting systems, drugs or drug conjugates must be designed so that they have a very strong affinity for hydroxyapatite. Thus, after systemic administration, the drug conjugate accumulates in bones.

A number of elements rule the binding effectiveness to the apatite surface, including the blood supply, the molecular structure of the apatite surface, the effective binding surface area and the local extravasation rate of the compound into the interstitial fluid where the bone surface is exposed.

To achieve this objective, a number of molecules and moieties can be used as selective bone-targeting ligands. A bone-targeting moiety should preferably have a strong affinity for hydroxyapatite, be chemically modifiable to allow its conjugation to carriers or other molecules used to build the drug delivery system. The introduction of bone-targeting ligands must not affect the drug delivery system in terms of toxicity but also in terms of overall biological activity. A variety of bone targeting agent owning these characteristics are recognised and described briefly in the subsequent sections.

#### 1.5.4.1 Tetracyclines

Tetracycline was discovered in the late 1940s by the American botanist Benjamin Duggar from soil near cemeteries (Figure 1-12). The yellow crystalline substance, derived from the metabolites of the *Streptomyces rimosus* bacteria, is an amphoteric substance which inhibits aminoacyl-tRNA from entering into bacterial ribosomes and thus inhibits the protein elongation; it affects the general bacterial metabolism.

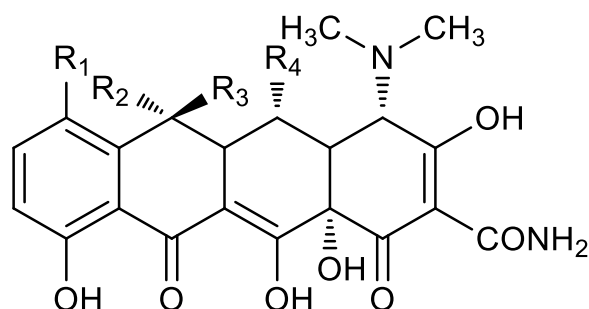


Figure 1-12 Tetracycline

Tetracycline was first used as an antibiotic in 1947 for a wide range of bacteria. Soon after its clinical use, it was noticed a considerable deposition into hard tissues including teeth enamel and bones, leading to the interruption of the prescription of the medicine to young children as the strong affinity to hard tissues caused the staining of children's teeth to a yellow colour. However, its use as bone targeting ligand as persevered for its interesting properties. Tetracycline belongs to a family of polycyclic naphthalene carboxamides. The atoms involved in the hydroxyapatite binding are the oxygen atoms in C<sub>2</sub>, C<sub>10</sub> and C<sub>12</sub>, therefore allowing modifications around the C<sub>5</sub>, C<sub>6</sub> and C<sub>7</sub> carbon atoms without altering the binding and biological activity. The tetracycline binding properties to hard tissue were first attributed to the interaction of the molecule with organic compounds. Later, it was recognised that tetracycline have distinct metal complexing abilities and one explanation for their binding to bone apatite was their capacity to chelate with hydroxyapatite surface calcium ions<sup>25,26</sup>

#### **1.5.4.2 Acidic oligopeptides.**

Bone hydroxyapatite mineral is amphoteric and presents a complex variety of charges due to Ca<sup>2+</sup>, PO<sub>4</sub><sup>3-</sup>, OH<sup>-</sup> and other substituents under physiological environments. Such ionic species provide plenty of sites for the binding of proteins via electrostatic interactions.

In the last few years, new bone targeting drug delivery systems based on oligopeptides are evolving. Non-collagenous proteins based on the repetitive sequence of acidic amino acids (L-aspartic acid or L-glutamic acid) are well known for binding to hydroxyapatite after addition to osteoblastic cell culture; for example bone sialoproteins which are highly modified anionic phosphoproteins exclusively expressed in mineralized connective tissues and osteopontins which are multifunctional proteins containing various structural areas such as an integrin binding (RGD) adhesive area and aspartic acid rich calcium-binding area.

A minimum number of 6 amino acids in the sequence should be maintained to obtain high binding capacity to hydroxyapatite. Ionic interactions between the negatively charged acid groups of these proteins and the positively charged calcium ions within the mineral constituent of bone, explain the affinity of acidic oligopeptides to hydroxyapatite at physiological pH.

#### **1.5.4.3 Bisphosphonates**

Bisphosphonates are synthetic equivalents of a naturally occurring polyphosphate present in serum and urine, the inorganic pyrophosphate. They are able to stop bone calcification by binding to newly produced hydroxyapatite crystals. Bisphosphonates are composed of two phosphonate groups linked to a central (geminal) carbon atom by



phosphor-ether bonds. Effective bone targeting drug-delivery systems based on bisphosphonate as for site-specific delivery of other drugs to the osseous tissues have already been developed, fructifying the adsorption of the prodrug to the mineral component of the bone<sup>27</sup>.

The present thesis project uses this strategy; the role of bisphosphonate will be developed further in the next sections.

#### **1.5.4.4 Other targeting agents**

The increased knowledge of the bone metastasis mechanism has led to the development of novel bone-targeting agents including RANK ligand (RANKL) inhibitors (for example, denosumab), Src inhibitors (for example, deastinib, bosutinib and saracatinib), Cathepsin K, chemokine receptor type 4 and GPNMB inhibitors. These models are currently investigated in different phases of preclinical trials (Phase I–III), RANKL inhibitor denosumab being one of the most studied at present.

### **1.6 Drug release from polymer-drug conjugates**

The attachment of a drug to a polymeric carrier leads to a polymer-drug conjugate. The type of binding between the drug and the polymer defines the stability of the conjugate, influencing the rate of drug release. Polymer-drug conjugates designed for controlled release under specific physiological conditions uses two main mechanisms for the release, including an enzymatic hydrolysis or non-enzymatic hydrolysis. The hydrolysis rate constant depends on the chemical nature of the linkage, the structure of the polymer and the environmental parameters. Other factors may influence the cleavage rate, such as the distance between the polymer and the drug, in addition to steric hindrance and the hydrophilicity of vicinal groups. The choice of the bond type between the polymer and the drug is often restricted by the functional groups present on the drug and on the polymer. The introduction of a spacer may overcome this limitation. When polymer-drug conjugates are elaborated for tumour delivery, the linkage between the drug and the polymer must be necessarily stable under physiological conditions until the tumour target is reached. The drug should then be cleaved rapidly to be activated.

#### **1.6.1 Carboxylic esters**

Carboxylic esters have the ability to hydrolyse more easily than carbonates, carbamates and amides at physiological pH. Polymer-drug conjugates, hydrogels or micelles have been developed using the characteristic of carboxylic ester for drug delivery. The hydrolysis in these systems is primarily aqueous.

Factors influencing rates of hydrolysis of carboxylic esters include the steric hindrance and the distribution of the drug along the backbone. The more the distribution is homogeneous, the quicker the release might be<sup>27-28</sup>.

### 1.6.2 Carbonate esters

Carbonates hydrolyse nearly 3 times slower than esters of analogous architecture; they are generally tough to non-enzymatic hydrolysis at physiological pH. However, in vivo, carbonate may hydrolyse in presence of enzymes<sup>27-28</sup>.

### 1.6.3 Carbamate esters

As for carbonates, carbamates are not sensitive to enzymatic hydrolysis at physiological pH. However, their strong bonds become weaker at extreme pH, either basic or acid. This property has been used by Yoo et al. to free doxorubicin from a PGLA-doxorubicin conjugate connected through carbamate bonding<sup>2a</sup>.

Carbamates are generally less sensible to esterases than carbonates. However, N-substituted or mono-substituted carbamates derived from phenolic compounds show a greater lability than aliphatic hydroxyl carbamates which are very stable, and therefore, phenolic carbamates are favourable to enzymatic hydrolysis.

### 1.6.4 Hydrazones

Hydrazones are widely used for targeted delivery. Their attractiveness is attributable to their property of hydrolysis in function of the environmental pH; hydrazones are stable at 7.4, physiological pH, but hydrolyse at pH 5.0. This characteristic has particularly been exploited in the design of polymer-drug conjugates for tumour or lysosome targeting<sup>28b</sup>.

### 1.6.5 Amide

Amides are generally very stable entities. They are not affected neither by aqueous nor by enzymatic hydrolysis and are particularly adapted for systems which need a permanent polymer-drug linkage.

### 1.6.6 Peptidyl spacers

Peptidyl spacers are usually used as enzyme substrates. In the case of cancer, proteases are very much involved in the development of tumours and can be used as triggers. Proteolysis is an irrevocable regulatory mechanism in which enzymes selectively cleave specific substrates based on amino acids. The bond rupture occurs at the amide bond between the C-terminal of the peptide and the amine group of the drug.

Proteases are an essential factor in numerous biological and pathological developments by the proteolysis regulatory mechanism; they are present in a large amount in normal lysosomes as well as in metastatic cancer. In neoplastic diseases, unusual proteolytic activity results either from greater protease expression, reduced levels of proteinase-inhibitors, altered subcellular distribution patterns or a combination of them. Proteases themselves originate not only from tumour cells but also from the various cell types present in the tumour microenvironment, where stromal cells such as fibroblasts, inflammatory cells such as macrophages, mast cells and neutrophils, and blood vessel cells such as endothelial cells interrelate in a complex network

Alterations in protease expression and substrate proteolysis are important elements in the pathogenesis of many diseases. Deregulated, excessive or incorrect proteolysis are characteristic features of neoplastic as well as inflammatory, cardiovascular, neurodegenerative, bacterial, viral and parasitic diseases.

In the case of tumour-specific targeting, the enzyme exploited for drug release and activation should be exclusively present in the tumour cell.

Perhaps the most direct way to design protease-sensitive prodrugs is to attach a cytotoxic agent covalently to a peptide substrate of the enzyme to be targeted. Ever since the early reports by Carl et al., several variants of this concept have been explored using different peptide substrates and chemotherapeutics.

Acetylation of the terminal amine function of the peptide is a frequent way to synthesise peptide-based prodrugs.

Designing a polymer-drug conjugate bound together via a peptidyl spacer has been investigated by several groups as exemplified in section 1.6.

## **1.7 Examples of drug release triggered by small proteases**

A commonly acknowledged approach to improve efficiency of chemotherapeutics is to direct anti-tumour drugs to their target site. The release of these drugs can be achieved by insertion of a spacer that is receptive to a disease-specific trigger. Methods using protease-sensitive spacers have attracted wide interests among researchers and more particularly polymer-drug conjugates involving activation by cleavage of small protease-sensitive peptide spacers.

A first example is the use of the Cathepsin-B sensitive spacer Gly-Phe-Leu-Gly in the synthesis of several N-(2-hydroxypropyl)-methacrylamide-copolymer (HPMA)-based drug conjugates in order to achieve lysosomal drug release.

N-(2-hydroxypropyl)methacrylamide (HPMA) copolymer conjugates with anti-tumour agents have been most extensively studied. Generally, the drugs are bound to the polymer backbone using peptidyl spacers designed for cleavage by lysosomal. The most

promising conjugate of this type is PK1; the polymer-drug conjugate went through to Phase I and Phase II clinical trials.

The first synthetic polymer-drug conjugate is a HPMA copolymer doxorubicin (PK 1), in which the anti-tumour agent doxorubicin is bound to the polymer backbone by a Gly-Phe-Leu-Gly peptidyl side chain. The conjugate displays anti-tumour activity and is five to ten times less toxic than free doxorubicin and shows evidence of tumour selective targeting. Studies demonstrated that an increase of lysosomal Cathepsin B activity was associated with a higher amount of free doxorubicin in the tumour tissue. Clinical trials established that the maximal tolerated dose (MDT) was found to be approximately 5 times higher compared to free doxorubicin and no cardiac failure were reported.

Other drugs using were covalently attached to HPMA via the Gly-Phe-Leu-Gly spacer, including Adriamycin, daunomycin, 5-fluorouracil or Pt(II)complexes.

Using the same peptide linker, but using alendronate as a therapeutic agent, HPMA-copolymer conjugates were developed by Satchi fainaro et al. These studies confirmed a strong affinity for bone tissues of the conjugate.

Gly-Gly-Pro-Nle is another linker which has been employed to connect HPMA copolymer to prostaglandin E1 for bone targeting. The Cathepsin K sensitive spacer was intended to achieve site- release with potential applications in osteoporosis or other bone diseases. In vitro studies validated that the osteoclasts activated efficiently the prodrug.

Another example uses a MMP-2/-9 sensitive dextran-methotrexate conjugate. The polymer, developed by Chau et al., contained a Pro-Val-Gly-Leu-Ile-Gly peptide linker. In vitro experiments showed release of 89% and 61% of the methotrexate after incubation with MMP-2 and MMP-9, respectively, for 24 hours. Moreover, it was shown that the liberated methotrexate-Pro-Val-Gly digestion product had cytotoxic effects in cell culture, although with a lower potency than free methotrexate.

In opposition to free methotrexate, the MMP-sensitive conjugate demonstrated acceptable in vivo side effects and successful inhibition of tumour growth by 83% in two independent MMP-overexpressing tumour models. MMP-insensitive conjugates, though able to inhibit tumour growth, caused toxicity in the small intestine and bone marrow.

## 1.8 Material involved in the project – Design of Pullulan-paclitaxel alendronate with Cathepsin K sensitive spacer

The concept of macromolecular carrier had already been defined at the beginning of the last century, when in 1906 Ehrlich created the term "magic bullet" to indicate the transport of drugs with a high molecular weight.

In the seventies, Helmut Ringsdorf proposed the first model of polymer therapeutics, in which the cytotoxic agent could be conjugated to different polymeric backbone<sup>29</sup>.

The model proposed by Ringsdorf consisted of an inert water soluble polymeric carrier on which different components were attached<sup>29</sup>:

- A biodegradable spacer interposed between the polymer backbone and the drug, allowing a sensitive chemical or enzymatic hydrolysis only at the site of action, releasing the active drug (intracellularly cleavable linker).
- A drug covalently linked to the spacer.
- Optionally, a targeting agent bound to the polymer structure can be added, promoting the guiding and the uptake to specific targeted cells, while minimising the non-specific interactions.
- Another optional element is the addition of solubilisers able to modulate the solubility of the polymer-drug conjugate.

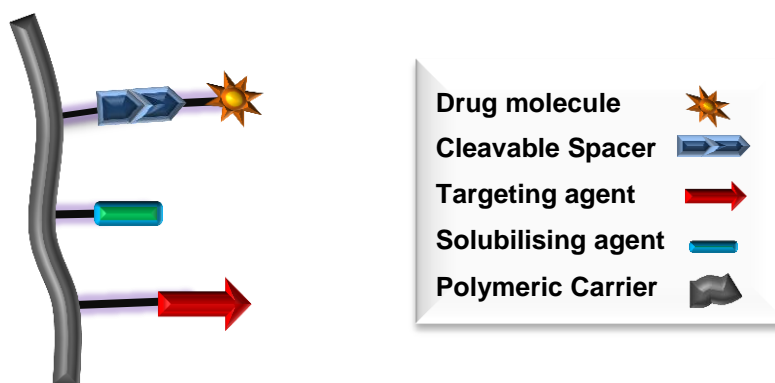


**Figure 1-13 Model of polymeric carrier**

Bio-conjugation is a strategy particularly encouraging for increasing the efficiency of injectable drugs since it allows to obtain new chemical entities with special chemical-physical and biological characteristics that positively influence the pharmacokinetics and pharmacodynamics of the drug itself<sup>30</sup>.

However, there are still many hurdles to overcome before succeeding in finding the ideal ligand for the polymer-drug conjugate.

One of the objectives to be attained is the improvement of the chemical bond so that the activation and coupling does not affect the properties of the polymer, and that the active site of the drug remains available.

A further challenge is to obtain well characterised polymers with low polydispersity.

Finally, there is a need to develop appropriate analytical methods for the characterisation of the conjugate and its components.

Although bio-conjugation is challenging, it is still considered as a key method with numerous benefits, among which:

- The disguise of the antigenic sites of the drug resulting in a reduced uptake by the immune system; especially in case protein drugs,
- The greater plasma half-life and the reduction of the renal excretion due to the high hydrodynamic volume;
- The greater solubility of drugs in water normally poorly soluble if used alone.
- The specific targeting of the drug in the tumour tissue due to the presence of targeting agents.
- The accumulation of the drug in the tumour tissue by passive targeting.
- The likelihood of less frequent administrations, and at lower doses reducing systemic toxicity.

The main advantage is still the ability to direct and release the drug only to the target site, exploiting the characteristics of the tumour tissue and the polymer-drug linkage or spacer.

Many polymer-drug conjugates are currently in clinical trial at various phases. As mentioned earlier, PK1 was among the first to be tested on humans, where HPMA is used as a carrier for the anti-tumour drug doxorubicin. Studies showed that the bio-conjugation permitted an increase of up to five times the maximum tolerated dose of doxorubicin alone, without presenting phenomena of cardiotoxicity, which appears to be the most harmful side effect of this drug<sup>31</sup>.

The same polymer was further modified with the introduction of galactosamine, a selective ligand for the hepatic asialoglycoprotein, in order to obtain a liver targeting. The polymer obtained named PK2 also entered clinical trials. It confirmed an accumulation capacity in the hepatic tumour cells, up to 50 times greater than that of the free drug<sup>32</sup>. However, it was evidenced that the bio-conjugate ligand was not selective for cancer cells but amassed equally in healthy hepatocytes. Other bio-conjugate were synthesised to increase the solubility of poorly soluble drugs such as paclitaxel and camptothecin. The derivatives of these drugs conjugated to HPMA have revealed issues related to the

stability of the spacer between the polymer and the drug, As a result, the polymer released the drug into the bloodstream, result of a too fast kinetic of hydrolysis of the ester bond, causing record phenomena of neurotoxicity, attributable to the circulation of the paclitaxel but not the conjugate<sup>33</sup>.

In a similar fashion, following Ringsdorf's model, the present project investigates the engineering and design of a new polymer-drug conjugate, involving a natural polymer, the Pullulan polysaccharide, a Cathepsin K sensitive spacer, an anti-tumour drug, Paclitaxel and a targeting agent, Alendronate.

### 1.8.1 Pullulan

Pullulan was first discovered by Bauer in 1938<sup>34</sup>. It is a neutral water-soluble polysaccharide, a random coil glucan, aerobically grown and produced extracellularly by some strains of the polymorphic yeast-like fungus *Aureobasidium pullulans* which is found commonly in the environment such as soil, wood or decaying leaf.

The biopolymer is composed of the trisaccharide maltotriose  $G_3 \alpha\text{-}(1\rightarrow4)\text{Glup-}\alpha\text{-}(1\rightarrow4)\text{Glup-}\alpha\text{-}(1\rightarrow6)\text{Glup-}$  and a small percentage of tetramer maltotetraose  $\alpha\text{-}(1\rightarrow4)\text{Glup-}\alpha\text{-}(1\rightarrow4)\text{Glup-}\alpha\text{-}(1\rightarrow4)\text{Glup-}\alpha\text{-}(1\rightarrow6)\text{Glup-}$  (maximum 7%). Therefore, pullulan possesses a molecular structure between amylose and dextran as the single polymer holds both types of glycosidic bonds.

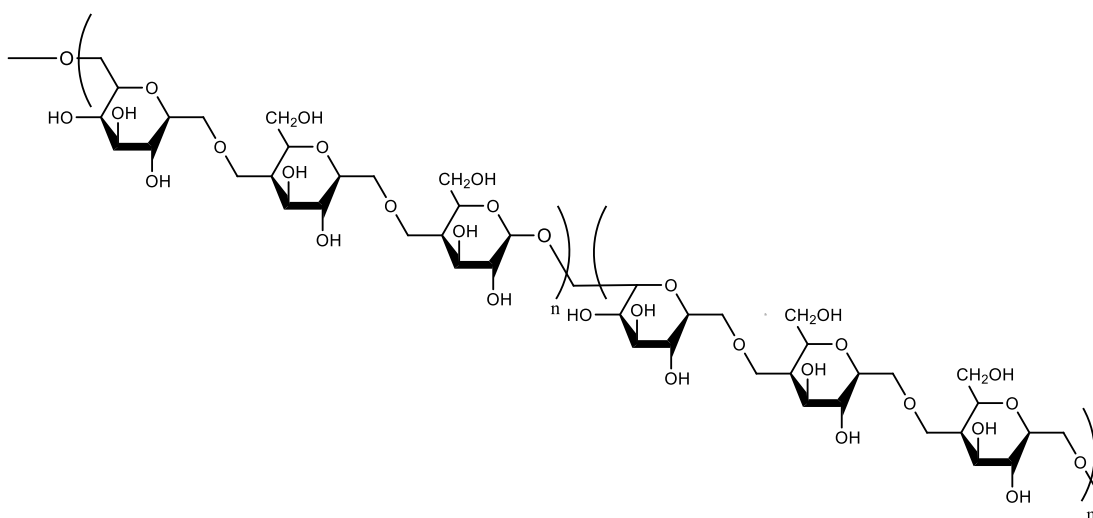


**Figure 1- 1 Pullulan**

Pullulan is soluble in water which gives stable low viscosity solutions, in respect to other polysaccharides. It decomposes at high temperature (250°C-280°C). It is only soluble in the two organic solvents dimethylformamide and dimethylsulfoxide.

Pullulan number-average molecular weight ( $M_n$ ) is about 100-200kDa and the weight – average ( $M_w$ ) between 362-480kDa. The polydispersity ( $M_w/M_n$ ) is frequently reported as being between 2.1 and 4.1, significantly lower than other common hexo-polysaccharides such as amylose and dextran.

The polysaccharide chain contains hydroxyl groups in position 2,3 and 4 which all possess a different chemical reactivity. Its non-toxic, non-immunogenic, non-mutagenic and non-carcinogenic properties make it an ideal candidate for numerous medical or biomedical applications including polymer therapeutics, gene delivery and tissue engineering<sup>35</sup>.

The biocompatibility of the polymer was confirmed by some studies on human fibroblast. After prolonged incubation periods with high concentrations of pullulan nanoparticles, no significant decline of the cellular vitality or morphological variations nor interferences with cell adhesion could be observed<sup>36</sup>. The adhesion is mediated by the interactions between surface proteins such as integrin, and proteins of the extracellular matrix (or the ones present on the surface of other cells or particles). The test of cell adhesion is of crucial importance in the growth, migration, differentiation, survival and organisation of tissues, thus, it is fundamental to make sure that the carrier is not responsible of such interferences or of other kinds of inflammatory phenomena.

As for many other polysaccharides, after intravenous administration pullulan is disseminated mainly to liver. Biodistribution studies in rats showed that the asialoglycoprotein receptor (ASGPR) contributes in a crucial way to the liver distribution. The inhibition of such receptor reduces the connection and the internalisation of the polymer at the level of the liver parenchyma. On the base of such observations, it can be thought of the use of pullulan as a potential passive carrier or active one via indirect endocytosis via receptors for the delivery to the liver. However, pullulan uptake is achieved via a specific path of recognition resulting in a high sensitivity towards the stereo chemical configuration of the molecule and to the position of the hydroxyl groups in the pyranose unit. Consequently, structural alterations can alter significantly the behaviour of the polymer.

Kaneo et al. proved that pullulan strongly binds to the asialoglycoprotein receptors expressed on the sinusoidal surface of hepatocytes<sup>37</sup>.

Pullulan accumulates in the liver in a higher amount than other water soluble polymers and is widely used for targeting gene/drug in the liver. In the treatment of hepatic C virus induced liver disease, interferons (IFN) are commonly used, however, they are clinically insufficient. Suginosita et al developed a method to target IFN to liver by complexation with modified pullulan DTPA12. They noticed an enhanced activity of the IFN from IFN-DTPA-pullulan conjugate in respect to the free IFN<sup>38</sup>.



In recent years, polysaccharides play an important role in the development of drug delivery systems for tumour targeting. Researchers have shown an increased interest in using pullulan for this application. A few examples include the self-assembly of hydrophobised pullulan, pH sensitive modified pullulan nanoparticles or else, anionic or amphiphilic microparticles.

Nogusa H et *al.* showed that the carboxymethylation of pullulan introduces negative charges onto the polysaccharide, leaving a derivative with low affinity for asiaglycoprotein unlike the native pullulan. Consequently, the liver uptake of pullulan decreased by more than a hundred fold. This property was exploited in the field of chemotherapy; for example, the anti-tumour agent Doxorubicin has been conjugated to the modified pullulan via a peptide linker. The authors found the conjugated drug was more efficient on solid tumours than the free drug<sup>39</sup>.

Other research focuses on the modification of pullulan to render it hydrophobic. The new material can then self assemble to form nanoparticles.

### 1.8.2 Polyethylene glycol

Polyethylene glycol (PEG) is the product of polymerisation of ethylene oxide by ring opening polymerisation. The polymer is ordinarily prepared by anionic polymerisation, The polymerisation occurs in three steps including an initiation steps which involves a nucleophilic attack of a hydroxide ion on the epoxide ring, a propagation step by epoxide addition and a termination step.

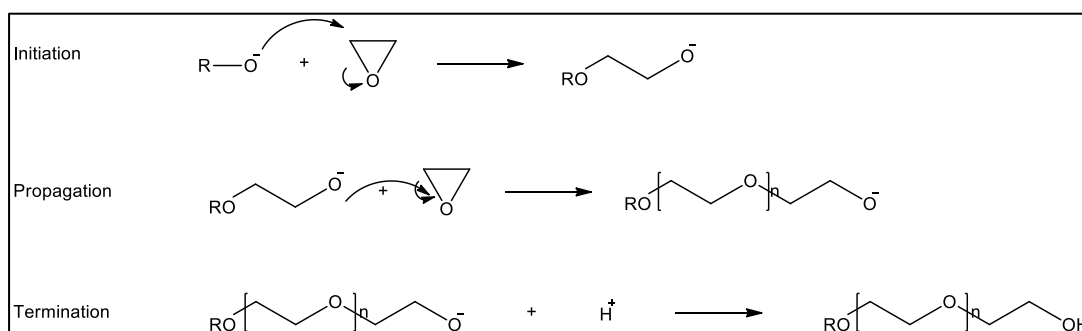


**Figure 1-14 Synthesis of polyethylene glycol.**

PEGs are often functionalised in order to increase their reactivity towards biomolecules. For example, the conjugation with amino acids will use a PEG-epoxide, PEG aldehyde, or PEG succinidyl. Molecules bearing hydroxyl groups will react with PEG-NHS or PEG nitrophenyl chloroformate.

A large number of derivatives of PEG have been developed to give chemical groups with different reactivity. PEGs have several applications in drug development, they are used for enhancing the load of low-molecular weight drugs with reduced biological activity or increase the solubility of a drug in the physiological environment as it has got unique solvation properties. PEG conveys properties to conjugates such as biocompatibility, anti-immunogenicity, and antigenicity.

The alcohol function of PEG is poorly reactive under the conditions needed for bioconjugation. Consequently, the polymer must be functionalised to increase its reactivity, introducing epoxide, aldehyde, thiol or succinimidyl functions for the conjugation of amino groups or N-hydroxysuccinimide and *p*-nitrophenyl chloroformate for the coupling with hydroxyl groups for example.

Bifunctional PEG can also contain protective groups such as t-Boc and Fmoc to prevent the reaction between the active ester and the amino group present onto the same PEG chain but also to ensure selective modifications of PEG. Bifunctional PEGs can also be used for crosslinking reactions. t-Boc and Fmoc are easily removed with trifluoroacetic acid and the mild base piperidine respectively.

Polyethylene glycol is widely used for pharmaceutical applications to obtain bioconjugates with new chemical and physical characteristics, and the enhancement of pharmacokinetic and pharmacodynamics of drugs without drastically altering the biological activity. Active PEGylated molecules gain new properties such as the increase of plasma half-life, the reduction of renal excretion and biodistribution for the increase of the molecular weight, the reduction of the hydrolytic and enzymatic degradation, the reduction of uptake into the reticulo-endothelial system, the increased solubility in water and the reduction of immunogenicity and antigenicity.

The PEGylation was initially used to conjugate peptides and proteins, but issues of stability occurred. Mild chemistry is needed so not to disable or denature the protein<sup>40</sup>.

Several conjugates in both clinical trials and market are currently available including:

- ADAGEN: PEG and bovine conjugate adenosine deaminase is promoted by Enzon, Inc., for the treatment of combined immunodeficiency syndrome
- PEG-INTRON: PEG 12000 Da and  $\alpha,2b$ -interferon conjugate ( $\alpha$ -IFN) to treat hepatitis C.

More recently PEG was conjugated with insulin, superoxide dismutase, interleukin- 2, haemoglobin.

PEGylation has also been widely used in cancer therapy in order to target the drug specifically to tumour tissue, preventing the distribution to other areas and normal tissues, avoiding side effects. ONCOSPAR ® conjugate between PEG and L-asparaginase is an example, used in the treatment of cancer Acute lymphocytic leukemia;

Other examples of PEG conjugated with anticancer drugs include camptothecin, an anti-tumour alkaloid whose solubility is increased by binding to the polymer<sup>41</sup>, or doxorubicin, which substantially reduced the cardio toxic effects.

AraC, methotrexate and taxanes PEG conjugates are currently being developed in order to target the antineoplastic agent in the tumour tissue, consequently reducing systemic toxicity and improving the pharmacodynamic and pharmacokinetic profiles.

PEGylation of antiviral, antimalarial and anti-AIDS drugs are also being studied to improve their pharmacological properties.

PEG is also used for other applications than pharmacological ones. Its very flexibility, its strong ability to coordinate water molecules and its high hydrodynamic volume is exploited in the "two phases partitioning" purification technique.

Furthermore, PEG is used for protein or nucleic acid precipitation and for peptide and oligonucleide synthesis in liquid or solid phase. The polymer is also very present in the field of cosmetics.

In recent years, it has been widely used in the pharmaceutical industry for the preparation of drug delivery systems such as liposomes, nanoparticles, nano-and microspheres, dendrimers and hydrogels and for the preparation of prodrugs by bioconjugation with peptides, proteins or low molecular weight drugs.

The delivery of biologically active molecules using various types of polymer systems has many advantages including a less frequent dosing, lower doses necessary, and being below the minimum toxic concentration. Using PEG allows the protection of the drug from inactivation resulting in prolonged half-life.

### 1.8.3 Paclitaxel

Paclitaxel, also known as Taxol, is extracted from the bark of the Pacific Yew tree (*Taxus brevifolia*), and is one of the main effective anti tumoural drug used to treat various solid tumours such as in head and neck human carcinomas, AIDS-related Kaposi's carcinoma as well as lung, metastatic breast and advanced ovarian cancers.

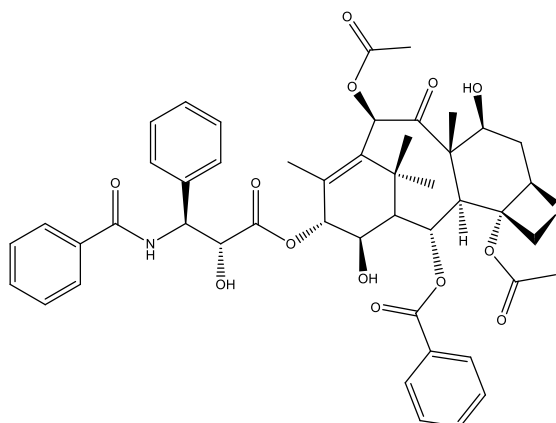


Figure 1-15 Paclitaxel

The paclitaxel structure is composed of a tetracyclic core, an eight-membered ring, a four-membered ring and two six membered rings. Several functional groups are attached to this skeleton, including a benzoyl group, particularly essential for maintaining the molecule's bioactivity. Other functional groups, present on paclitaxel's side chain are also crucial for its anti-tumour activity and particularly an amide-acyl group at the end of the chain. Due to this structure, paclitaxel is a particularly hydrophobic molecule (solubility in water  $1\mu\text{g}\cdot\text{ml}^{-1}$ ).

Paclitaxel is a known cytotoxic agent used in anti-tumour therapy, alone or in association with cis-platinum, in affected patients from ovarian carcinoma, or like medicine of second choice in the breast cancer when not responding to other treatments. It is also indicated treatment for pulmonary carcinoma and sarcoma of Kaposi AIDS-correlated.

The biological activity of taxols is attributable to the specific and stoichiometric connection to tubules, constituent protein of the microtubule skeleton. Microtubules are cellular components involved in the correct separation of the chromosomes during cellular division.

When paclitaxel binds with tubulin, it encourages the polymerisation and stabilises the micro tubular structure, modifying a normal equilibrium. A stabilised cell with microtubule undergoes a programmed process of cellular death or apoptosis.

An albumin bound paclitaxel (named Abraxane®), is actually used clinically. This alternative formulation where paclitaxel is bound to albumin nano-particles is formulated with Cremophor EL which leads to numerous side effects of the drug including reactions of hypersensitivity, neurotoxicity and nephrotoxicity. These effects are sometimes very serious and in some cases, a preventive medication with corticosteroids and antihistaminic is necessary.

In order to overcome these side effects, researchers concentrate on developing new drug delivery systems which would increase the solubility of paclitaxel and even target the drug to the tumour tissues.

The intravenous administration of the medicine requires long times and slow flow. Recent studies seem to confirm a reduction of the efficiency of the anti-tumour drug due to the presence of the Cremophor EL. For these reasons, a special attention is drawn to the development of alternative drug delivery systems, Cremophor-free. Among these, can be included the use of liposomes, cyclodextrin, micro emulsions, microspheres or polymeric nanoparticles.

Such systems are used not only to increase the solubility of the medicine, but also to target the drug to the tumour. Restricted delivery of paclitaxel would give sustained drug exposure to tumour cells and enhance the tumour penetration of cytotoxic agents and decrease the rate of replication of tumour cells.

Targeting chemotherapeutics delivery to the tumour site is also thought to enhance the chemo responsiveness by exposing tumours and adjacent metastases to high drug concentrations at the same time as reducing its systemic exposures.

Encouraging results were obtained for chemically modified paclitaxel (prodrugs) incorporated into lipidic systems using acid folic as targeting agent. Liposomes have been also synthesised using folic acid, offering a greater half-life with respect to the traditional carriers. The cytotoxicity was four times superior with respect to the same liposomes without folic acid.

Other polymeric micelles having an average diameter of 130 nm have been achieved using the copolymer (NIPAAm-co-DMAAm)-b-PLGA, in which a large amount of paclitaxel was physically loaded, ensuring the same sustained release<sup>42</sup>. Similar features were observed for micellar aggregates based on triblock copolymer-PLA-PEG-PLA synthesised by ring opening polymerisation at different molar ratios of ethylene glycol/lactic acid<sup>43</sup>. Other micellar systems based on low molecular weight diblock copolymer mPEG-block-poly(D,L-lactide) maintained a comparable cytotoxicity to the free drug on a MCF-7 cell line. However, in vivo bio distribution assays showed greater drug levels, from 2 to 3 times higher in the liver, kidney, spleen, lung and tumour tissue<sup>44</sup>.

A micellar type system was also developed by preparing immune-micelle of PEG-phospholipids, chemically modified by covalent binding with specific monoclonal antibodies capable of recognising a wide range of tumour cells and showed that these systems increase the cytotoxicity<sup>45</sup>.

Among the drug delivery systems for paclitaxel based on polysaccharides, the most encouraging ones were obtained by using amphiphilic derivatives of chitosan such as the conjugate N-octyl-O-sulfate chitosan micellar system, able to solubilise up to 25% by weight of paclitaxel<sup>46</sup>, the derivative N-mPEG-N-octyl-O-sulfate-chitosan which reached 40% loading by weight and the N-lauryl-carboxymethyl chitosan conjugate, which led to a 1000 fold increase solubility in an aqueous environment, ensuring the in vitro cytotoxic activity<sup>47</sup>.

Hydrophobised glycol-chitosan with 5 $\beta$ -cholanic acid has also been developed to produce nanoparticles of 400 nm in diameter, able to upload up to 10% by weight of paclitaxel. The nanoparticles were stable in PBS for up to 10 days. It was determined that 50% of the drug was released in the first 24 h, and stabilised progressively up to 80% over the next 10 days. However in vitro cytotoxicity studies show a lower efficiency of the micellar systems with respect to commercial preparation with Cremophor<sup>48</sup>.

#### **1.8.4 Bisphosphonates and Alendronate**

The “seed and soil” Paget’s theory of bone metastases describes the travel of metastatic cells in all body once entered in the bloodstream and their attachment only in favourable environments, bone marrow being one of those. Once in the bone, bone anabolism and catabolism causes patients severe bone pain and increases mortality.

Small drug molecules are often used as osteoclast target for the treatment of these metastases such as Cat K inhibitors, Reveromycin or bisphosphonates (BPs).

As bone metastases progress, hydroxyapatite (HAp) is exposed to blood and constitutes a target for BP attachment. This characteristic can also be utilised to deliver high drug loads specifically to disease tissue. Macromolecular therapeutics are able to travel into the tissue due to vascular pressure and be retained into the tumour tissue due to the poor tumour vasculature.

Alendronate belongs to the family of bisphosphonates which constitutes the most important category of anti-resorptive agents.

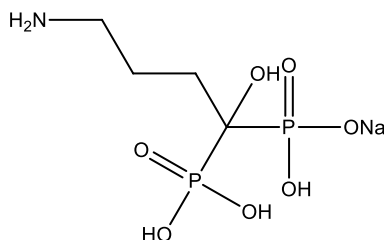


**Figure 1-16 Sodium alendronate**

This class of drug is characterised by a high affinity for bone and hydroxyapatite.

In the 1960s, original investigations revealed that inorganic pyrophosphates (IPP) were capable of inhibiting calcification by binding to hydroxyapatite crystals, suggesting that regulation of IPP levels could be the mechanism by which bone mineralization is regulated.

Bisphosphonates are analogous to inorganic pyrophosphate in which the hydrolysable oxygen bridge between the two phosphate atoms has been replaced by a more stable carbon with various side chains to give a high affinity to bone and retain much of the binding affinity after conjugation to other molecules and carriers.

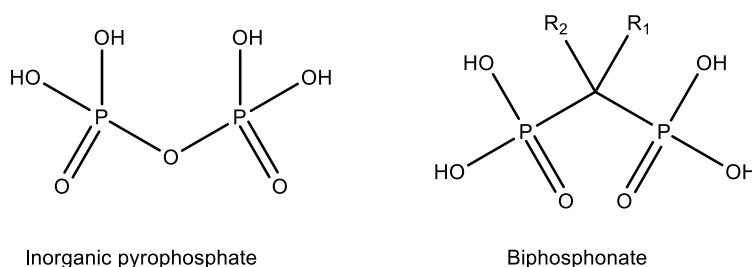


**Figure 1-17 Comparison inorganic pyrophosphate and bisphosphonate**

Bisphosphonates are preferably assimilated into sites of active bone remodelling, as it normally takes place in disorders characterized by accelerated skeletal turnover. The free

bisphosphonate, not retained by the skeleton, is rapidly cleared from the circulation by renal excretion. Moreover, bisphosphonates inhibit hydroxyapatite breakdown and efficiently prevent bone from resorption<sup>49</sup>.

Bisphosphonates increase the calcium balance and the mineral density of bones. They are used in the treatment of metabolic bone diseases, including tumour-associated osteolysis, hypercalcemia, Paget's disease and osteoporosis. The potency of inhibiting bone resorption is very variable between different bisphosphonates and can increase up to 10 000 fold.

They are resistant to enzymatic hydrolysis due to the carbon atom in their structure. The composition of their derivatives induces diverse cellular and molecular mechanisms; their activity varies from one another depending on the length and substitution of the aliphatic carbon atom. Modifications of the R2 side chain demonstrates that the presence of a nitrogen atom onto the alkyl chain, as in alendronate, ibandronate or pamidronate, increases the anti-resorptive potency of the drug (10 to 1000 fold) in respect to the earlier generation of bisphosphonates such as etidronate (Figure 1-18<sup>50</sup>).

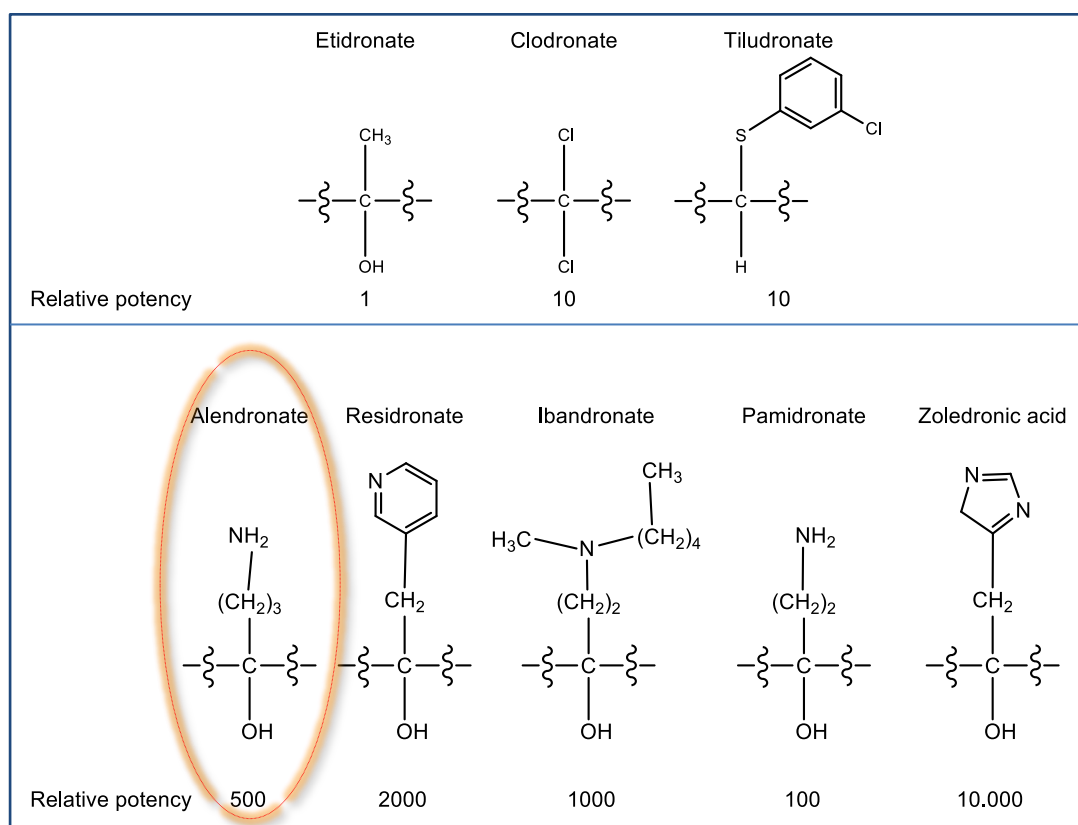


**Figure 1-18 Bisphosphonate structures and approximate relative potencies for osteoclast inhibition.**

The more the nitrogen atom on the  $R_2$  chain is distant from the P-C-P group, the greater is the potency of the bisphosphonate (Figure 1-19).

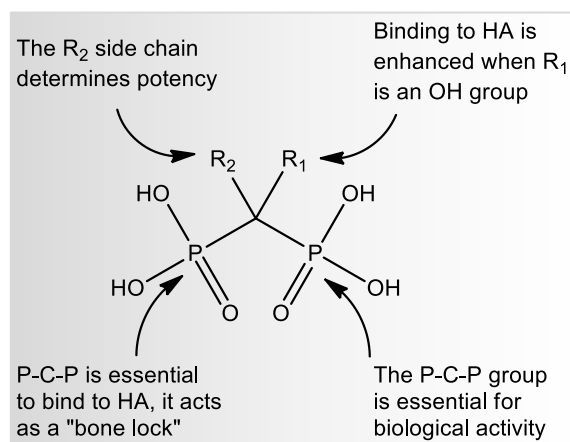


**Figure 1-19 General features of bisphosphonates**

If an OH group in  $R_1$  is replaced by a methyl group, the bone activity is noticeably reduced as well as the anti-resorptive activity.

The increasing antiresorptive activity of common bisphosphonate is as follow: etidronate < clodronate < pamidronate < alendronate < risedronate

In recent years, the amino bisphosphonate alendronate (ALN) has arisen as an efficient therapeutic method for the prevention of skeletal troubles produced by bone metastases. Similar to all bisphosphonates (BPs), it exhibits a remarkably high affinity to the bone-mineral hydroxyapatite (HAp). ALN is approved by the FDA for the treatment of bone related diseases and cancer connected hypercalcaemia.

Considerable efforts have been made to conjugate BPs with non-specific bone therapeutic agents in order to obtain osteotropy because of their high bone affinity. ALN was successfully conjugated with polymer-drug delivery systems.

Recent works have shown that both low doses ALN and PTX may selectively inhibit endothelial functions important to angiogenesis, phenomenon now recognized as an important mechanism in tumour progression and metastasis formation.

This high affinity for bone mineral allows bisphosphonates to reach a high local concentration throughout the entire skeleton. Consequently, bisphosphonates have come to be the primary therapy for skeletal disorders characterised by extreme or imbalanced skeletal remodelling, in which osteoclast and osteoblast activities are not strongly united, leading to excessive osteoclast-mediated bone resorption.



### 1.8.5 Cathepsin K

Cathepsins, found in various types of cells, break apart other proteins by hydrolysis of amide bonds and belong to papain-like cysteine proteases. The twelve constituents of this enzyme family are distinguished by their structure, catalytic mechanism and which molecule they cleave, i.e. by their substrate specificities. They include plant enzymes (papain and bromelain), parasite proteases (cruzipain and falcipain) and human cysteine Cathepsins (B, H, L, S, C, K, O, F, and V, X, W)<sup>51</sup>.

Most of human Cathepsins are activated in lysosomes where pH is low. Their main localisation in the endosomal/lysosomal compartment affords cysteine Cathepsins with optimum conditions for substrate cleavage. Together with their physiological functions, they are significantly involved in several pathological disorders. This often implicates relocation from their usually lysosomal compartment to extracellular sites. Amplified expression of cysteine Cathepsin arises often in premalignant or early lesions. For example Cathepsin B is over-expressed in Barrett's oesophagus and stage I oesophageal tumours or Cathepsin H in lymph node-negative lung tumours. Bio-responsive release is achieved by insertion of a spacer that is responsive to a disease-specific trigger. Therefore, a substantial and homogeneous expression at the diseased site is required, with low or no activity in normal tissues or serum.

In the case of breast cancer bone metastasis, an over-expressed enzyme is Cathepsin K, highly present at osteolytic lesions and site of active bone resorption.

Cathepsin K works extracellularly subsequent to the secretion of osteoclasts, leading to destruction of bone matrix through type I collagen degradation, a known substrate of Cathepsin K containing multiple glycine-proline sequences<sup>52</sup>.

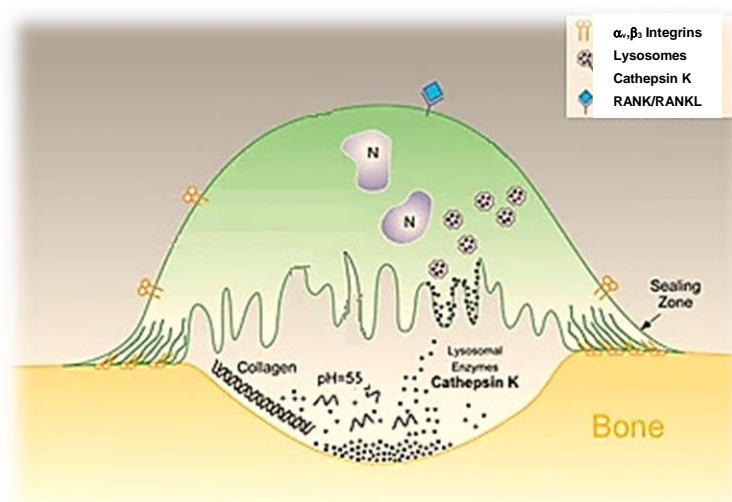


**Figure 1-20 Osteoclast morphology**

The highly overexpressed Cathepsin K in osteoclasts has also been found in the serum of Gaucher patients, in lung epithelial cells, in cancer prostate cells and in macrophages. Beside their physiological function by protein degradation/turnover in endosomal/lysosomal system, they also are involved in pathological processes such as Alzheimer's disease, tumour invasion, muscular dystrophy, osteoporosis or rheumatoid arthritis.

# MATERIALS AND METHODS

---



## 2. Materials and methods

### 1.9 Reagents

- Fmoc-proline, Fmoc-glycine, Fmoc-Norceuline-Wang resin (Fmoc-Nle-Wang-R) were procured by Bachem (Bubendorf, Switzerland)
- HOBt and HBTU were acquired from ABI S.r.l (Milano, Italy)
- Reactors for solid phase peptide synthesis (SPPS) were purchased from Grace Davison Discovery Sciences (Columbia, USA)
- Cathepsin K was obtained from Calbochem, (Darmstadt, Germany)
- Alendronate was acquired from LTBio (Shanghai, China) and alendronic acid from Surfactis Technologies (Angers, France)
- Paclitaxel was obtained from LC Laboratories (Woburn, USA)
- Pullulan and all other chemical reagents, including salts, silica gel, trifluoro acetic acid, coupling agents and solvents, were purchased from Sigma-Aldrich (Saint Louis, USA).
- Alpha-t-Butyloxycarbonylamino-omega-carboxy succinimidyl ester poly(ethylene glycol) (tBoc-NH-PEG3000-NHS, 3000Da) was purchased from Iris biotech (Marktredwitz, Germany) or from JenKem Technology USA (Allen, USA)
- Deuterated solvents used for NMR spectroscopy analysis, including chloroform, water and dimethylsulfoxide, were obtained from Sigma Aldrich (Saint Louis, USA)
- All solvents of appropriate purity (HPLC or higher degree of purity) were obtained from Sigma Aldrich (Saint Louis, USA), VWR (Milan, Italy) or Carlo Erba (Milano, Italy).
- All reactions requiring anhydrous conditions were performed under N<sub>2</sub> atmosphere.
- Chemicals and solvents were analytical grade reagents and anhydrous solvents were obtained by distillation and conservation on molecular sieves.

### **1.10 Cell culture**

- Dubelcco's modified Eagle's medium (DMEM), RPMI 1640, Fetal Bovone Serum (FBS), Penicilin, Streptomycin, Nystatin, L-Glutamine, Hepes buffer, Sodium pyruvate, and fibronectin were procured by Biological Industries Ltd (Kibbutz Beit Haemek, Israel). growth factor reduced medium EBM-2, and EGM-2 medium was purchased from Cambrex (Walkersville, MD, USA). Matrigel was from BD Biosciences (USA).
  
- MTT was purchased from Sigma Aldrich (aint Louis, USA)
- MDA-MB231 human mammary adenocarcinoma, SAOS-2 osteosarcoma and 4T1 murine adenocarcinoma cell lines were purchased from American Type Culture Collection (ATCC). Human Umbilical Vein endothelial cells (HUVEC) were obtained from Cambrex (Walkersville, USA).

## **1.11 Instruments**

- Ultraviolet-Visible Spectrophotometry measurements were performed using a UV-Vis  $\lambda$ 25 Perkin Elmer (Norwalk, CT, USA) apparatus.
- Spectrofluorimetric analyses were performed using a FP 6500 Jasco Spectrofluorimeter (Tokyo, Japan).
- A plate reader was used for 96 well plates using the Microplate Autoreader (mod. EL311SK) from Biotek instrument Inc. (Highland, Vermont, USA)
- A Fourier Transform Infrared spectroscopy instrument FT/IR-6000 series from Jasco (Tokyo, Japan) was used. Samples were dispersed in KBr pellets and recorded with an instrumental resolution of  $2\text{ cm}^{-1}$  and an average of 256 scans on the FTIR spectrometer, with a resolution of  $3\text{ cm}^{-1}$ .
- A Jasco HPLC equipped with two P1580 pumps, a UV-1575 detector, a Hercule Lite fornito recorder from JMBS, and a RP Phenomenex Luna C18 250x4.60 mm column.
- Solid Phase Peptide Synthesis (SPPS) was performed using a PS3 peptide synthesiser from Protein Technologies Inc. (Tucson, USA)
- Freeze drying was performed on a Hetosic HETO Lab Equipment freeze drier or Speed Vac, Vacuum Centrifuge HETO Lab Equipment apparatus (Birkerod, Denmark)
- Solvents were removed using a R114 BÜCHI Labortechnik AG rotavapor (Postfach, Switzerland)
- pH of solutions were measured using a Seven Easy S20-K Mettler Toledo pHmeter with Mettler Toledo Inlab 413 electrode (Schwerzenbach, Switzerland)
- Aldehyde titrations were performed using a Fisherbrand Hydrus600 pHmeter (Illkirch, France)
- Centrifugation was achieved using a CENTRIKON T-42K Kontron Instruments, Z300 Hemle (Eching , Germany) and with a ALC micro centrifuge 4214 from ALC international (Cologno Monzese, Italy)

- The NMR spectroscopy analyses were performed using a Spectrospin AMX 300 MHz Bruker NMR instrument (Billerica, MA, USA).
- The ESI-MS measurements were achieved using an Applied Biosystem Mariner ESI-TOF mass spectrometer (Monza, MI, Italy).
- Ultra-filtrations were carried out using an Amicon system (Denver, MA, USA) equipped with an YM1 membrane (cut-off 10.000 Da) and an Amicon ultraFree-MC Millipore with a 1kDa or 30kDa cut-off.
- Buffer solutions were filtered using a Millipore (Bendford, MA, USA) fritted glassware with a 0.22  $\mu\text{m}$  filter
- An ultrasonic bath from Branson Ultrasonics (Danbury, USA) was used to sonicate buffers and eluents prior to chromatographic analysis.
- The size of polymeric nanoparticles was estimated by Dynamic Light Scattering using a Zetasizer NanoZS instrument (Malvern Instruments Ltd, UK).
- TLC plates used were covered with silica gel (60ALUGRAM SIL/UV254, Sigma Aldrich, Saint Louis, USA) and were eluted using the solvents mixtures indicated. Products were detected using a UV lamp at 254nm.
- Dialysis tubes used for drug release studies and purifications were made of regenerated cellulose (Visking, cut-off 3.5kDa and 14kDa) and supplied by Delchimica Scientific Glassware (Naples, Italy).
- Endothelial cells and 4T1 cells were counted using Coulter Counter Cell and Particle Counters, Coulter Z series from Beckman Coulter Inc. (Highland, Vermont, USA).

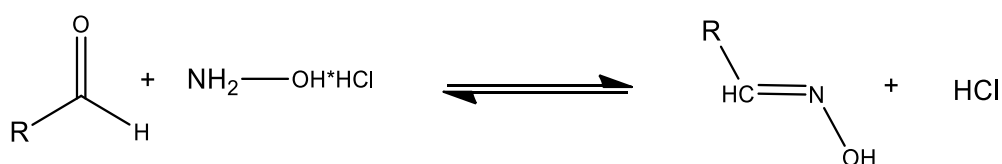


## 1.12 Methods

### 1.12.1 Analytical methods

#### 1.12.1.1 Determination of aldehyde groups

Aldehyde groups react instantaneously with hydroxyl amine to form an oxime and free a molecule of hydrochloric acid. This later can be titrated using sodium hydroxide (NaOH, 0.1mol.l-1) and the quantity of aldehyde groups can be deduced from the titration (Scheme 2-1).



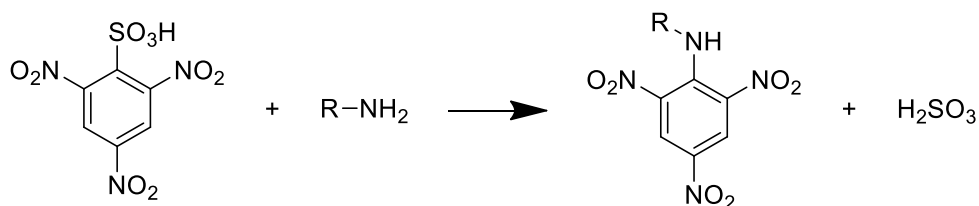
**Scheme 2-1 Titration of aldehydes by hydroxylamine**

Protonation induces an increase of electrophilicity of the carbon-oxygen double bond of the carbonyl, which encourages the nucleophilic attack of the hydroxylamine with release of water from a tetrahedral intermediate to form an oxime.

In the case of using hydroxylamine chloride, hydrochloric acid is released and can easily be titrated using a standard solution of sodium hydroxide or other alkali standards to quantify the number of carbonyl groups in the compound. The reaction of oximation is equilibrium and it must be remembered that the reaction does not go to completion for all carbonyl groups so that a fraction of the compound remains in carbonyl form. The presence of an excess of hydroxylammonium hydrochloride, which is also an acid, could cause a lack of precision in the determination point. For this reason, a potentiometric titration is more suitable to obtain an accurate result.

#### 1.12.1.2 Determination of primary amine content by Snyder test

The quantification of primary amino groups was determined using the trinitrobenzenesulfonic acid (TNBS) also referred as Snyder test.



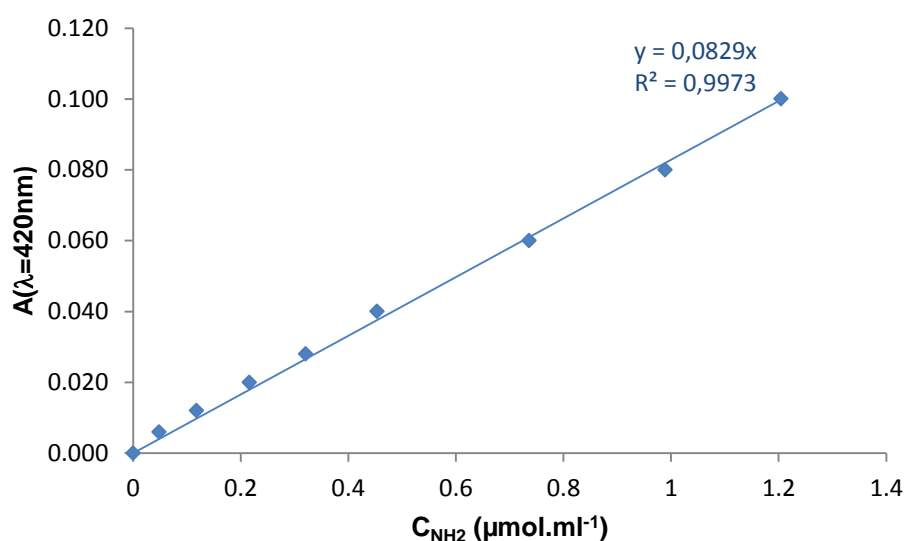
**Scheme 2-2 Titration of primary amine group containing compounds by Snyder colorimetric assay**

TNBS reaction with amine is preferred over its reaction with hydroxyl groups if under low ionic strength and temperature conditions and a pH value, 0.5 unit below the pKa amine value. Therefore, the spectrophotometric quantification of amino groups can be realised in aqueous solution due to the slow rate of reaction of TNBS with hydroxide ions in comparison with amino groups (two to three times more rapid than with hydroxide ions).

A calibration curve using the simplest of dipeptides glycyl-glycine ( $\text{H}_2\text{Ngly-glyOH}$ ) was first plotted as reference to deduce the amount of primary amines in primary amine containing compounds. A gly-gly solution ( $0.4\text{mmol.l}^{-1}$ ) was prepared in milliQ water.

Briefly, to some vials, were added  $\text{NH}_2\text{gly-glyOH}$  various quantities ranging from 0 to  $250\mu\text{l}$ . Subsequently, a borate buffer solution at pH 9.3 (acid boric,  $0.1\text{mol.l}^{-1}$ ) was added to obtain a volume of  $970\mu\text{l}$ . Finally  $30\mu\text{l}$  TNBS solution in water ( $1\%_{\text{w/w}}$ , freshly prepared to avoid hydrolysis) was added to make a total volume of  $1000\mu\text{l}$ . A blank sample - not containing  $\text{NH}_2\text{gly-glyOH}$  - was prepared as reference for spectrophotometric measurements.

All mixtures were left at room temperature for 30min to allow the reaction of TNBS with  $\text{NH}_2\text{gly-glyOH}$  primary amino group. The calibration curve was drawn as a linear regression between absorbance and primary amine concentration.



**Graph 2-1 Primary amine calibration curve by Snyder test – Reference compound:  $\text{NH}_2\text{gly-glyOH}$**

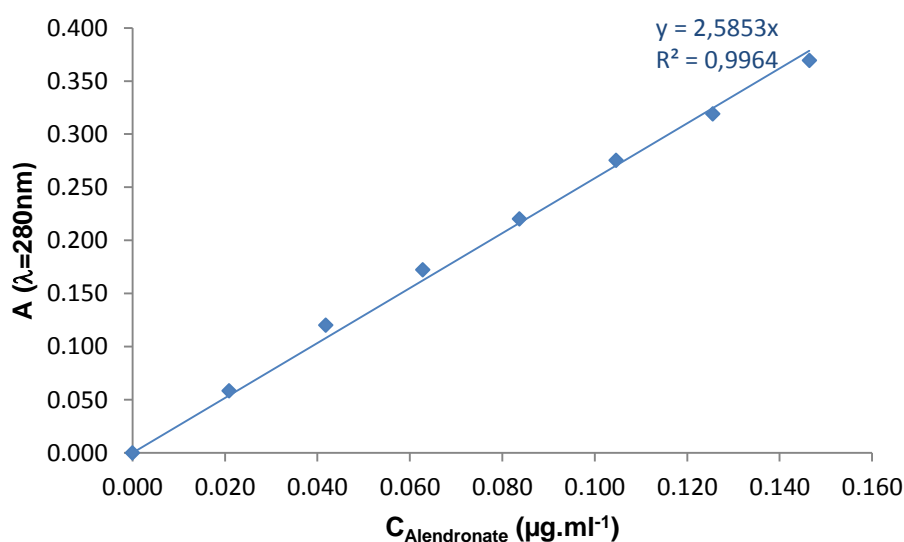
### 1.12.1.3 Determination of alendronate content by spectrophotometry

The formation of a complex between alendronate and ferric ions (Fe(III)) in perchloric acid solution ( $\text{HClO}_4$ ,  $2\text{mol.l}^{-1}$ ) allowed the determination of alendronate content in all derivatives prepared with the bisphosphonate.

A calibration curve was obtained by using a series of alendronate solution at concentration varying from 0 to  $3\text{mol.l}^{-1}$ .

A ferric standard solution was made by dissolution of ferric chloride hexahydrate into an  $\text{HClO}_4$  solution ( $2\text{mol.l}^{-1}$ ). A stock solution of alendronate ( $5\text{mmol.l}^{-1}$ ) in perchloric acid ( $2\text{mol.l}^{-1}$ ) was prepared and conserved at a temperature below  $6^\circ\text{C}$ .

Standard solutions of alendronate were freshly prepared from the stock solution by suitable dilution into perchloric acid solution ( $2\text{mol.l}^{-1}$ ).



**Graph 2-2 Alendronate calibration curve by spectrophotometry**

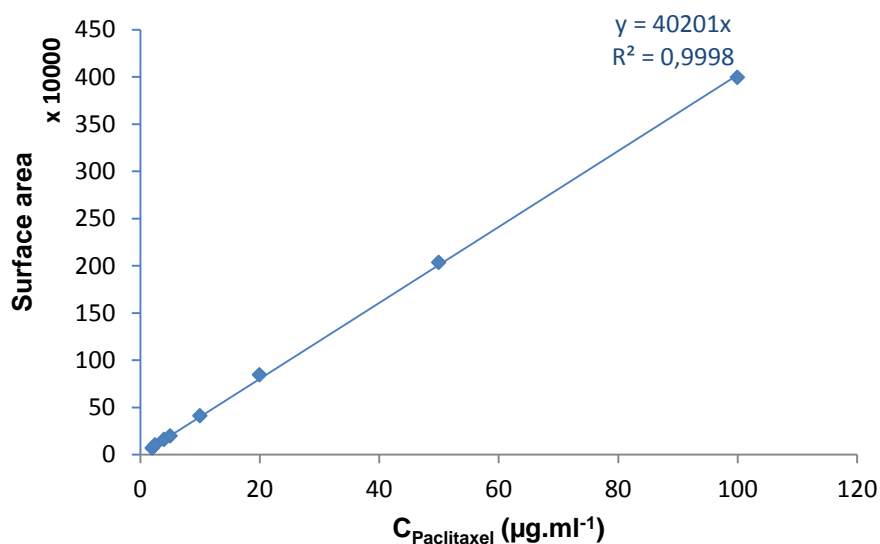
Alendronate content in conjugates was determined as follow:

Succinctly, the conjugate ( $0.1\text{ml}$ ,  $2\text{-}10\text{mg.ml}^{-1}$ ) was added to  $\text{FeCl}_3$  ( $0.1\text{ml}$ ,  $4\text{mol.l}^{-1}$ ) in  $\text{HClO}_4$  ( $0.8\text{ml}$ ,  $0.2\text{mol.l}^{-1}$ ) at room temperature to instantaneously form a complex. Absorbance was immediately read against blank, at a wavelength  $\lambda$ =of  $280\text{nm}$ .

### 1.12.1.4 Determination of paclitaxel content by Reverse Phase High Performance Liquid Chromatography (RP-HPLC)

Standard solutions ranging from  $2\mu\text{g.ml}^{-1}$  to  $100\mu\text{g.ml}^{-1}$  were prepared in acetonitrile. All solutions were centrifuged for  $5\text{min}$  at  $6000\text{rpm}$  prior to RP-HPLC analysis.

Samples were eluted in isocratic mode, using a C<sub>18</sub> type column at room temperature and a UV detector. The acetonitrile/water (55/45 vol/vol, 0.05%TFA) eluent was ran at 1ml.ml<sup>-1</sup> and paclitaxel absorbance was read at  $\lambda=227\text{nm}$  to give the following calibration graph.



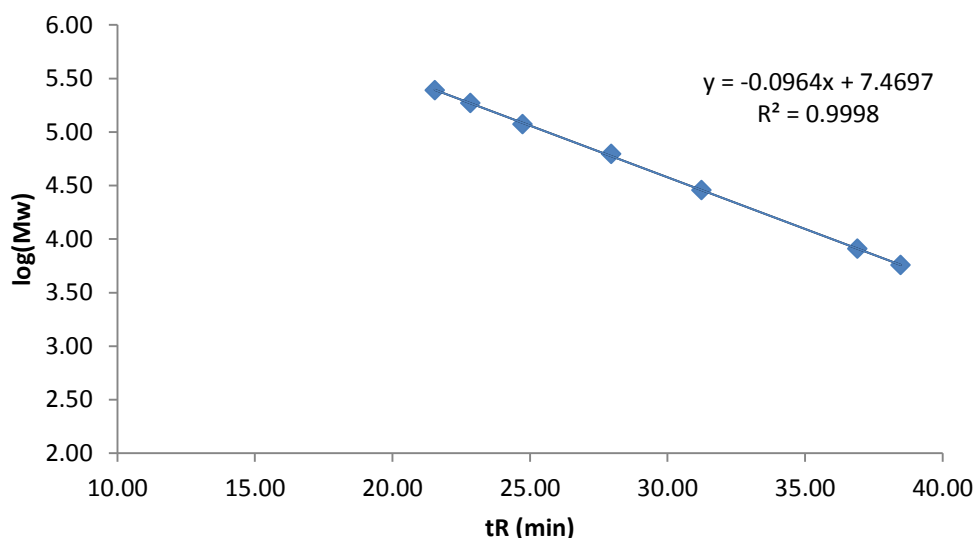
**Graph 2-3 Paclitaxel calibration curve by HPLC**

#### **1.12.1.5 Determination of pullulan Molecular Weight ( $M_w$ )**

Molecular weight ( $M_w$ ) of native, oxidised pullulan and pullulan conjugates were determined by SEC-HPLC using two columns TSK G3000SWXL and TSK G4000SWXL (7,8 X 300 mm, Tosoh) in series. The samples were eluted in isocratic mode at room temperature using a Refractive Index (RI) detector. MilliQ water was used as eluent and ran at 0.6ml.ml<sup>-1</sup>

A calibration curve was obtained employing pullulan standards of known molecular weights (270 kDa, 150 kDa, 80 kDa, 50kDa, 25 kDa, 12kDa).

The pullulan standards  $M_w$  were expressed in logarithmic scale ( $\log(M_w)$ ) and plotted against time retentions ( $t_R$ ) to give a linear calibration curve.



**Graph 2-4 Pullulan calibration curve by GPC**

Molecular weights of final polymer conjugates were determined by comparing the elution times of samples with the linear calibration curve.

#### **1.12.1.6 Determination of molecular size**

Size distributions of the polymer conjugates were determined using Dynamic Light Scattering (DLS), allowing the determination of hydrodynamic radius. Polymers were dissolved in water or acetate buffer (pH5.5) or phosphate buffer (PBS, pH7.4) at a concentration of  $1\text{mg}\cdot\text{ml}^{-1}$ .

#### **1.12.2 Synthesis**

##### **1.12.2.1 Kinetic of oxidation of pullulan**

Sodium periodate is used in the oxidation of polysaccharides by converting the free vicinal hydroxyl groups of the polymer units into aldehyde functions. The resulting modified polysaccharide becomes highly reactive towards amine<sup>12</sup>.

To a solution of native pullulan ( $M_w \sim 100$  kDa, 100mg,  $617\mu\text{mol}$  glucosidic monomer units) in ultrapure water (8.15ml), was added sodium periodate (4.3mg,  $20.4\mu\text{mol}$ ). The final solution obtained was maintained in the dark at room temperature under stirring. Sampling ( $500\mu\text{l}$ ) was performed after 30min, 1h, 2h, 3h, 4h, 6h, 20h and mannitol (10mg,  $50\mu\text{mol}$ ) was added. After 1 hour, the solution was ultra-filtered using a with 10 kDa cut-off

membrane. The determination of aldehyde content on the polysaccharide backbone was then performed using the method described previously.

### 1.12.2.2 Synthesis of 30 % oxidised pullulan (*Pullox<sub>30</sub>*)

Pullulan (500mg, 3.09mmol glucosidic monomer unit) was dissolved in milliQ water (50ml). The mixture was heated at 40°C under stirring to ease the dissolution. After cooling, sodium periodate (21.7mg, 0.102mmol) was added to the pullulan solution under stirring and left to react overnight protected from the light.

After 16h, the oxidation of the polymer was stopped using mannitol (27.7mg, 0.154mmol). Past 2h, the excess mannitol was removed from the reaction mixture by ultra-filtration using an Amicon system equipped with a 10 kDa cut-off membrane.

Once ultra-filtered, the oxidised polysaccharide was lyophilised to give a light white cotton-like solid.

For the synthesis of 95% oxidised pullulan, a ratio Pullulan glucosidic monomer:sodium Periodate of 1:0.95 was used. The procedure of synthesis remained the same.

The quantification of aldehyde groups on the oxidised pullulan chain was performed by titration as reported in the 2.3.1.1.

### 1.12.2.3 Synthesis of *Fmoc-Gly-Gly-Pro-Nle-OH* by solid phase peptide synthesis (SPPS)

The peptide synthesis was performed on a 0.5 mmol scale, using a synthesiser after setting up the reaction conditions beforehand, by manual peptide synthesis.

Wang-Nle-Fmoc resin was chosen as a solid phase matrix. It was approximately 65%<sub>n/w</sub> Nle activated. Therefore, 770mg of resin were used for the synthesis of the four amino acid oligopeptide.

Each amino acid was placed into an assigned vial, together with the HBTU and HOBt activators.

To a first vial, was added Fmoc-Proline (674.8mg, 2mmol), O-Benzotriazole-N,N,N',N'-tetramethyl-uronium-hexafluoro-phosphate (HBTU – 758.6mg, 2mmol) and N-Hydroxybenzotriazole (HOBt – 234.25mg, 2mmol) coupling agents.

To a second vial, was added Fmoc-Proline (674.8mg, 2mmol), O-Benzotriazole-N,N,N',N'-tetramethyl-uronium-hexafluoro-phosphate (HBTU – 758.6mg, 2mmol) and N-Hydroxybenzotriazole (HOBt – 234.25mg, 2mmol) coupling agents. Proline was more difficult to couple so it was chosen to perform a double coupling without deprotection in order to ensure maximum yield.

To a third vial, was added Fmoc-Glycine (594.6, 2mmol), O-Benzotriazole-N,N,N',N'-tetramethyl-uronium-hexafluoro-phosphate (HBTU – 758.6mg, 2mmol) and N-Hydroxybenzotriazole (HOBt – 234.25mg, 2mmol) coupling agents.

To a fourth vial, was added Fmoc-Glycine (594.6, 2mmol), O-Benzotriazole-N,N,N',N'-tetramethyl-uronium-hexafluoro-phosphate (HBTU – 758.6mg, 2mmol) and N-Hydroxybenzotriazole (HOBt – 234.25mg, 2mmol) coupling agents.

A deprotection cocktail was prepared, adding a 20%<sub>mol</sub> pyridine solution in 1-methyl-2-pyrrolidone (NMP (17.2g, 0.21mol) and NMP (82.4g, 0.83) into the appropriate synthesiser bottle. Finally, a coupling cocktail containing 5%<sub>mol</sub> N,N-Diisopropylethylamine (DIPEA – 4.52g, 5mol) in dimethylformaldehyde (DMF- 89.3g, 95mol) was added into a second synthesiser bottle.

The synthesiser was programmed so that it started with the deprotection of the Fmoc-Norleucine Wang resin (Fmoc-Nle-Wang) in order to free the amino acid primary amine, followed by the coupling of Fmoc-Pro. A second batch of Fmoc-Pro was added to optimise the coupling yield without preliminary deprotection of the first Fmoc-Pro batch. Successively, a Fmoc-deprotection was performed on Fmoc-Pro and the coupling of Fmoc-Gly was performed. Finally, Fmoc-Gly was deprotected and a second Fmoc-Gly, the ultimate amino acid in the sequence, was added to yield Wang-Nle-Pro-Gly-Gly-Fmoc modified resin.

#### *Isolation of the peptide from Wang resin –Analytical cleavage*

After completion of the synthesis, a small aliquot of the reaction mixture was taken from the reaction vessel and the peptide was cleaved from the resin. Before cleavage, the aliquot was washed three times with NMP, three times with DCM and three times with methanol (MeOH), corresponding to an increasing solvent hydrophobicity. Between each wash, the resin was vacuum dried. After the final wash, the resin was carefully air dried. The cleavage procedure was then performed. The Wang-NleProGlyGlyFmoc solid was left to react for 30min in the dark with a 95/5 %<sub>vol</sub> solution of trifluoroacetic acid (TFA) in water. After the peptide was extracted by filtration; the solid phase corresponding to the resin was discarded and the liquid phase containing the peptide was kept, diluted 10 times in water. After centrifugation and lyophilisation, a white/off white powder was obtained. The product was analysed by mass spectrometry (ESI-TOF, Positive mode).

#### **1.12.2.4 Synthesis of FmocGGPNlePTX**

Multiple approaches were considered for the synthesis of peptylpaclitaxel including, the two step synthesis using first N,N'-dicyclohexylcarbodiimide (DCC) coupling in presence of 4-(dimethylamino)pyridine (DMAP) catalyst, and 1-ethyl-3-(3-dimethylaminopropyl) carbodiimide (EDC) coupling in presence of DMAP. These techniques led to very poor yield and a new approach was used to include a phenyl ring between the tetrapeptide and paclitaxel. Only this new approach is reported in this chapter in the following sections.

#### 1.12.2.5 Synthesis of FmocGGPNle $\phi$ OH

To a solution at -18°C (freezer) of Fmoc-Gly-Gly-Pro-Nle (100mg, 177 $\mu$ mol) in a dioxane/THF solvent mixture (20/80%<sub>v/v</sub>, 4ml) under stirring, was added N-methylmorpholine at once (NMP, 19 $\mu$ l, 177 $\mu$ mol) and isobutylchloroformate (28 $\mu$ l, 212 $\mu$ mol). The reaction was left under stirring for 20min and 4-aminobenzyl alcohol (4-ABA, 32.7mg, 265 $\mu$ mol) was then added. The reaction was left in freezer and stirring was performed manually every 20min for 16h. Upon this time, the prodrug was filtered and the filtrate concentrated by roto evaporation to give a yellow viscous substance.

FmocT $\phi$ OH was purified by two silica column chromatographies using ethylacetate (100%) first and ethylacetate/acetone solvent mixture (20/80%<sub>v/v</sub>) then. Fractions were analysed by TLC and mass spectrometry (ESI-TOF, positive mode, acetonitrile:H<sub>2</sub>O:Formic acid 49:50:1) to collect the ones containing FmocT $\phi$ OH. After elimination of the solvents under vacuum, FmocT $\phi$ NO<sub>2</sub> was recovered as a white powder.

#### 1.12.2.6 Synthesis of FmocGGPNle $\phi$ NO<sub>2</sub>

To a solution at 0°C (ice bath) of Fmoc-Gly-Gly-Pro-Nle $\phi$ OH (113mg, 168 $\mu$ mol) in anhydrous THF (4ml) under stirring, was added diisopropylethylamine at once (DIPEA, 117 $\mu$ l, 674 $\mu$ mol), *p*-nitrophenyl chloroformate (102mg, 506 $\mu$ mol) and a catalytic amount of pyridine. The reaction was left under stirring at 0°C for 16h. Upon this time, the reaction mixture was concentrated under vacuum and dissolved in ethylacetate (5ml).

The organic phase washed three times with ammonium chloride (saturated solution, 3x5ml), dried over sodium sulphate and finally filtered off. The filtrate was concentrated by rotoevaporation.

#### 1.12.2.7 Synthesis of FmocGGPNle $\phi$ PTX

To a solution at room temperature of Fmoc-Gly-Gly-Pro-Nle $\phi$ NO<sub>2</sub> (59mg, 71 $\mu$ mol) in anhydrous THF (4ml) under stirring, was added paclitaxel at once (PTX, 72mg, 85 $\mu$ mol), and dimethylaminopyridine (DMAP, 13mg, 106 $\mu$ mol). The reaction was left under stirring at room temperature for 8h.

The reaction mixture was then concentrated under vacuum using a roto evaporator. The residue was then purified by two silica column chromatographies using ethylacetate (100%) first and ethyl acetate/acetone solvent mixture (20/80%<sub>v/v</sub>) consecutively. Fractions were analysed by TLC and mass spectrometry (ESI-TOF, positive mode, acetonitrile:H<sub>2</sub>O:Formic acid 49:50:1) to collect the ones containing Fmoc-Gly-Gly-Pro-Nle $\phi$ NO<sub>2</sub>. After elimination of the solvents under vacuum, Fmoc-Gly-Gly-Pro-Nle $\phi$ PTX was recovered as a white powder.



#### 1.12.2.8 Synthesis of $\text{NH}_2\text{GGPNle}\phi\text{PTX}$ – Deprotection of $\text{FmocGGPNle}\phi\text{PTX}$

To a solution of  $\text{FmocT}\phi\text{PTX}$  (93mg, 90 $\mu\text{mol}$ ) in dichloromethane (DCM, 4ml), was added DMAP (11mg, 77.4 $\mu\text{mol}$ ) at once. The reaction mixture was left under stirring at room temperature for 48h and monitored by mass spectrometry ESI-TOF, positive mode, acetonitrile:H<sub>2</sub>O:Formic acid 49:50:1).

$\text{NH}_2\text{T}\phi\text{PTX}$  was recovered by precipitation of reaction mixture into cold diethyl ether three times, collection of the precipitate and evaporation of solvents to yield a white powder.

#### 1.12.2.9 Synthesis of $\text{Fmoc-GGPNle-Alendronate}$

Multiple tactics were considered for the synthesis of peptylalendronate including, N,N'-dicyclohexylcarbodiimide (DCC) coupling in presence of 4-(dimethylamino)pyridine (DMAP) catalyst, and 1-ethyl-3-(3-dimethylaminopropyl) carbodiimide (EDC) coupling in presence of DMAP, solution phase O-Benzotriazole-N,N',N'-tetramethyl-uronium-hexafluoro-phosphate / Hydroxybenzotriazole (HBTU/HOBt) coupling, EDC in presence of N-hydroxysuccinimide (NHS) coupling, 4,5-dihydrothiazole-2-thiol (TT) in presence of DCC coupling, pH were varied from 7 to above 11. These synthesis trials are not described in details here as the synthesis were not successful and did not lead to the desired product. Possible reasons will be discussed in the result and discussion paragraph.

A new approach was thought, which would include a relatively low molecular weight poly(ethylene glycol) (PEG) in the alendronate derivative. By attaching the PEG in its form tBoc-NH-PEG-NHS to alendronate first, tBoc-NH-PEG-alendronate would be produced and facilitate the attachment of this first compound to the pullulan aldehyde groups after tBoc deprotection.

#### 1.12.2.10 Synthesis of $\text{tBoc-NH-PEG-Alendronate}$

To a stirred solution of alendronate (50mg, 153.84 $\mu\text{mol}$ ) in borate buffer (0.1mol.l<sup>-1</sup>, pH 8, 5ml), tBoc-NH-PEG<sub>3000</sub>-NHS (3000Da, 165mg, 55 $\mu\text{mol}$ ) was added at once. The reaction mixture was stirred for 5h at room temperature, under atmospheric pressure.

Upon this time, the pH was adjusted at 4.5 using a hydrochloric acid solution (0.2mol.l<sup>-1</sup>). tBoc-NH-PEG-Alendronate was extracted in dichloromethane (6x5ml), the organic phase dried over sodium sulphate and lastly, precipitated into diethyl ether after filtration.

Determination of free alendronate was made by measuring free primary amino groups by Snyder test and showed the absence of free amine in the white powder product. Alendronate content was assessed by spectrophotometric method, showing 24%<sub>mol</sub> alendronate

#### **1.12.2.11 Synthesis of NH<sub>2</sub>-PEG-Alendronate**

A solution of trifluoroacetic acid/dichloromethane (TFA/DCM, 50/50%<sub>v/v</sub>, 1 ml) was added to tBoc-PEG-alendronate (60mg, 20 $\mu$ mol) at once. The reaction mixture was left at room temperature under stirring for 30min.

Upon this time, DCM and TFA were removed under vacuum and NH<sub>2</sub>-PEG-ALN recovered by precipitation into diethyl ether to obtain a white powder.

#### **1.12.2.12 Synthesis of Pull-PTX**

To a solution of 30% oxidised pullulan (Pullox<sub>30</sub>, 15mg, 185 $\mu$ mol eq aldehyde) in DMSO (2ml), was added NH<sub>2</sub>-GGPNle $\phi$ PTX (60mg, 45 $\mu$ mol) at once. The reaction mixture was left at room temperature under stirring for 12h. Upon this time, sodium borohydride (NaBH<sub>4</sub>, 7mg, 155 $\mu$ mol) was added at once. The reaction mixture was left for 24h under stirring at room temperature.

#### **1.12.2.13 Synthesis of Pull-PEG-ALN**

To a solution of 30% oxidised pullulan (Pullox<sub>30</sub>, 15mg, 185 $\mu$ mol eq aldehyde) in milliQ water (2ml), was added NH<sub>2</sub>-PEG-Alendronate (60mg, 30 $\mu$ mol) at once. The reaction mixture was left at room temperature under stirring for 4h. Upon this time, sodium borohydride (NaBH<sub>4</sub>, 7mg, 155 $\mu$ mol) was added and the reaction mixture was left for 72h under stirring at room temperature.

The conjugate was then dialysed against water for 48h using a 3500Da cut-off dialyse membrane in order to remove salts and excess NH<sub>2</sub>-PEG-alendronate. The product was lyophilised to yield a white brittle powder.

#### **1.12.2.14 Synthesis of Pull-PTX-ALN**

To a solution of oxidised pullulan (24%<sub>mol</sub> oxidation, 100mg, 296 $\mu$ mol aldehyde eq) in dimethylsulfoxide (DMSO, 8ml) was added a solution of NH<sub>2</sub>GGPNle $\phi$ PTX (124mg,93 $\mu$ mol) in DMSO (2ml). After 12 h, was added sodium triacetoxyborohydride (20mg, 93 $\mu$ mol).

The reaction mixture was left under stirring for 6 hours. Upon this time, NH<sub>2</sub>PEGALN (170mg,56 $\mu$ mol) dissolved in DMSO (1ml) as added to the pullulan solution. The reaction was maintained overnight at room temperature under stirring.

Subsequently, sodium borohydride (NaBH<sub>4</sub>, 11mg, 296 $\mu$ mol) was added at once. The reaction mixture was left at room temperature, under stirring overnight.

Purification was conducted by dialysis against water for two days (release medium renewed 4 times a day). The product was then freeze-dried, followed by washes with

methanol (5 times 5ml) to ensure the full removal of unreacted  $\text{NH}_2\text{GGPNle}\phi\text{PTX}$ . Solvents were evaporated under vacuum to yield a white/off-white brittle powder.

#### **1.12.2.15 Determination of total paclitaxel content in the conjugates**

*All solutions were prepared in sodium acetate buffer at pH5.5 (50mM, 100mM NaCl).*

To a L-cysteine solution (303 $\mu\text{l}$ , 2.5mM), was added a solution of Ethylenediaminetetraacetic acid (EDTA, 146 $\mu\text{l}$ , 5mM) and DL-Dithiothreitol (DTT, 84 $\mu\text{l}$ , 5mM). The solution was warmed up at 37°C for 5min. Cathepsin K (162 $\mu\text{l}$ , 150nM) was then added to the mixture.

Finally, a Pull-PTX-ALN solution (305 $\mu\text{l}$ , 75 $\mu\text{M}$   $\text{PTX}_{\text{eq}}$ ), was added to the Cathepsin K containing reaction mixture.

The mixture was incubated at 37 °C. After 480min, the drug was extracted by dichloromethane. The organic phase was evaporated and the residue was solubilised in acetonitrile.

The amount of free paclitaxel in the conjugates was evaluated by reverse phase HPLC using a  $\text{C}_{18}$  (4.6  $\times$  250 mm; 5  $\mu\text{m}$ ) column, with the UV detector set at 227 nm. MilliQ  $\text{H}_2\text{O}$  (0.05% TFA) and acetonitrile (0.05% TFA) were used as eluent A and B respectively. Elution was performed in isocratic mode at a flow rate of 0.7ml.min<sup>-1</sup>, using a 45/55%<sub>v:v</sub>  $\text{H}_2\text{O}$ /acetonitrile ratio.

The total drug content was evaluated by RP-HPLC following the release of PTX from the conjugates.

As second check, the total drug content of the polymer-drug conjugates was also analysed by UV spectrophotometry at  $\lambda=234\text{nm}$  and results were confronted with the ones obtained by RP-HPLC.

#### **1.12.2.16 Determination of alendronate bound to PEG**

The formation of a chromophoric complex between alendronate and Fe(III) ions in perchloric acid solution ( $\text{HClO}_4$ , 0.2mol.l<sup>-1</sup>) was used to determine spectrophotometrically the quantity of alendronate bound to PEG.

Conjugates (2.5, 5 and 10 mg) were dissolved in a mixture of 100 $\mu\text{l}$  Fe(III)Cl (4mmol.l<sup>-1</sup>) solution in  $\text{HClO}_4$  and 900 $\mu\text{l}$  of  $\text{HClO}_4$  solution. The alendronate content in the conjugates was determined against a calibration graph of serial dilutions of alendronate solution from 0 to 3mmol.l<sup>-1</sup>

Sample absorbance was measured by UV spectrophotometry at a wavelength of 300nm.

#### **1.12.2.17 Determination of Critical Micelle Concentration (CMC)**

The critical micelle concentration (CMC) of the modified pullulan Pull-PTX-ALN was determined by a fluorescence spectroscopy method, using pyrene monomer fluorescence as a hydrophobic probe.

Briefly, the polymer conjugate was dissolved in 750 $\mu$ l Phosphate Buffer Saline (PBS, 20mmol.l<sup>-1</sup>) containing sodium chloride (NaCl, 0.15mol.l<sup>-1</sup>) at pH7.4. Polymer concentrations ranged from 0.2 to 100.0 $\mu$ g.ml<sup>-1</sup>. To 750 $\mu$ l of polymer solution, was added a pyrene solution in acetone (5 $\mu$ l, 0.18mmol.l<sup>-1</sup>).

Samples were incubated under gentle shaking at room temperature and were left overnight and protected from the light to allow equilibration.

Prior to measurements, polymer solutions were incubated at 37°C for 15min. Fluorescence excitation spectra were recorded using a Jasco FP-6500 Spectrofluorometer.

The emission wavelength ( $\lambda_{em}$ ) was set at 390nm and excitation spectra were recorded in the 300 to 360nm wavelength range. The excitation and emission band slits were set at 4 and 2nm respectively.

The  $I(\lambda_{ex\ 339nm})/I(\lambda_{ex\ 334nm})$  intensity ratios were plotted as a function of the logarithm of the polymer conjugate concentration (logC).

The CMC was determined from the intersection point at low polymer concentration.

#### **1.12.2.18 Determination of particle size and charge in solution**

The particle size, polydispersity and zeta potential were measured by Dynamic Light Scattering (DLS) using a Malvern Instrument Ltd Zetasizer Nano ZS (Malvern, UK). Polymer conjugate samples were analysed at a concentration of 1mg.ml<sup>-1</sup>, in sodium acetate buffer at pH5.5 (20mmol.l<sup>-1</sup>) and PBS at pH7.4(20mmol.l<sup>-1</sup>, NaCl 0.15mol.l<sup>-1</sup>), and milliQ water.

#### **1.12.2.19 Stability assay**

The drug release assay was carried out in sodium acetate buffer at pH5.5 (20mmol.l<sup>-1</sup>) and PBS at pH7.4 (20mmol.l<sup>-1</sup>, NaCl 0.15mol.l<sup>-1</sup>), Polymer solutions (3mg.l<sup>-1</sup>, 3ml) were placed into a dialysis bag (regenerated cellulose, 3.5kDa cut-off). Then, the dialysis bag was quickly immersed in the appropriate release medium (50ml, pH=pH inside bag) kept under controlled temperature at 37°C and under continuous stirring. At given time intervals, 600 $\mu$ l sample was withdrawn from the dialysis bag and the equal volume of fresh medium was refilled. The sample was divided into two equivalent volumes, one

designated for the determination of released alendronate by spectrophotometry after complexation with Fe(III) ions and the other one for the determination of paclitaxel release by UV spectrophotometry and RP-HPLC as reported previously.

#### **1.12.2.20 In vitro-drug release assay in presence of Cathepsin K**

*All solutions were prepared in sodium acetate buffer at pH5.5 (50mM, 100mM NaCl).*

To a L-cysteine solution (303 $\mu$ l, 2.5mM), was added a solution of Ethylenediaminetetraacetic acid (EDTA, 146 $\mu$ l, 5mM) and DL-Dithiothreitol (DTT, 84 $\mu$ l, 5mM). The solution was warmed up at 37°C for 5min. Cathepsin K (162 $\mu$ l, 150nM) was then added to the mixture.

Finally, a Pull-PTX-ALN solution (305 $\mu$ l, 75 $\mu$ M PTX<sub>eq</sub>), was added to the Cathepsin K containing reaction mixture.

The mixture was incubated at 37 °C and aliquots (75 $\mu$ l) were taken after 0 min, 15 min, 30 min, 45, 60 min 120, 240, 480 and 1220 min and analysed by HPLC.

The assay was produced in triplicate.

#### **1.12.2.21 Hydroxyapatite binding assay**

In order to assess the affinity between the bisphosphonate containing polymer conjugates and the bone mineral hydroxyapatite, a hydroxyapatite binding assay was designed.

Polymer conjugates solutions (3mg.ml<sup>-1</sup>) were prepared in acetate buffer at pH5.5 (20mmol.l<sup>-1</sup>) and PBS at pH 7.4 (20mmol.l<sup>-1</sup>, NaCl 0.15mol.l<sup>-1</sup>). Solutions were incubated under stirring at 37°C. After equilibration, hydroxyapatite (30eq) was added at once to the polymeric solutions.

Hydroxyapatite binding was monitored spectrophotometrically by determination of the decrease over time, of the polymer conjugate concentration in the supernatant, measuring the quantity of paclitaxel and alendronate by UV spectrophotometry.

The percentage of binding to hydroxyapatite was calculated as follow:

#### **Equation 2-1 Equation used for the calculation of the %binding onto hydroxyapatite**

$$\% \text{binding} = \frac{[(\text{sample concentration without hydroxyapatite} - \text{sample concentration with hydroxyapatite})]}{[\text{sample concentration without hydroxyapatite}]} \times 100$$

### 1.12.3 Cell culture

MDA-MB-231 human mammary adenocarcinoma, SAOS-2 osteosarcoma and 4T1 murine mammary adenocarcinoma cell lines were provided by American Type Culture Collection (ATCC).

MDA-MB231 cells were cultured in DMEM supplemented with 10% FBS, 100µg/ml Penicillin, 100U/ml Streptomycin, 12.5U/ml Nystatin and 2mM L-Glutamine.

SAOS-2 cells were cultured in DMEM supplemented with 10% FBS, 100µg/ml Penicillin, 100U/ml Streptomycin, 12.5U/ml Nystatin, 2mM L-Glutamine and 1mM sodium pyruvate.

4T1 cells were cultured in RPMI 1640 supplemented with 10% FBS, 100µg/ml Penicillin, 100U/ml Streptomycin, 12.5U/ml Nystatin, 2mM L-Glutamine, 10mM HEPES buffer, and 1mM sodium pyruvate.

Human Umbilical Vein Endothelial Cells (HUVEC) were obtained from Cambrex (Walkersville, USA) and grown according to manufacturer's protocol in EGM-2 medium (Cambrex). All cells were grown at 37°C, 5% CO<sub>2</sub>.

#### 1.12.3.1 MTT assay

A solution of 1-(4,5-Dimethylthiazol-2-yl)-3,5-diphenylformazan, Thiazolyl blue formazan (MTT, 5mg/ml) was prepared in sterile PBS at 37°C. After centrifugation, 20µl of MTT solution was added into each well of a 96-well plate. After incubation at 37°C, 5%CO<sub>2</sub>, the mixture of medium and MTT was removed by vacuum and replaced by 200µl dimethylsulfoxide. After dissolution of the crystals, the 96-well plate was read by UV spectrophotometry at  $\lambda=565\text{nm}$ .

#### 1.12.3.2 Cell proliferation assays

MDA-MB231 cells were plated onto a 96-well plate ( $5 \cdot 10^3$  cells/well) in DMEM supplemented with 5% FBS and incubated for 24h (37°C, 5% CO<sub>2</sub>). Following 24h incubation, the 5%FBS supplemented DMEM medium was replaced by a 10%FBS supplemented DMEM medium. Cells were challenged with free paclitaxel and free alendronate, unmodified native pullulan, Pull-PTX, Pull-ALN and Pull-PTX-ALN at serial concentrations for 72h. Following incubation, MDA-MB231 cells viability was measured by MTT assay.

SAOS-2 cells were plated onto a 96-well plate ( $2 \cdot 10^3$  cells/well) in DMEM supplemented with 5% FBS and incubated for 24h (37°C, 5% CO<sub>2</sub>). Following 24h incubation, the 5%FBS supplemented DMEM medium was replaced by a 10%FBS supplemented DMEM medium. Cells were challenged with free paclitaxel and free alendronate, unmodified native pullulan, Pull-PTX, Pull-ALN and Pull-PTX-ALN at serial concentrations for 72h. Following incubation, MDA-MB231 cells viability was measured by MTT assay.

4T1 cells were plated onto a 24-well plate ( $4 \cdot 10^3$  cells/well) in RPMI supplemented with 5% FBS and incubated for 24h (37°C, 5% CO<sub>2</sub>). Following 24h incubation, the 5%FBS supplemented RPMI medium was replaced by a 10%FBS supplemented RPMI medium. Cells were challenged with free paclitaxel and free alendronate, unmodified native pullulan, Pull-PTX, Pull-ALN and Pull-PTX-ALN at serial concentrations for 72h. Following incubation, 4T1 cells viability was measured Coulter Counter.

HUVEC cells were plated onto a 24-well plate ( $1.5 \cdot 10^3$  cells/well) in growth factor reduced media EBM-2 supplemented with 5% FBS and incubated for 24h (37°C, 5% CO<sub>2</sub>). Following 24h incubation, the 5%FBS supplemented EBM-2 medium was replaced by EGM-2. Cells were challenged with free paclitaxel and free alendronate, unmodified native pullulan, Pull-PTX, Pull-ALN and Pull-PTX-ALN at serial concentrations for 72h. Following incubation, HUVEC cells viability was measured Coulter Counter

### **1.12.3.3 *In Vitro Tube Formation assay***

Matrigel (50 µl) was carefully added in a thin layer into each well of a 24-well plate and allowed to solidify at 37°C for 30 min. After the solidification of the Matrigel, HUVEC ( $3 \cdot 10^4$  cells/well) were added in 500 µl of EGM-2 medium. Cells were incubated for 24 h at 37°C in a humidified incubator (95% air/5% CO<sub>2</sub>).

HUVEC were challenged with free PTX (10nM), a combination of free PTX and ALN (23nM), free ALN, Pull-ALN, Pull-PTX, Pull-PTX-ALN at equivalent concentrations, and were seeded on the coated plates in the presence of complete EGM-2 medium. After 8 h of incubation (37°C; 5% CO<sub>2</sub>), wells were imaged using Nikon TE2000E inverted microscope integrated with Nikon DS5 cooled CCD camera by 4X objective, bright field technique. The tube networks were quantified by image analysis using ImageJ.

### **1.12.3.4 *Wound healing assay***

MDA-MB231 cells were plated onto a 6 well plate ( $4 \cdot 10^5$  cells/well) 24h prior performing the scratch wound assay. The confluent monolayer was scratched by a pipette tip, rinsed with PBS to remove detached cells and fresh medium was added.

Digital images of cells were taken immediately after scratching (t = 0). Cells were challenged with free paclitaxel and free alendronate, unmodified native pullulan, Pull-PTX, Pull-ALN and Pull-PTX-ALN for 24h, at a concentration just below the IC<sub>50</sub> of PTX. After 24h incubation, the distance between cells in the scratched area was evaluated using ImageJ. Results were normalized to untreated control cells.

#### 1.12.3.5 Red Blood Cells Lysis assay

Rat Blood Cells were obtained from whole rat blood. Blood was first diluted in PBS at pH 7.4 (20mmol.l<sup>-1</sup>, NaCl 0.15mol.l<sup>-1</sup>).

After mixing for 10 s and incubating for 2 min at room temperature, the mixture was centrifuged at 1000rpm for 5 min at 4°C using a refrigerated centrifuge. The supernatant was discarded and the packed cells washed again, repeating the procedure twice more, using PBS at pH 7.4 (20mmol.l<sup>-1</sup>, NaCl 0.15mol.l<sup>-1</sup>).

Rat RBC solution (2%<sub>w/w</sub>) was incubated for 1h at 37°C, with serial dilutions in PBS (pH 7.4, 20mmol.l<sup>-1</sup>, NaCl 0.15mol.l<sup>-1</sup>) of free paclitaxel and free alendronate, unmodified native pullulan, Pull-PTX, Pull-ALN and Pull-PTX-ALN at equivalent concentration of PTX and ALN.

Negative controls were PBS (pH 7.4, 20mmol.l<sup>-1</sup>, NaCl 0.15mol.l<sup>-1</sup>) and Dextran (MW 70kDa) whereas positive controls were Triton X100 (1%<sub>w/v</sub>) and poly(ethylenimine).

Following centrifugation (7min, 3000rpm), the supernatant was drawn off and its absorbance measured at 550nm using a micro-plate reader. The results were expressed as percent of haemoglobin released relative to the positive control (Triton X100).

#### 1.12.3.6 Statistical methods

*In vitro* data are expressed as mean ± s.d. Statistical significance was determined using an unpaired *t*-test. *P* < 0.05 was considered statistically significant. All statistical tests were two-sided.



# Results

---



### 3. Results

#### 1.13 Synthesis of Pullulan-Paclitaxel-Alendronate – Pull-PTX-ALN

The following sections describe the different stages in the creation of the polymer-drug conjugate Pullulan-Paclitaxel-Alendronate (Pull-PTX-ALN), main compound in this project.

##### 1.13.1 Carrier function: Periodate oxidation of pullulan

Preliminary studies in agreement with Brunel<sup>53</sup>, allowed to assess the conditions of activation of pullulan by sodium periodate and showed that the oxidation of vicinal diols was a rapid process. The oxidation reached 24% and 60% after 30min for 30% and 100% oxidation targets, to reach a plateau after 6h (Figure 3-1).

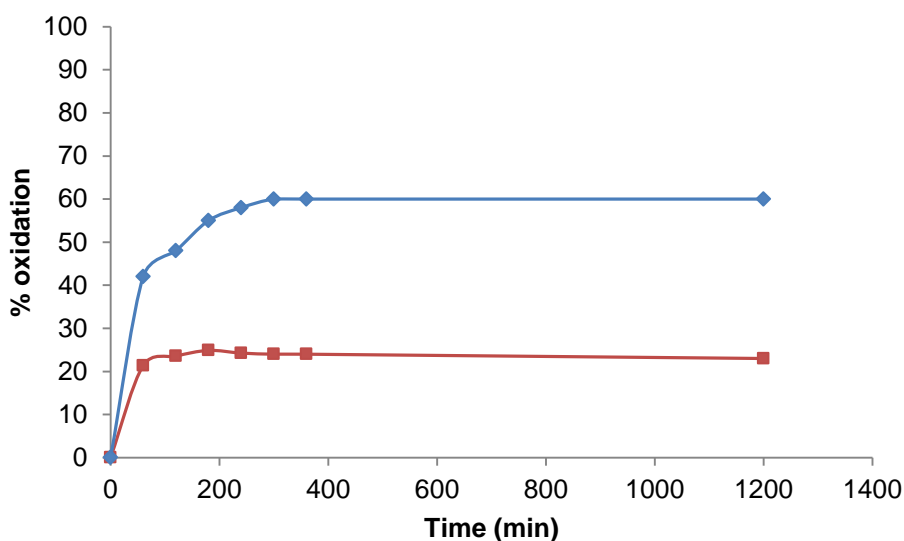
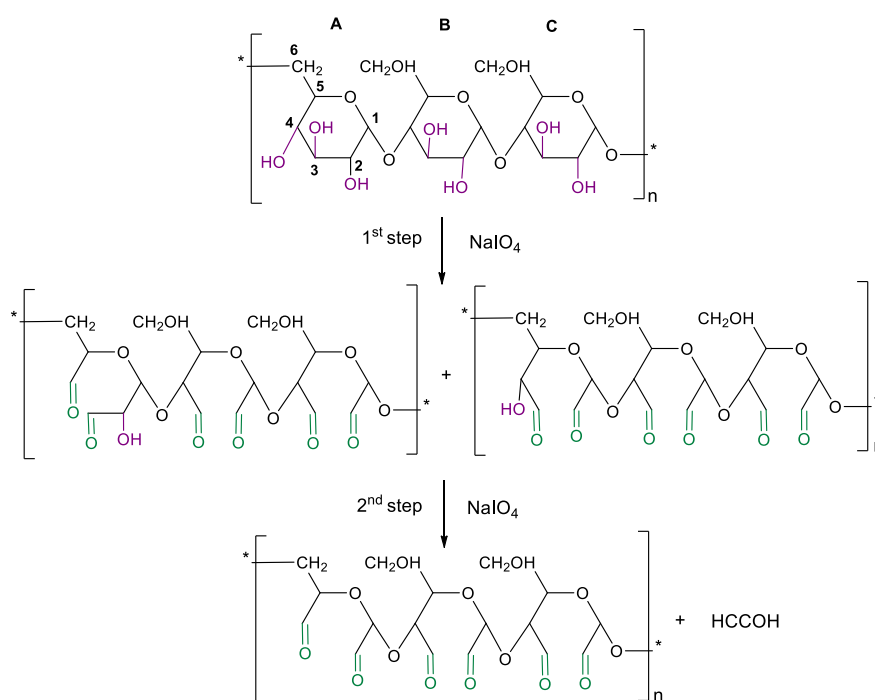


**Figure 3-1 Kinetics of oxidation of pullulan by periodate oxidation – 30% target (■) and 100% target (◆)**

The use of periodate ions enabled the selective oxidation of the vicinal diols to form aldehydes, with simultaneous disruption of the connection C2-C3 and consequent opening of the glucopyranose polysaccharide ring as shown in Scheme 3-1.



**Scheme 3-1 Periodate oxidation of pullulan**

The target oxidation for the matter of this project was 30%, leading to the oxidised pullulan Pull<sub>ox30</sub>. The success of the reaction was determined by qualitative and quantitative analysis.

#### *<sup>1</sup>H NMR spectroscopy*

<sup>1</sup>H NMR spectroscopy performed in deuterated water D<sub>2</sub>O allowed to confirm the presence of aldehyde groups on pullulan backbone after oxidation, as revealed by the appearance of a peak at  $\delta=9.26\text{ppm}$  as shown in Figure 3-2 <sup>1</sup>H NMR Spectra in D<sub>2</sub>O of native Pullulan- Top (-) and Pull<sub>ox30</sub>-Bottom (-). This peak corresponded to the aldehyde formyl hydrogen which was strongly deshielded: aldehyde compounds have a distinctive chemical shift which appears to be between 9-10 ppm, Aldehyde hydrogens are also slightly deshielded because of the electron withdrawing from the oxygen from the carbonyl group. The peak at 2.21ppm represents the acetone solvent, commonly used in laboratories.

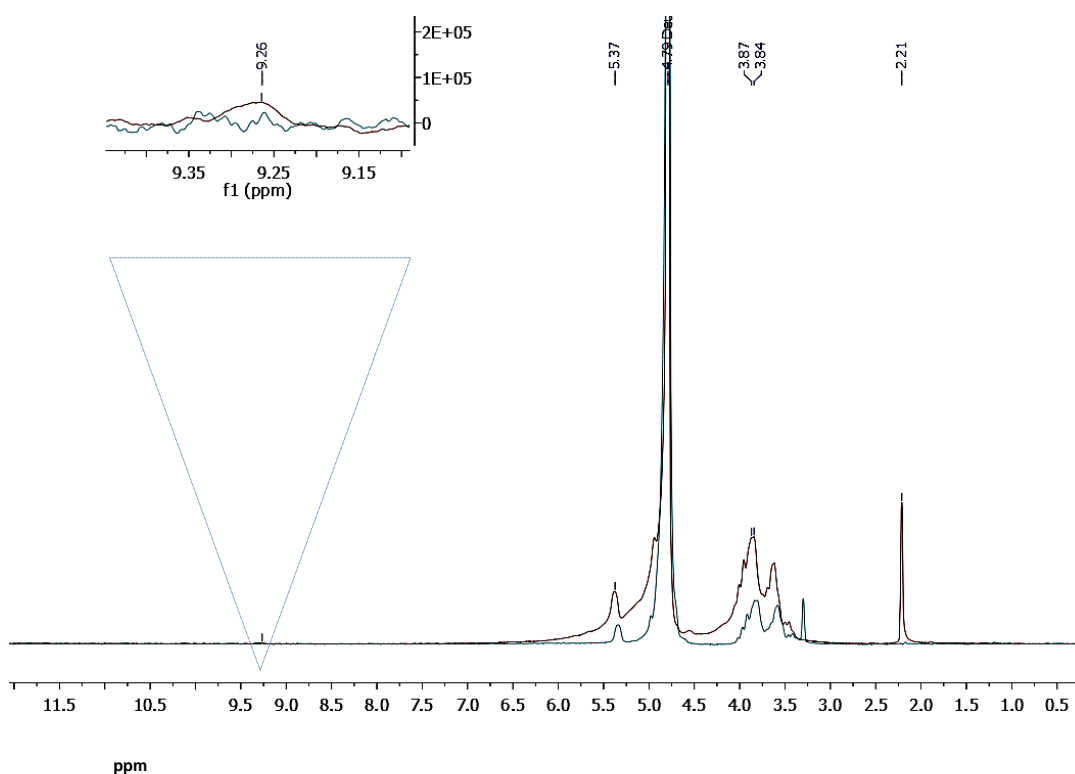


**Figure 3-2**  $^1\text{H}$  NMR Spectra in  $\text{D}_2\text{O}$  of native Pullulan- Top (-) and Pull<sub>ox30</sub>-Bottom (-)

Oxidised pullulan (Pull<sub>ox30</sub>) was also analysed by Fourier Transformed InfraRed Spectroscopy (FT-IR) as presented in Figure 3-3. Native pullulan and oxidised pullulan differed from each other in the region of  $600\text{-}800\text{cm}^{-1}$ . Indeed, after oxidation, the formation of aldehyde on the polysaccharide's chain could be observed by the apparition of two peaks in this region, typical from C-O stretching from carbonyl groups. However, regions were stretching vibrations (CO) C-O-C of the glycosidic bridge in oligosaccharides were observed for both modified and non-modified polysaccharides, in the range of  $1100\text{-}970\text{cm}^{-1}$  as expected.

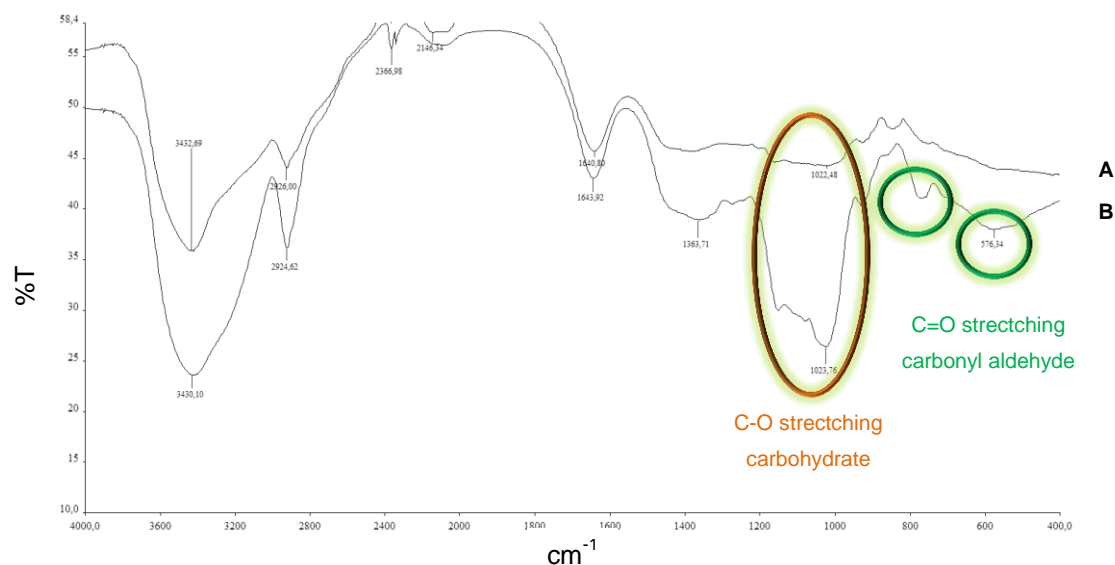
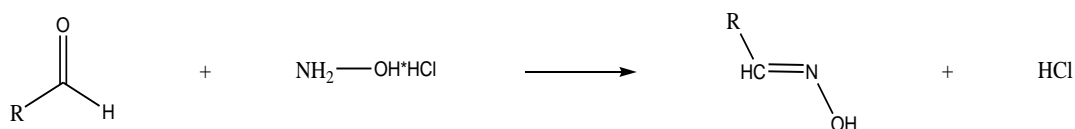


**Figure 3-3** FT-IR spectra on KBr plate of native Pullulan (A) and Pull<sub>ox30</sub> (B)

#### Potentiometric titration of aldehydes

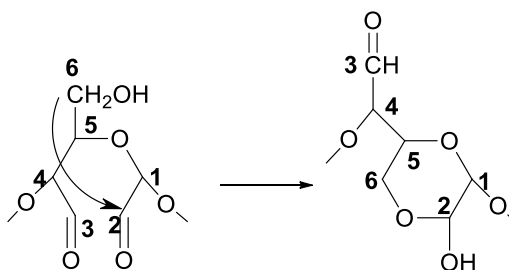
In addition to qualitative analysis, Pull<sub>ox30</sub> was analysed quantitatively, the amount of aldehyde generated in the oxidised polysaccharide was estimated by the hydroxylamine hydrochloride reaction. This reagent is involved in a nucleophilic attack of one aldehyde that leads to formation of an oxime and stoichiometric release of hydrochloric acid (HCl). HCl can then be potentiometrically titrated with sodium hydroxide (NaOH) (Scheme 3-2).



**Scheme 3-2** Titration of aldehyde groups in oxidised pullulan

This analytical method allowed the determination of the amount of aldehydes produced after pullulan oxidation. The oxidation degree obtained was of 23%<sub>mol</sub> of glucopyranose units by using a periodate : maltotriose molar ratio of 0.3:1. This result matched with literature (Bruneel D., 1993) where it was reported that only 2/3 of all aldehydes formed could be detected.

Indeed, this quantification method uses a nucleophilic attack of the reagent onto the carbonyl carbon, but not all aldehydes are accessible. A possible explanation of such phenomenon is the spontaneous formation of a hemiacetal (with recyclisation) in  $\alpha$ -1,4 of the glycosidic residue as illustrated in Scheme 3-3.



**Scheme 3-3 Spontaneous hemiacetal formation occurring in a maltotriose unit.**

Consequently, this could be translated as a protection (and consequent loss of reactivity) of 2 of 6 aldehydes obtained in the completely oxidised maltotriose unit.

#### Gel Permeation Chromatography (GPC)

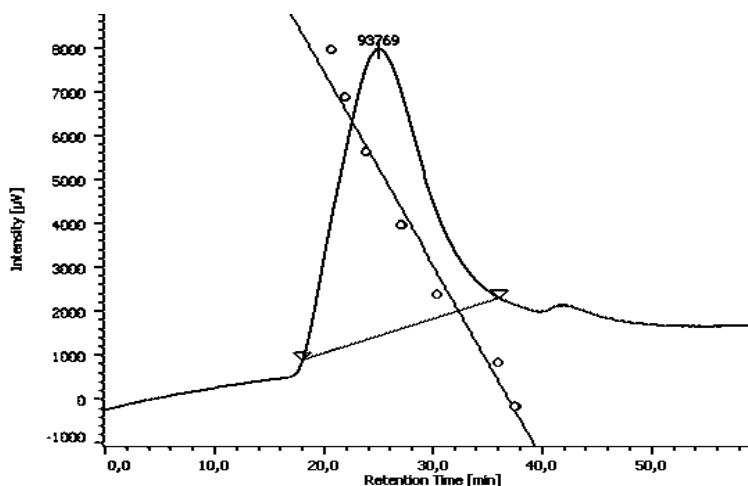


**Figure 3-4 GPC chromatogram of aldehyde pullulan Pull<sub>ox30</sub>**

The periodate oxidation caused a reduction of the polysaccharide molecular weight from ~110kDa to ~93769kDa and a PDI decrease from 2.35 to 1.90.

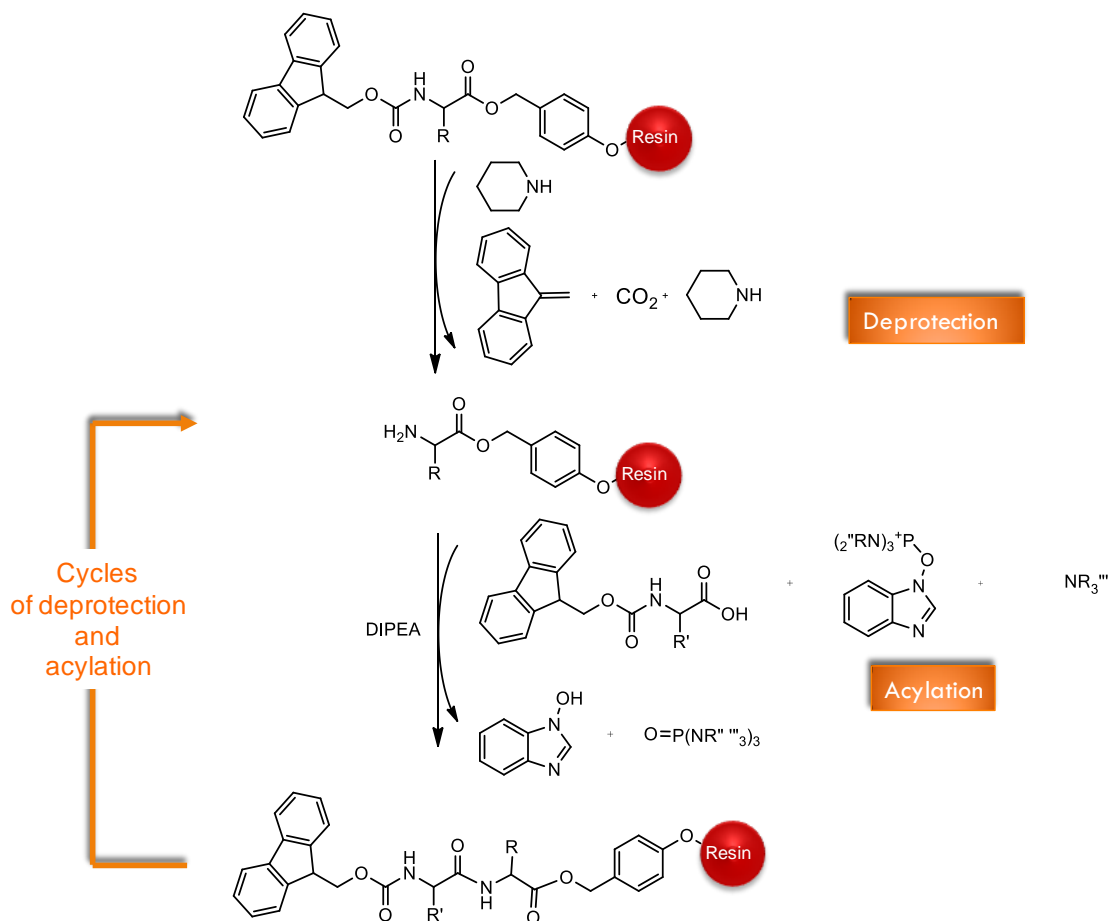
#### **1.13.2 Enzyme triggered release function: Synthesis of the FmocGlyGlyProNle peptide**

The method chosen for the synthesis of the Cathepsin K sensitive spacer Gly-Gly-Pro-Nle was the widely used solid phase peptide synthesis (SPPS) in which chemical transformations are performed onto a solid support. This concept was first introduced by Bruce Merrifield to synthesise polypeptides and earned him the Nobel Prize in 1984. Wang resin was selected as support matrix, a 4-Benzyloxybenzyl alcohol, polymer-bound

resin which allows the peptide to remain covalently bonded to the insoluble, yet porous bead until cleavage. This is advantageous as the immobilised peptide could be retained during filtration process while liquid reagents and by products could be flushed away. The resin was provided with the first protected amino acid Norleucine already anchored.

As 99% of coupling sites are located inside the resin beads and not at their surface, the resin must be prepared before synthesis. It was swollen using 1-methyl-2-pyrrolidone (NMP) for 30min in order to ensure an optimal permeation of the N-protected amino-acids in the polymer matrix.

The succession of coupling and deprotection cycles permitted the growth of the tetrapeptide in a linear fashion using a C-N strategy, from C-terminus to N-terminus. N-protected C-terminal amino acid residues were anchored via their carboxyl group to the amino group ending resin to yield an amide linked peptide (Scheme 3-4).



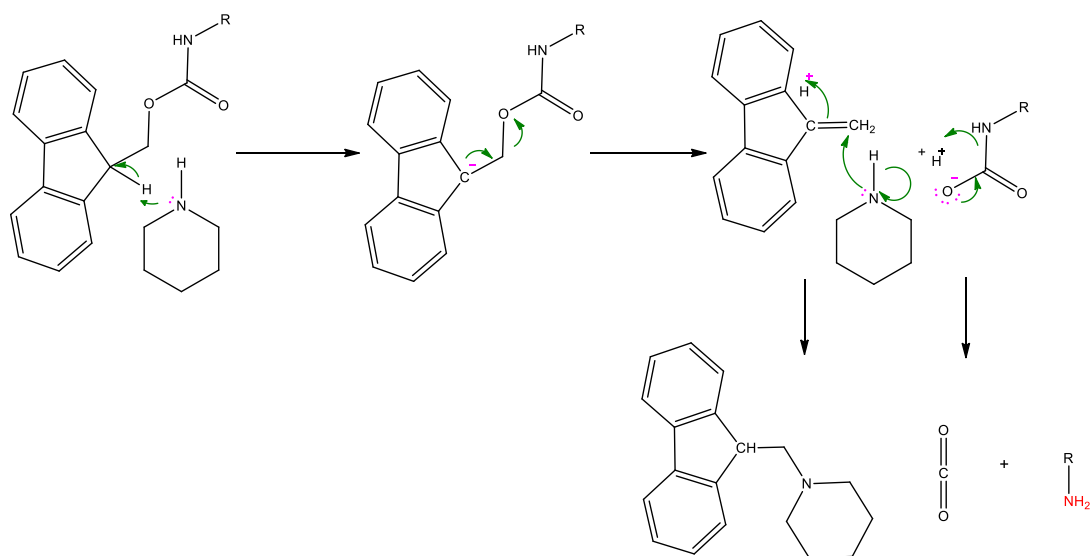
**Scheme 3-4 Solid Phase Peptide Synthesis general principle**

Amino acids were added in large excess to ensure complete coupling for each step. Two N-terminal protecting groups are much used namely tBoc and Fmoc. Such groups protect the amine by carbamate formation which lability allows the release of CO<sub>2</sub> during the deprotection process. The base labile Fmoc protecting group was selected for the



protection of the amine group of the amino acids as it allows the use of mild conditions for deprotection and for the cleavage of the peptide from the resin,

The removal of the Fmoc protecting group from the N-terminus of the resin-peptyl was achieved by treating the beads with a 20%<sub>v/v</sub> of piperidine in 1-methyl-2-pyrrolidone for 20min to ensure a complete deprotection. The deprotection results in the formation of a dibenzofulvene-piperidine adduct as shown in Scheme 3-5.

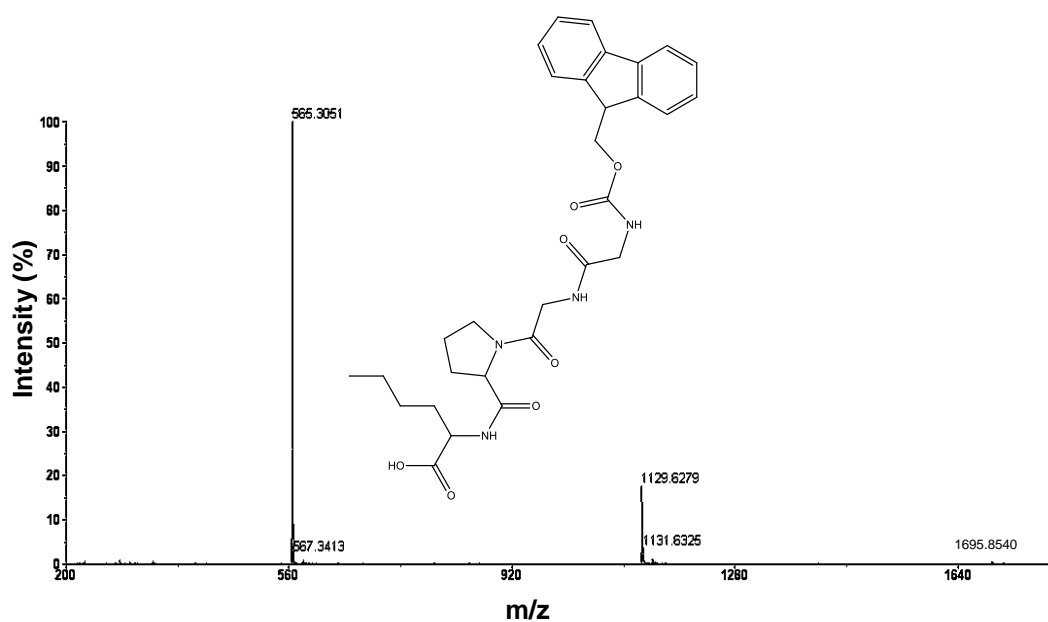


### **Scheme 3-5 Mechanism of Fmoc protected amine deprotection by piperidine**

Soluble side products and the excess of reactants were removed by washing steps during coupling and deprotection steps.

Concentrated trifluoroacetic acid solution in ultrapure water (95/5%<sub>v/v</sub>) was used for the cleavage of the peptide from the resin after several wash of the resin-peptyl with a series of solvents in order of increasing hydrophilicity NMP < dichloromethane < methanol.

After extraction of the tetrapeptide FmocGlyGlyProNle into iced cold water, the white product was analysed by mass spectrometry (positive mode, ESI-TOF) as exposed in Figure 3-5.

Mass Spectrometry

**Figure 3-5 Mass spectrum (ESI-TOF, positive mode) of tetrapeptide FmocGlyGlyProNle**

The analysis by mass spectrometry showed a peak at  $m/z=565.3051$  corresponding to the protonated tetrapeptide Fmoc GGP<sub>Nle</sub>OH  $[M+H]^+$ .

At  $m/z=1129.6279$ , was observed the aggregate of two tetrapeptides and at  $m/z=1695.8540$ , the aggregate of 3 tetrapeptides a common artefact of mass spectrometry.

All the peptide was then cleaved from the resin as mass spectrometry analysis showed the success of the synthesis.

<sup>1</sup>H NMR spectroscopy

The chemical composition of the final product was also checked by <sup>1</sup>H NMR performed in deuterated dimethylsulfoxide (DMSO-*d*<sub>6</sub>) spectroscopy. The spectrum of Figure 3-6 reports the characteristic signals of the tetrapeptide.

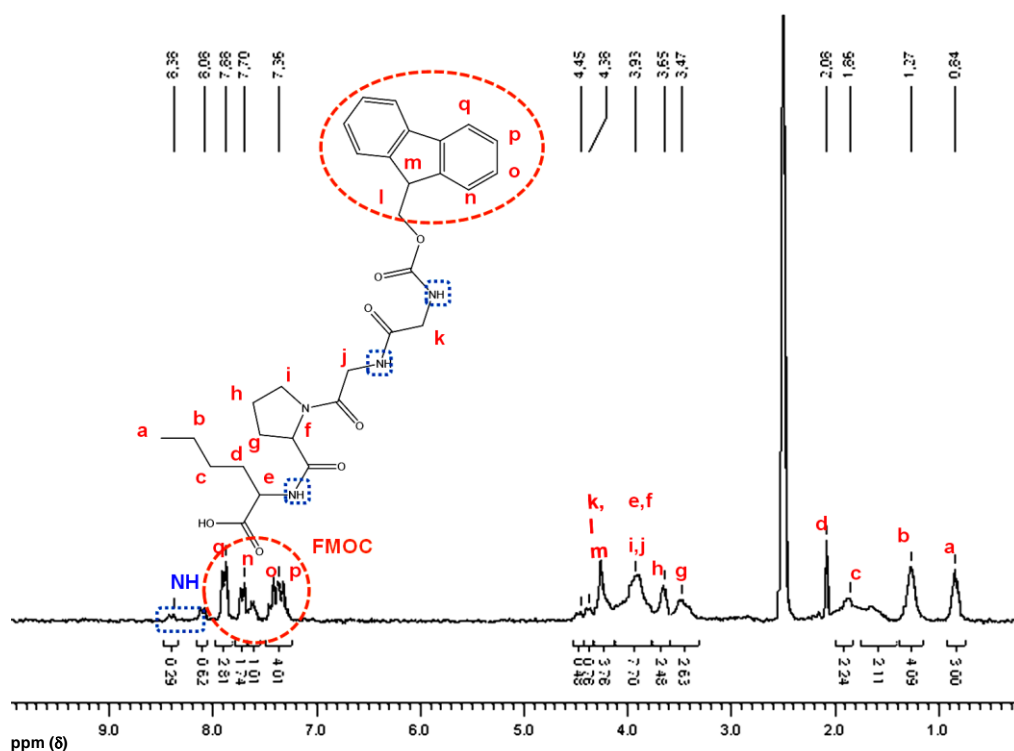


**Figure 3-6** <sup>1</sup>H NMR spectrum in DMSO-d<sub>6</sub> of FmocGlyGlyProNle

The methyl protons (a) at  $\delta=0.84\text{ppm}$  were set as reference and were attributed to 3H from the  $\text{CH}_3$  of the norleucine amino acid since the protons were the most shielded in the tetrapeptide molecule. Integrations of all peaks allowed the determination of all protons present in the molecule. The amide protons were detected at  $\delta=8.38\text{ppm}$  (1H,  $\text{NH}$ ) and 8.05 ppm (1H,  $\text{NH}$ ). Fmoc protecting group was present in the range between  $\delta=7.36$  and 7.88ppm, typical from cyclic molecules where protons are highly deshielded. More particularly, Fmoc protecting group was found at  $\delta=7.36\text{ppm}$  (m, 4H,  $\text{CH}$ , Fmoc),  $\delta=7.70\text{ppm}$  (m, 1H+1H,  $\text{CH}$ , Fmoc) and  $\delta=7.88\text{ppm}$  (m, 2H,  $\text{CH}$ , Fmoc). Norleucine methylene protons (b,c,d) could be identified at  $\delta=1.27\text{ppm}$  (m, 4H,  $\text{CH}_2\text{-CH}_2$ ) and  $\delta=2.11\text{ppm}$  (m, 2H,  $\text{CH}_2$ ). In the table hereafter, are recognised all protons from FmocGlyGlyProNle, integrations corresponded to the theoretical values (Table 3-1).

**Table 3-1** <sup>1</sup>H NMR chemical shifts ( $\delta$ ) and proton number for FmocGlyGlyProNle

Proton	$\delta$ (ppm)	Theoretical number	Experimental number
a	0.84	3	3.00
b	1.27	2	4.09
c	1.27	2	
d	1.86	2	2.11
e	3.93	1	e,f,i,j→7.70
f	3.93	1	
g	3.47	2	2.63
h	3.65	2	2.48
i	3.93	2	e,f,i,j→7.70
j	3.93	2	
k	4.38	2	K,l,m→5
l	4.38	2	
m	4.45	1	
n	7.70	2	1.74
o	7.36	2	4.01
p	7.36	2	
q	7.88	2	2.61

Mass spectrometry and  $^1\text{H}$  NMR spectroscopy showed the successful synthesis of the tetrapeptide sensitive spacer FmocGmyGlyProNle.

### 1.13.3 Anti-tumour function: Synthesis of $\text{NH}_2\text{T}\phi\text{PTX}$ paclitaxel prodrug

Multiple approaches were considered for the attachment of the N-terminus of the tetrapeptide spacer (S1) Gly-Gly-Pro-Nle to the hydroxyl group of paclitaxel (Figure 3-7-A) including common techniques also used in protein coupling such as the N,N'-dicyclohexylcarbodiimide (DCC) coupling in presence of 4-(dimethylamino)pyridine (DMAP) catalyst or the 1-ethyl-3-(3-dimethylaminopropyl) carbodiimide (EDC) coupling in presence of DMAP. These techniques were worked on different conditions (temperature, atmosphere, solvents) but none of them led to successful synthesis or the yield was unreasonably poor.

To overcome these issues, it was decided to insert a 1,6-elimination spacer based on 4-aminobenzyl alcohol (Figure 3-7-B). The latter was used to link the N-terminus of the peptide to the OH-group of the paclitaxel. The insertion of this second spacer (S2) would not modify the aim of the project, which was to use the enzymatic environment in bones

to cleave the tetrapeptide spacer and release paclitaxel. It was also reported in literature by Greenwald and co-workers<sup>54</sup> that the strong electronic-donating amine group of the 1,6- elimination spacer would be exposed upon enzymatic cleavage of the peptide spacer and consequently, a *n*-electronic cascade commences, that leads to the cleavage of the ester bond and release paclitaxel.

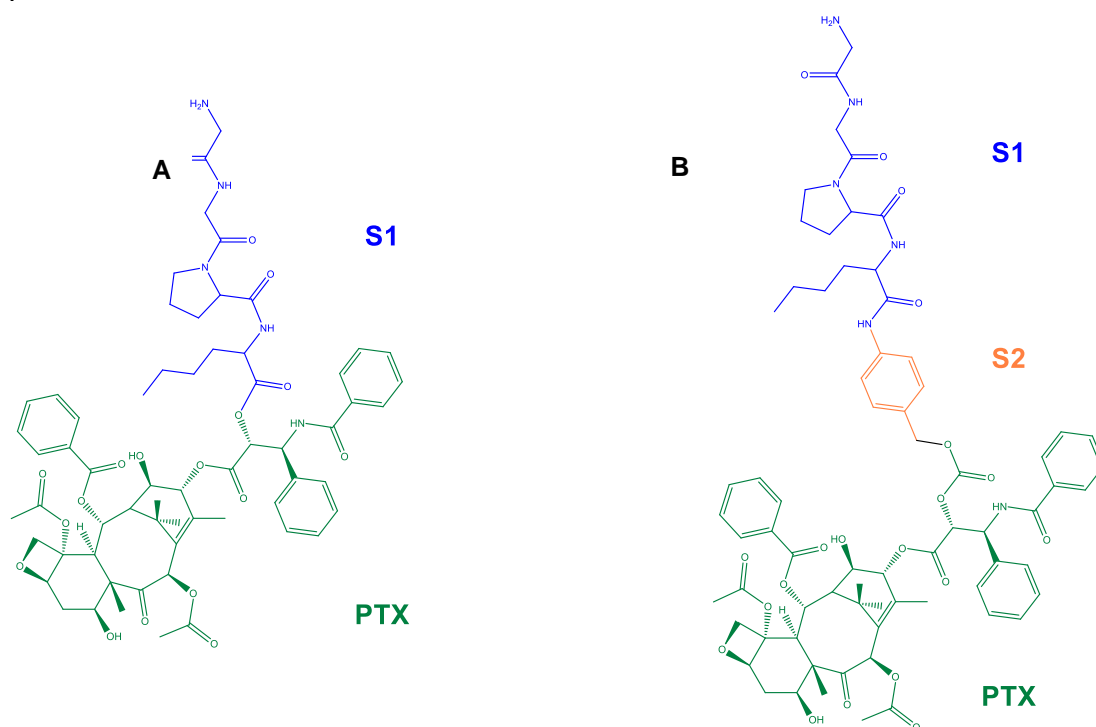
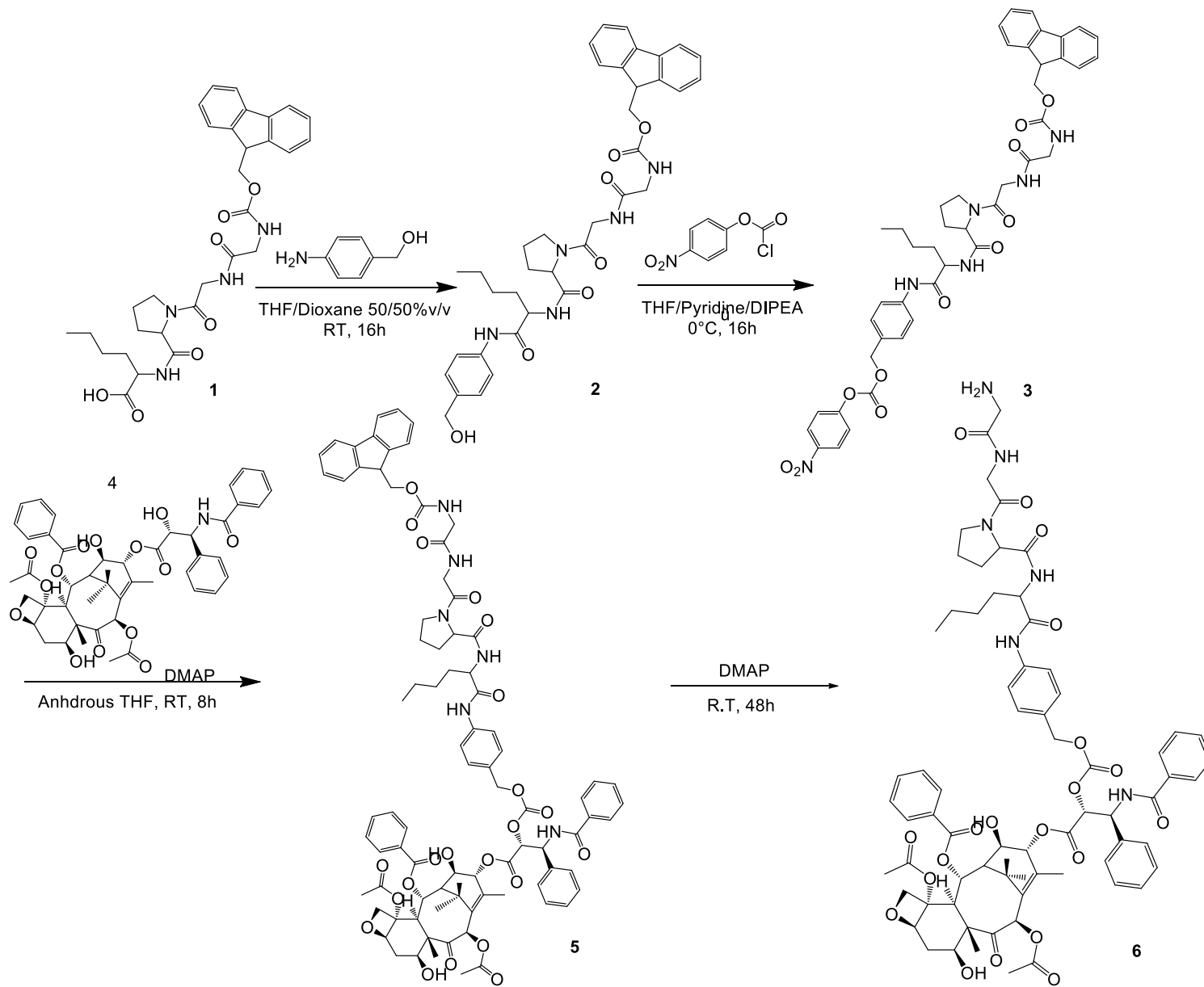


**Figure 3-7** Molecules designed for the synthesis of a Cathepsin K sensitive PTX prodrug. First design S1-PTX or NH<sub>2</sub>TPTX (A), second design S1-S2-PTX or NH<sub>2</sub>TφPTX (B)

In the following section, (T) will be used for the tetrapeptide GlyGlyProNle part of the prodrug and (φ) for the phenyl carbonate self immolative spacer. The detailed synthesis is described in Scheme 3-6.

Results



Scheme 3-6 Synthesis of the NH<sub>2</sub>T-PTX paclitaxel prodrug.

The previously synthesised (1.13.2) N-Protected tetrapeptide (T) FmocGlyGlyProNle (1) was mixed with isobutyl chloroformate in presence N-methylmorpholine. The carboxyl group was activated by the isobutylchloroformate to form a mixed carboxylic-carbonic anhydride intermediate. The intermediate was then reacted with 4-aminobenzyl alcohol to yield FmocT $\phi$ OH (2). The choice of solvent mixture tetrahydrofuran/dioxane was made in order to maximise the solubility of the tetrapeptide and ensure a successful coupling; traditional solvents such as chloroform, dichloromethane, tetrahydrofuran alone, and toluene were not able to dissolve to dissolve the tetrapeptide. The reaction temperature was lowered at -18°C in order to avoid the degradation of the tetrapeptide as observed at higher temperatures. Two column chromatography purifications allowed the separation of by-products from final products and starting materials. The first column chromatography using the highly hydrophobic hexane allowed the elimination of NMP originated by-products, while the second column chromatography used a mixture of acetone and ethylacetate (80/20%<sub>v/v</sub>) in order to separate the eventual non-reacted tetrapeptide from the product (2). The yield of the reaction was of 99%<sub>mol</sub>. Mass spectrometry (Figure 3-8) allowed to check the purity of FmocT $\phi$ OH and pursue to the next step.

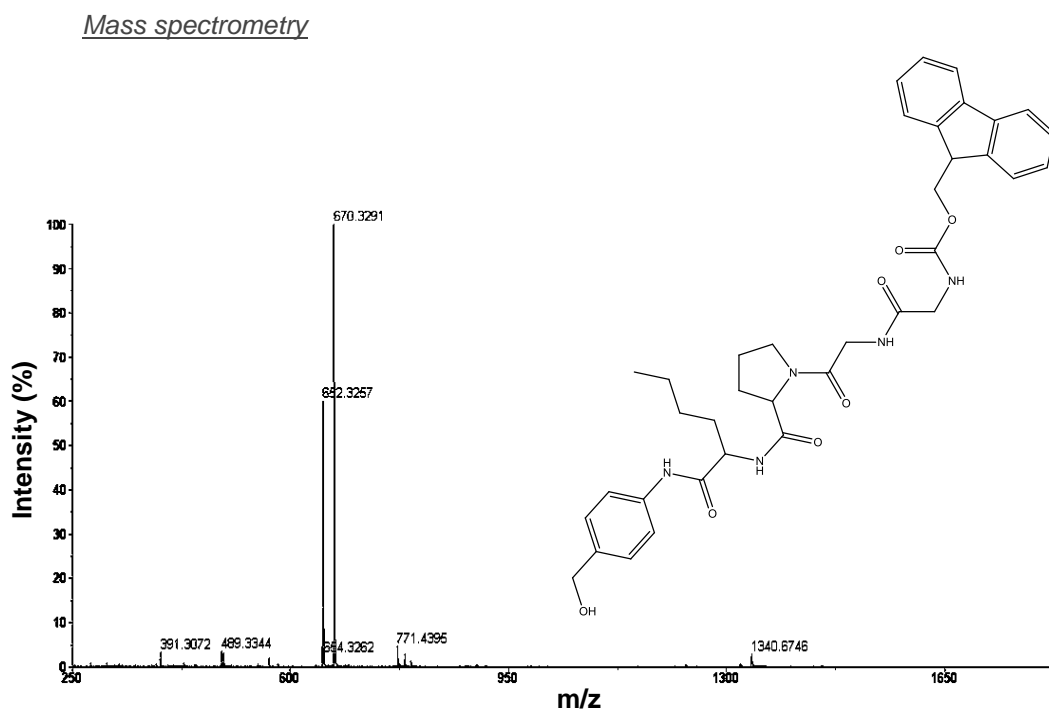


**Figure 3-8** Mass spectrometry (ESI-TOF, positive mode) of FmocT $\phi$ OH

The analysis by mass spectrometry (Positive mode, ESI-TOF) showed a peak at  $m/z=670,3291$  corresponding to the protonated modified tetrapeptide FmocT $\phi$ OH  $[M+H]^+$ . At

$m/z=652.3257$  was observed the dehydrated form  $[M-H_2O]^+$  of FmocT $\phi$ OH, and finally, at  $m/z=1340.6746$  was observed the aggregate of two modified tetrapeptides.

These results were considered satisfying to pursue to the next step as high purity was obtained, shown by the absence of starting material.

In a second step, the resulting benzylic alcohol FmocT $\phi$ OH (2) was activated with 4-nitrophenyl chloroformate in presence of pyridine and diisopropylethylamine to yield to yield the corresponding *p*-nitrophenyl carbonate FmocT $\phi$ NO<sub>2</sub> (3). The reaction was performed at 0°C under anhydrous conditions. In order to favour the formation of FmocT $\phi$ NO<sub>2</sub>, a large excess of *p*-nitrophenyl chloroformate was necessary. The reaction did not always reach completion. A probable explanation is the fast degradation of *p*-nitrophenyl chloroformate. The chloroformate was highly unstable in ambient environment; even if carefully conserved under nitrogen at 6°C, it degraded in 3 main products (a, b, c) as presented in Figure 3-9.

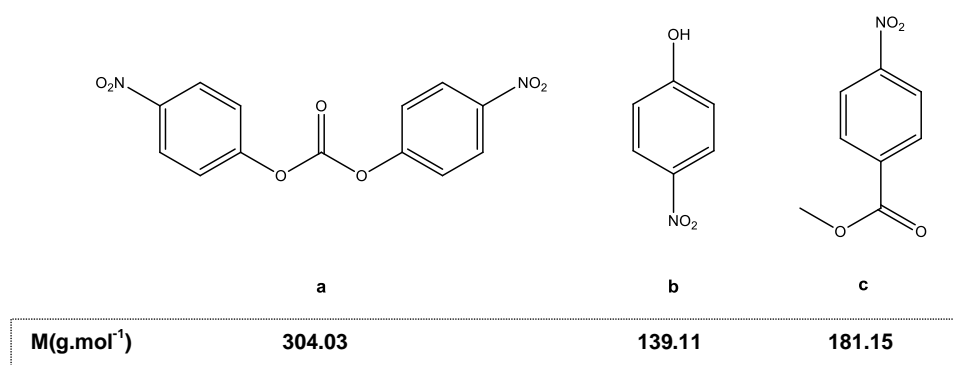


**Figure 3-9 Products of degradation of *p*-nitrophenyl-chloroformate (a, b, c)**

The best yield (44%<sub>mol</sub>) was obtained by double coupling; more specifically, a first coupling of FmocT $\phi$ OH with *p*-nitrophenyl chloroformate was performed followed by full purification (extraction and two silica gel chromatographies) and then a second coupling was performed in the same manner followed by full purification (extraction and two silica gel chromatographies).

The separation of FmocT $\phi$ OH and FmocT $\phi$ NO<sub>2</sub> was achieved by extraction in ethylacetate from a saturated solution of ammonium chloride after filtration, in order to remove pyridine and derivative by products soluble in water. The purification was then followed by two column chromatographies. The two compounds FmocT $\phi$ OH and FmocT $\phi$ NO<sub>2</sub> are very similar in term of polarity and it was always found some residual FmocT $\phi$ OH after purification as shown by the mass spectrometry in Figure 3-10 (positive mode, ESI-TOF).



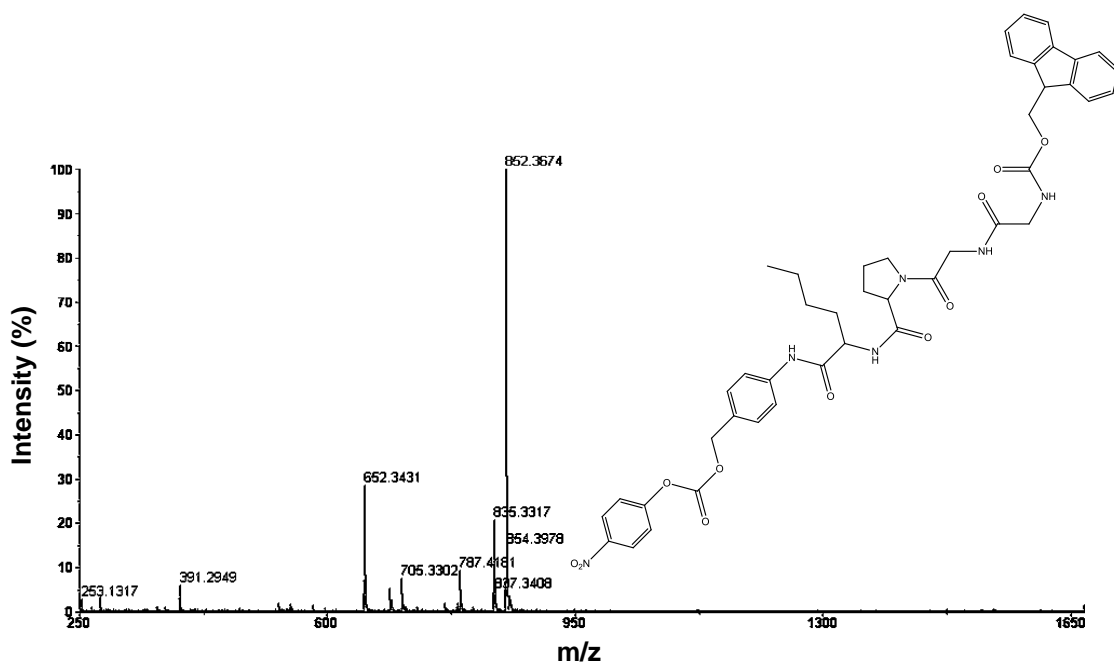


**Figure 3-10** Mass spectrometry (ESI-TOF, positive mode) of FmocT $\phi$ NO<sub>2</sub>

The analysis by mass spectrometry (Positive mode, ESI-TOF) showed a peak at  $m/z=852.3674$  corresponding to the protonated modified tetrapeptide FmocT $\phi$ NO<sub>2</sub> [M+H]<sup>+</sup>. At  $m/z=652.3431$ , was observed the dehydrated form [M-H<sub>2</sub>O]<sup>+</sup> of FmocT $\phi$ OH,

Mass spectrometry is not quantitative; consequently, it was not possible to determine the purity of FmocT $\phi$ NO<sub>2</sub>. <sup>1</sup>H NMR spectroscopy of FmocT $\phi$ NO<sub>2</sub> and FmocT $\phi$ OH were too similar to be able to distinguish characteristic peaks for **(2)** and **(3)** and quantify their ratio.

The presence of FmocT $\phi$ OH was not considered as an issue as it was hypothesised it should not react in the following step. Therefore, it was decided to move onto the next step where FmocT $\phi$ NO<sub>2</sub> was attached to paclitaxel **(4)** in presence of DMAP catalyst at room temperature. Paclitaxel was used in excess in order to optimise the yield of reaction and obtain FmocT $\phi$ PTX **(5)**.

The crude product was purified by column chromatography using hexane first, to remove PTX and then, ethylacetate/acetone (20/80%vol) to separate products from starting material **(3)**. The reaction yield was of 92%mol. The white product was analysed by TLC which revealed a strong spot for the product and no other spots from starting materials. The product was then examined by mass spectrometry (positive mode, ESI-TOF) presented in

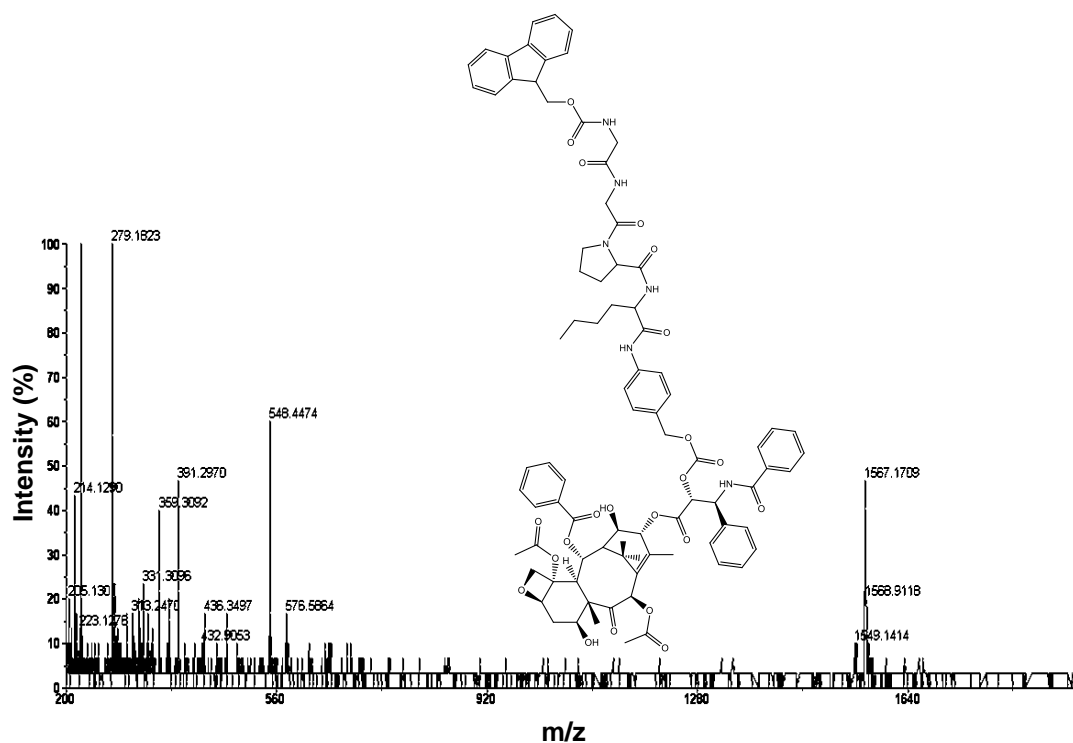


**Figure 3-11 Mass spectrometry (ESI-TOF, positive mode) of FmocT $\phi$ PTX**

The analysis by mass spectrometry (Positive mode, ESI-TOF) showed a peak at  $m/z=1549.1414$  corresponding to the protonated modified tetrapeptide FmocT $\phi$ PTX  $[M+H]^+$ . And at  $m/z=1567.1709$ , was observed the  $[M+NH_4]^+$  form of FmocT $\phi$ PTX.

FmocT $\phi$ PTX did not ionise easily in mass spectrometry, product ratios cannot be demonstrated in this analytical method. It was believed that the product purity was  $\geq 90\%$  as the reaction yield was high and TLC was clean. The presence of large phthalate peaks at  $m/z+=279.1823$ ,  $391.3130$  and  $548.4474$  coming from plasticisers (Diisobutyl phthalate, diisooctyl phthalate and Diisotridecyl phthalate respectively) of tools used in labs, represents only traces and show how much this type of analysis is not quantitative.

In the next step, FmocT $\phi$ PTX was deprotected to obtain NH<sub>2</sub>T $\phi$ PTX (**6**). Fmoc (9-fluorenyl-methyloxycarbonyl) amine protecting group is susceptible to be removed by weak bases. Usually, primary or secondary amines can be used. A first tentative was made using the classical method using a 20%<sub>v/v</sub> Piperidine/dichloromethane mixture where Fmoc is removed by piperidine which in turn scavenges the liberated dibenzofulvene to form a fulvene-piperidine adduct (Scheme 3-5).

The reaction was first carried out for 20min and revealed a degradation of FmocT $\phi$ PTX in several amino acid or combination of amino acid residues. The reaction time was then lowered to 10 then 5min but resulted to degradation of compound **(5)** in all cases.

Several other methods were experimented, such as the diisopropylethylamine/dichloromethane or ethanolamine methods, always varying the conditions of time for each one. In all cases, these reactions were too drastic for the deprotection of FmocT $\phi$ PTX as fragments of amino acids and paclitaxel were observed in mass spectrometry. Although fragmentation may occur in mass spectrometry analysis, in this present case, it was thought that the phenomenon was related to a degradation of the product as fragmentation by mass spectrometry did not occurred in the previous steps.

An innovative method (for that it is not reported in literature) was trialed using DMAP to deprotect FmocT $\phi$ PTX. The synthesis was monitored by mass spectrometry and TLC and showed that FmocT $\phi$ PTX primary amine gradually appeared, and the tetrapeptide structure was completely preserved since no fragments were measured in mass spectrometry: The method was validated.. After 48h, the product was precipitated in cold diethylether to yield a off-white product (80%<sub>mol</sub>) analysed by mass spectrometry (positive mode, ESI-TOF) as shown in Figure 3-12.

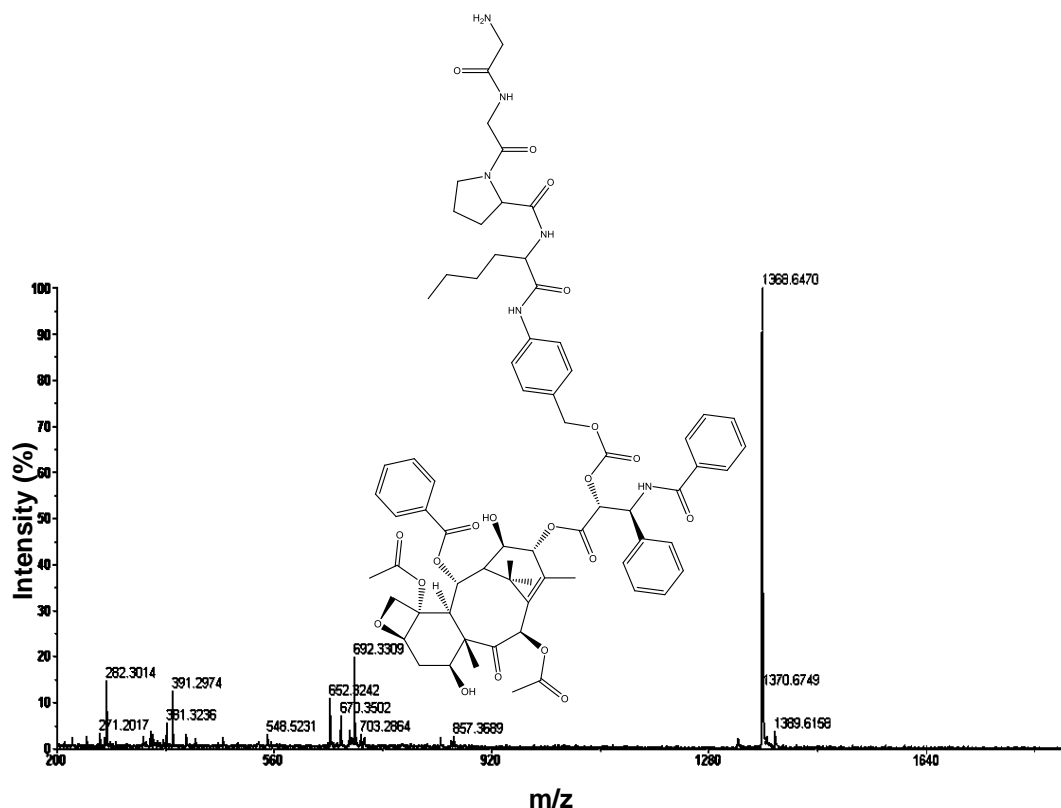


Figure 3-12 Mass spectrometry (ESI-TOF, positive mode) of  $NH_2T\phi PTX$

The analysis by mass spectrometry (Positive mode, ESI-TOF) showed a peak at  $m/z=1368.6470$  corresponding to the potassium ionised modified tetrapeptide  $\text{NH}_2\text{T}\phi\text{PTX}$ .

The synthesis was successful and the final  $\text{NH}_2\text{T}\phi\text{PTX}$  was kept for future attachment to the polymer carrier.

#### High Performance Liquid Chromatography (HPLC)

HPLC chromatograms of  $\text{NH}_2\text{T}\phi\text{PTX}$  and free PTX are showed in Figure 3-13. Retention time of both compounds obtained by RP-HPLC analysis, performed in identical conditions, were fundamentally different one from another.  $\text{NH}_2\text{T}\phi\text{PTX}$  eluted at  $t_R=12.783\text{min}$  while free PTX elution time was observed at  $t_R=7.797\text{min}$ . This was expected as the paclitaxel prodrug was less polar than the free drug due to the introduction of hydrophobic amino-acids (Gly, Pro, Nle) in the final structure. RP-HPLC demonstrated the high purity of  $\text{NH}_2\text{T}\phi\text{PTX}$  as well as the absence of free PTX peak.

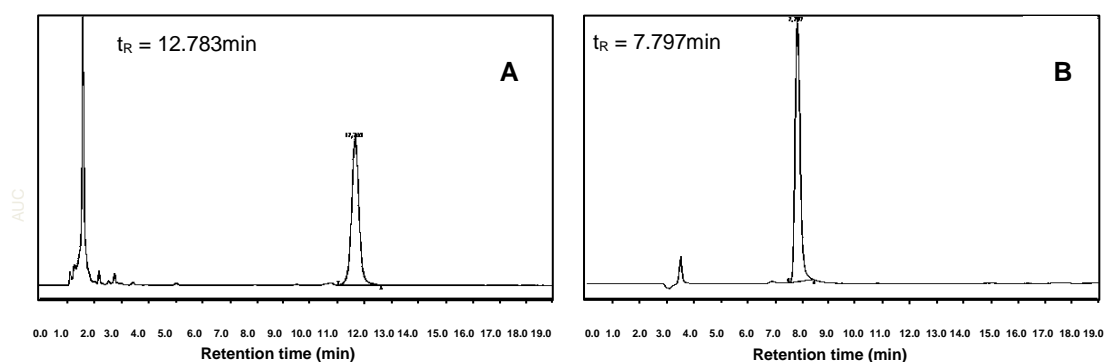


**Figure 3-13 HPLC chromatograms of  $\text{NH}_2\text{T}\phi\text{PTX}$  (A) and free PTX (B)**

The successful synthesis of the paclitaxel prodrug  $\text{NH}_2\text{T}\phi\text{PTX}$  allowed to continue on the next step, in the creation of the polysaccharide-drug conjugate aimed in this project. The next step was the synthesis of the targeting module based on the bisphosphonate alendronate.

#### **1.13.4 Targeting function: Synthesis of $\text{NH}_2\text{-PEG-Alendronate}$**

Several tactics were considered for the synthesis of the alendronate prodrug FmocGlyGlyProNleAlendronate including, N,N'-dicyclohexylcarbodiimide (DCC) coupling in presence of 4-(dimethylamino)pyridine (DMAP) catalyst, and 1-ethyl-3-(3-dimethylaminopropyl) carbodiimide (EDC) coupling in presence of DMAP, solution phase O-Benzotriazole-N,N',N'-tetramethyl-uronium-hexafluoro-phosphate / Hydroxybenzotriazole (HBTU/HOBt) coupling, EDC in presence of N-hydroxysuccinimide

(NHS) coupling, 4,5-dihydrothiazole-2-thiol (TT) in presence of DCC coupling, pH were varied from 7 to above 11. These synthesis trials were not successful since they did not lead to the desired product<sup>55</sup>.

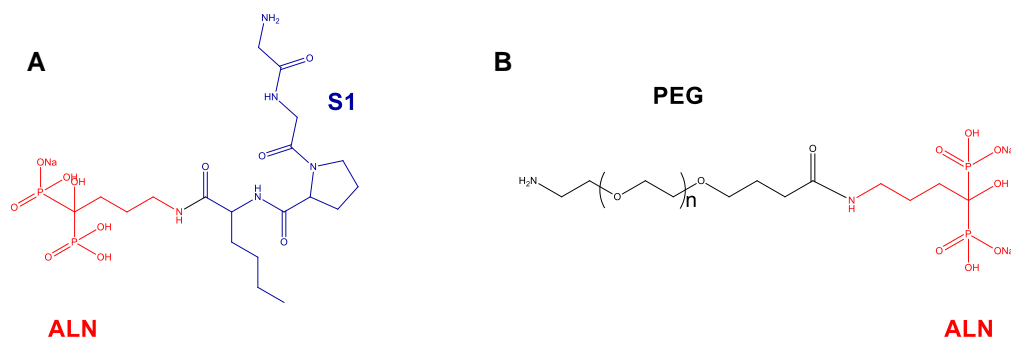
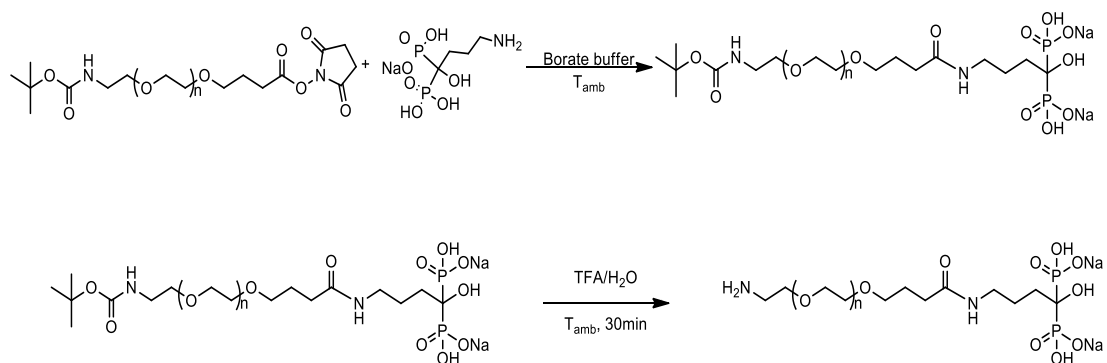


**Figure 3-14** Molecules designed for the synthesis of a Cathepsin K sensitive ALN prodrug. First strategy S1-ALN (A), second strategy PEG-ALN (B)

A new approach was elaborated, which would include a relatively low molecular weight poly(ethylene glycol) (PEG) in the alendronate derivative. By attaching the PEG in its form tBoc-NH-PEG-NHS to alendronate first, tBoc-NH-PEG-alendronate (tBocPEGALN) would be produced and facilitate the attachment of this first compound to the pullulan backbone after tBoc deprotection as described in Scheme 3-7. The bone targeting function of the final polymer-drug conjugate would be maintained.



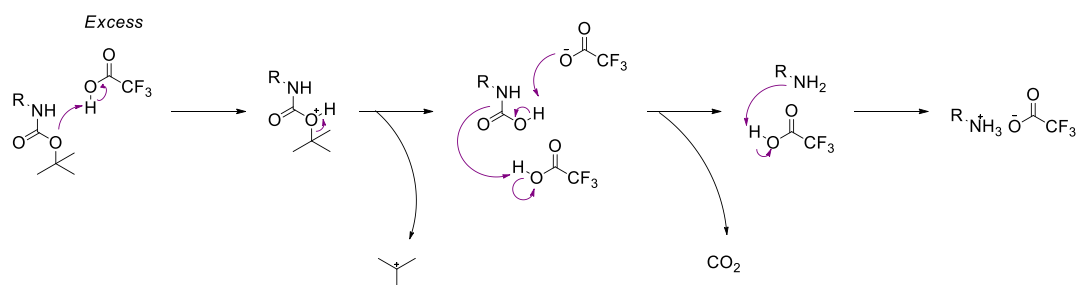
The reactive N-hydroxysuccinimide-ended PEG was directly coupled to alendronate primary amine to form an amide bond yielding tBocPEGALN, releasing N-hydroxysuccinimide (NHS) which was easily removed by dialysis. This reaction is strongly dependant on the pH conditions so it was chosen to perform the modification at pH 8.5. A low pH was not recommended as the alendronate primary amine group would be

protonated and the reaction would not take place. On the contrary, a too high pH would increase the rate of hydrolysis.

Dialysis to remove excess, unreacted alendronate and by-products was used. The absence of free alendronate was verified by TNBS assay which revealed to be negative.

The amine protected tBocPEGALN was finally deprotected using a mixture of Trifluoroacetic acid (TFA)/dichloromethane (50/50%v/v) to yield NH<sub>2</sub>PEGALN. The generally accepted mechanism for the cleavage of the Boc group under acidic conditions involves the formation of carbon dioxide, and a tert-butyl cation resulting in a carbamic acid. Decarboxylation of the carbamic acid leads to the free amine.

#### <sup>1</sup>H NMR spectroscopy



#### **Scheme 3-8 General mechanism of deprotection of tBoc protected amine by TFA**

<sup>1</sup>H NMR spectroscopy (prior to dialysis) confirmed the full tBoc removal as its characteristic peak disappeared at  $\delta = 1.23$  ppm and shifted to 1.53 ppm and the formation of a NH<sub>2</sub> was shown with its distinctive protons at  $\delta = 4.65$  ppm.

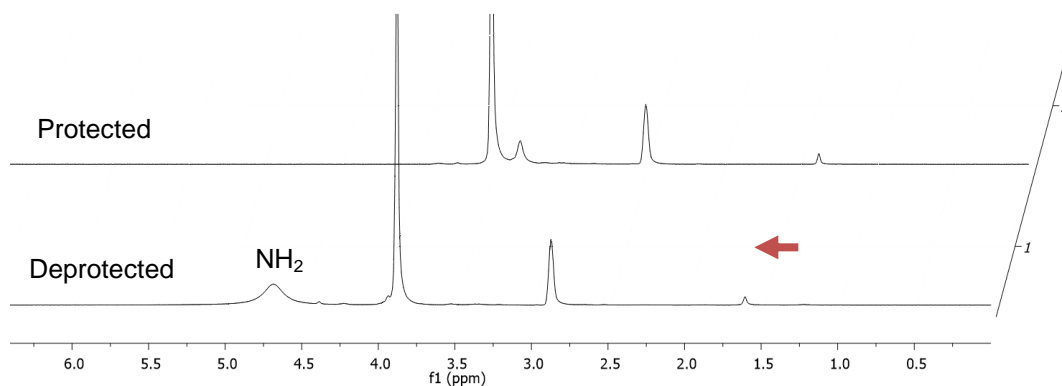


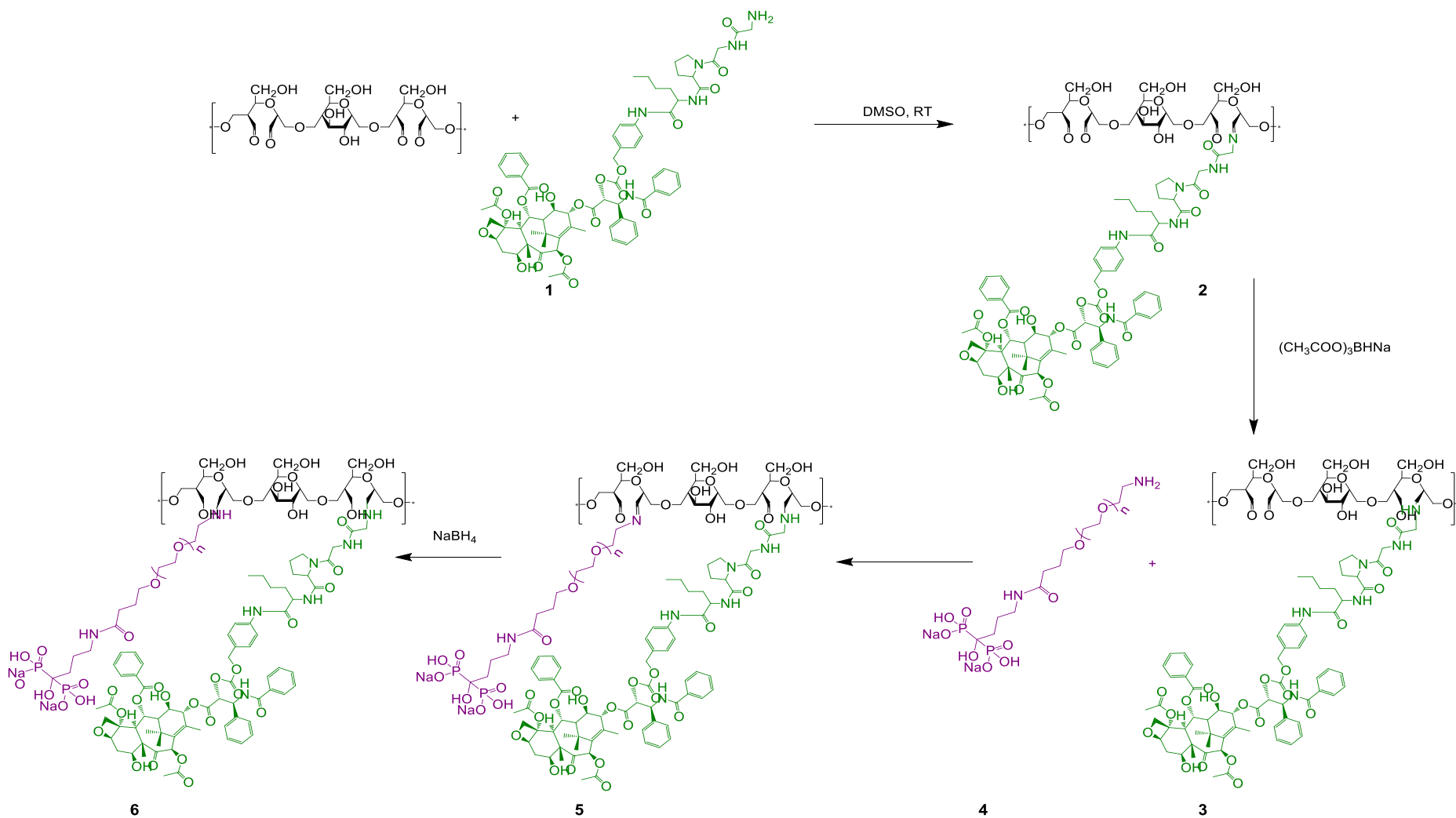
**Figure 3-15 <sup>1</sup>H NMR spectra in DMSO of protected and deprotected PEGylated alendronate**

The content of NH<sub>2</sub>PEGALN conjugate was determined by spectrophotometry by formation of a complex between alendronate and ferric ions (Fe(III)) in perchloric acid solution. The measure of the complex absorbance was performed by UV at  $\lambda=280\text{nm}$ . The quantification of alendronate in the conjugate was verified against a calibration curve. It was found a maximum alendronate content of 24%<sub>mol</sub> of alendronate in the conjugate. This low value could be explained by the strong competition with hydrolysis due to experimental conditions.

The synthesis could only and strictly be performed in aqueous environment as alendronate is only soluble in water. However, in these conditions, the active N-hydroxysuccinimide was very easily hydrolysable. Optimal conditions could be reached by use of anhydrous organic solvents instead of an aqueous environment if the solubility of alendronate allowed it. An additional reason for low alendronate content could also be due to the pH conditions. Although the reaction pH is optimal at around 8.3-8.5 when using NHS esters, it is important to note that this pH is a lot lower than the pKa of the alendronate primary amine group which is of 11. This means that at pH 8.5, the amine is protonated and the reaction of esterification becomes less favourable. In spite of this low alendronate concentration, the PEGylated alendronate was kept for further coupling onto the polymer backbone as the bisphosphonate is very potent and should play its role of targeting agent even in a small amount as reported in literature.

#### **1.13.5 Polymer therapeutics: Synthesis of Pullulan-Paclitaxel-Alendronate (Pull-PTX-ALN)**

Formerly synthesised paclitaxel and alendronate prodrugs were both conjugated to the modified pullulan by formation of a carbon-nitrogen double bond (Schiff base) followed by a selective reduction with sodium borohydride as described in Scheme 3.9.



Scheme 3-9 Synthesis of Pull-PTX-ALN



In a first step,  $\text{NH}_2\text{T}\phi\text{PTX}$  (**1**) was reacted onto oxidised Pullulan  $\text{Pull}_{\text{ox}30}$  in dimethylsulfoxide (DMSO) to form a Schiff base (**2**). The unstable bound is part of an equilibrium which is unfavourable for the successive reactions. Consequently, compound (**2**) was stabilised using sodium acetoxyborohydride, known selective reducing agent for imines<sup>56</sup>: the polysaccharide Schiff bases were reduced to stable secondary amines (**3**) while aldehyde groups remained available for further conjugation. Subsequently, a large excess of  $\text{NH}_2\text{PEGALN}$  (**4**) was added to the polymer mixture (**3**), followed by stabilisation with sodium borohydride which reduces the newly formed Schiff bases of compound (**5**) to simultaneously convert the unreacted aldehyde groups into alcohol groups and give the final compound (**6**) named Pull-PTX-ALN.

### GPC

The gel permeation chromatography analysis of the Pull-PTX-ALN showed a molecular weight  $M_w$  of 89124Da and a polydispersity index (PDI) of 1.88 as shown in Figure 3-16.

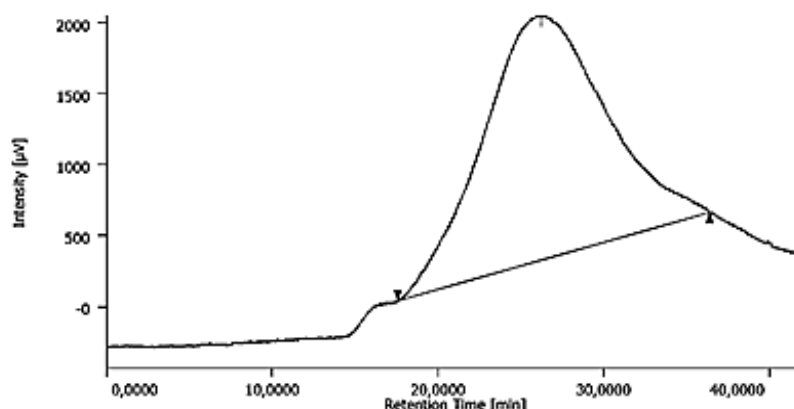


**Figure 3-16 GPC traces of Pull-PTX-ALN against Pullulan standards**

### Fourier Transform Infrared Spectroscopy (FT-IR)

The FT-IR spectra of Pull-PTX-ALN showed the disappearance of the strong  $\text{C}=\text{O}$  stretching band from the aldehyde ( $\text{Pullox}_{30}$  starting material) and the appearance of two strong characteristic bands at approximately  $1250\text{-}1100\text{ cm}^{-1}$  and  $1100\text{-}900\text{ cm}^{-1}$ , due to the vibrations ( $\text{P}=\text{O}$ ) ( $1200\text{-}1160\text{ cm}^{-1}$ ), ( $\text{P}-\text{OH}$ ) ( $\approx 1000\text{ cm}^{-1}$  and  $\approx 925\text{ cm}^{-1}$ ) and  $\delta(\text{POH})$  (around  $1080\text{ cm}^{-1}$ ) bands of the bisphosphonate alendronate.

Stretching bands were observed over the  $\nu(\text{O}-\text{H})$  band. The  $\nu(\text{O}-\text{H})$  band also overlapped with the very large and weak  $\nu(\text{PO}-\text{H})$  and  $\delta(\text{POH})$  bands, with maximum around  $2600\text{-}2800\text{ cm}^{-1}$ .

The amide band (between 1600 and 1700  $\text{cm}^{-1}$ ) was mainly associated with the C=O stretching vibration and related to the N-H from the tetrapeptide spacer GlyGlyProNle.

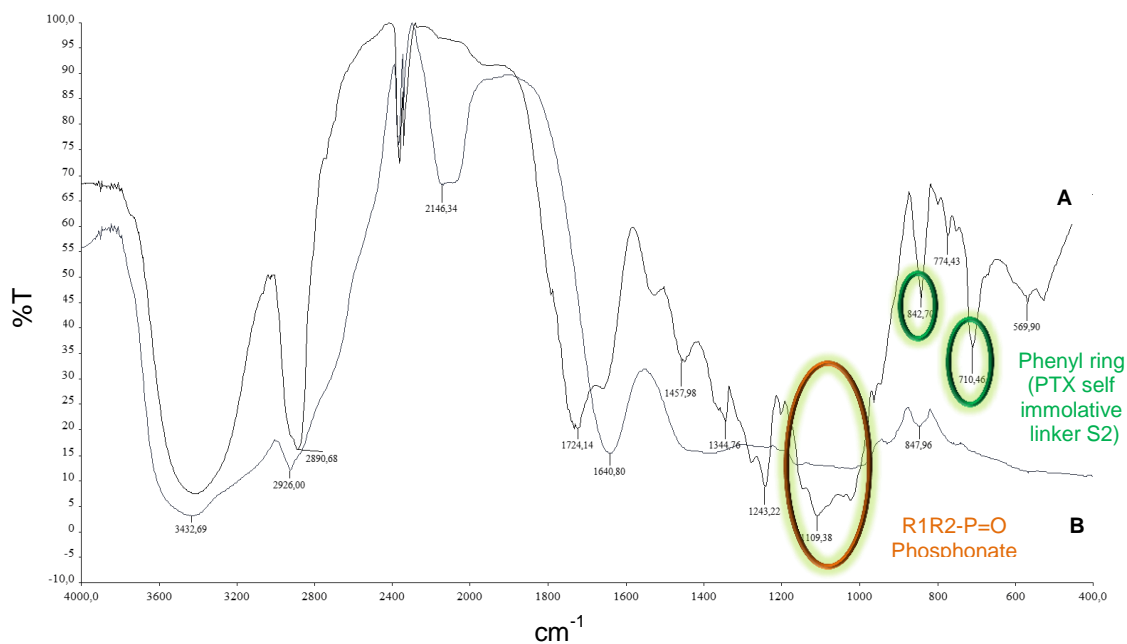


**Figure 3-17** FT-IR spectra of Pull-PTX\*ALN (A) and native Pullulan (B)

#### RP-HPLC characterisation

Pull-PTX-ALN was characterised by reverse phase chromatography to control its purity. As shown in Figure 3-18, the retention time obtained for Pull-PTX-ALN ( $t_R=18.093$  min) varied from free PTX ( $t_R= 7.840$  min) while native Pullulan was not detectable as expected. These results indicated a good purification of product and the absence of free PTX.

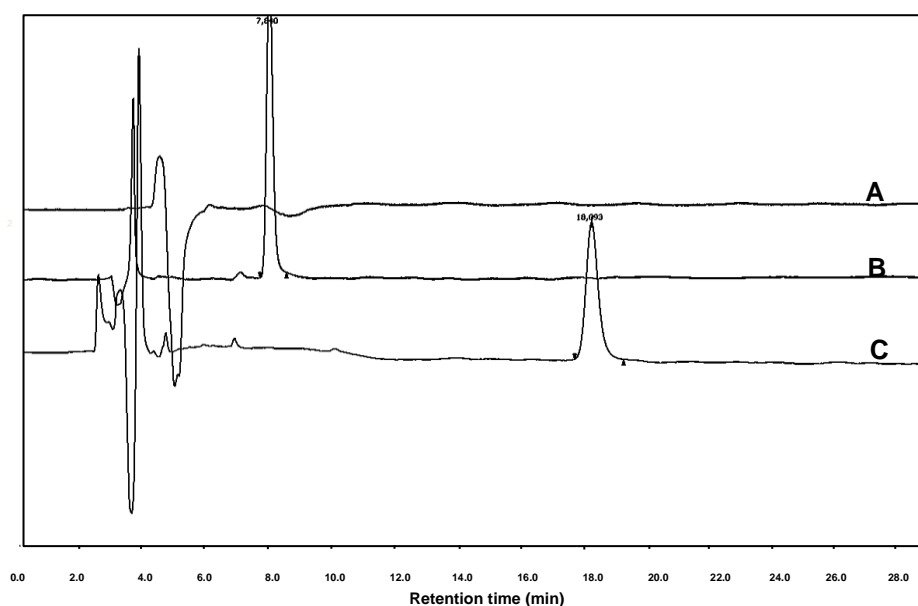


**Figure 3-18** HPLC chromatograms of native Pullulan (A) free PTX (B) and Pull-PTX-ALN (B)

The success of the synthesis of final polymer-drug conjugate Pull-PTX-ALN allowed to make further studies for understanding its physico-chemical properties and its properties on cancerous cells. The subsequent sections will investigate Pull-PTX-ALN in details, from its composition to its anti-tumour and anti-angiogenic properties without forgetting the study of its stability.

## 1.14 Properties of Pull-PTX-ALN

### 1.14.1 Solubility of Pull-PTX-ALN

The solubility of Pull-PTX-ALN was assessed by preparing sequential dilution of a polymer-drug suspension of known composition. The picture in Figure 3-19 shows the solubility of the free drug paclitaxel and Pull-PTX-ALN in water. The quantity of compound was normalised to get an equivalent amount of paclitaxel for both tests.

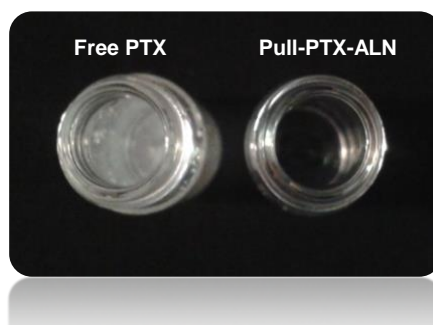


**Figure 3-19 Solubility of the free drug paclitaxel (left) and PullPTXALN (right) in ultrapure water at room temperature**

The final nano-carrier solubility was of about 513 $\mu\text{g/ml}$  equivalent paclitaxel which was 500 times higher solubility than the free drug, an encouraging result for one of the purpose of the project; to increase the solubility of the highly hydrophobic drug paclitaxel (free paclitaxel has a low water solubility of approximately 0.3 $\mu\text{g/ml}$ )<sup>57</sup>.

### 1.14.2 Identification of the polymer-drug conjugate composition

#### UV-VIS determination of ALN and PTX content

As showed in Figure 3-20 and Figure 3-21, Pull-PTX-ALN spectrum (–) was superimposable to free ALN and free PTX spectra indicating that the ALN and PTX attachment to the pullulan backbone through a spacer did not compromise the physicochemical characteristic of the drug in UV-VIS spectroscopy.

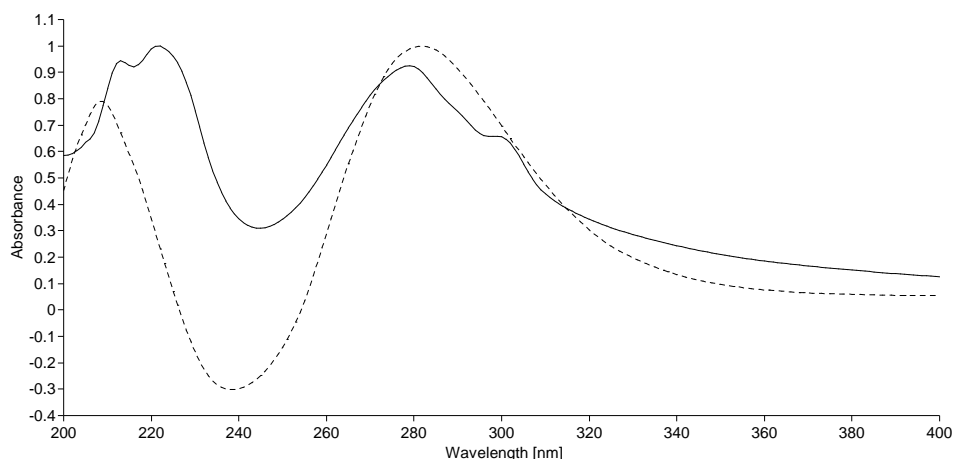


**Figure 3-20 UV-VIS spectra in perchloric acid of Pull-PTX-ALN (–) and ALN (---) after complexation with  $Fe^{3+}$**

UV-VIS determination of PTX content

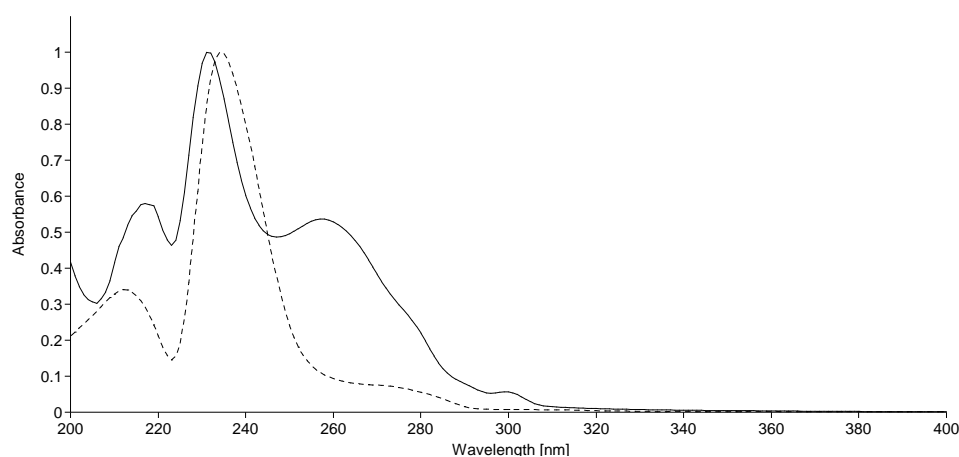


**Figure 3-21 UV-VIS spectra in MeOH of Pull-PTX-ALN (–) and PTX (---)**

Results obtained via spectrophotometry after complexation of Pull-PTX-ALN with Fe (III) indicated an alendronate weight percentage of 1.6%<sub>w/w</sub> while the quantity of paclitaxel present onto the polymeric carrier was of 7.8%<sub>w/w</sub> in weight corresponding to our initial loading target. The %<sub>w/w</sub> was also confirmed by another method using RP-HPLC using PTX as calibration standards.

Summary Pull-PTX-ALN composition

The composition of Pull-PTX-ALN is summarised in Table 3-2. These data were used as reference all through the cell studies.

**Table 3-2 Composition of Pull-PTX-ALN in comparison with non-modified pullulan**

		Pull-PTX-ALN composition	Native Pullulan
Mw (DA)	SEC	89124	104000
PDI	SEC	1,88	1.92
% <sub>w/w</sub> Alendronate	UV-VIS (complexation with Fe(III))	1.6	0
% <sub>w/w</sub> Paclitaxel	UV-VIS	7.8	0

It is worth noting that higher loading of paclitaxel onto the polymer backbone was attempted to identify the maximum conjugation capacity. The NH<sub>2</sub>T<sub>φ</sub>PTX:Pullo<sub>x</sub><sub>30</sub> ratios were varied from 2:100, 5:100 10:100 to 20:100. The value of 7.8%w/w of PTX reported above was the maximum conjugation obtained.

### 1.14.3 Molecular size and surface charge of conjugates

The hydrodynamic diameter and size distribution profile of Pull-PTX-ALN conjugate was evaluated using Dynamic Light Scattering (DLS).

The mean hydrodynamic diameter of the nano-carrier in PBS, pH5.5 was of 163.30±18.25nm and the polydispersity index (PDI) was of 0.20±0.02. In water the particle size was of 100.2±7.3 nm and the PDI of 0.17±0.03nm. Finally, in PBS, pH7.4 the particle size was of 69.88±6.27nm and the PDI of 0.15±0.01 (Figure 3-22).

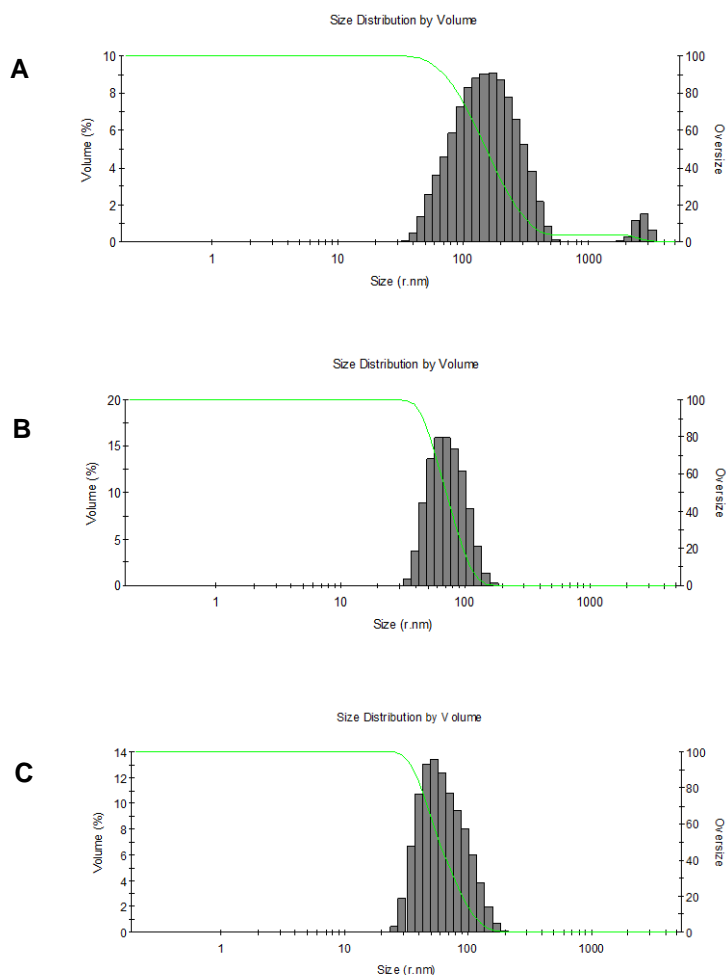


**Figure 3-22 Size analysis by DLS of Pull-PTX-ALN in PBS, pH5.5 (A) at 25°C in water (B) at 25°C and in PBS, pH 7.4 (C) at 25°C**

This particle size was in agreement with the recommended size to allow drug delivery to the bone, considering the anatomical fenestrations of the bones known to be between 80nm and 150nm.

As a control, a solution of native Pullulan in water was analysed in the same conditions as for Pull-PTX-ALN and demonstrated that the unconjugated polymer was of about 10nm; meaning ten times smaller than the conjugated one (Figure 3-23).

This result suggested the formation of self-assemblies of the polymer-drug conjugate in solution.

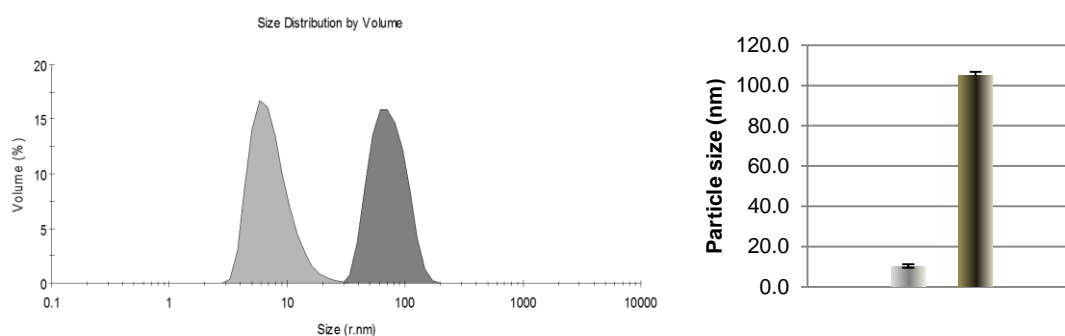


**Figure 3-23 Comparison of the size by DLS of native pullulan (-) and the Pull-PTX-ALN (-) conjugate in water at 25°C**

Measure of the Zeta potential

The  $\zeta$ - potential of the Pull-PTX-ALN conjugate was measured in water to evaluate the global charge on the polymer surface at pH 7.4 in HEPES.

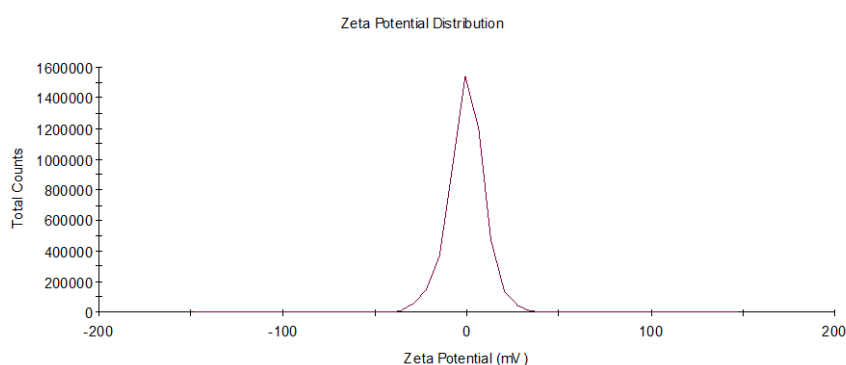


**Figure 3-24  $\zeta$ - potential of Pull-PTX-ALN in water at 25°C**

The analysis indicated that the polymer-drug conjugate had a  $\zeta$ - potential of  $-0.33967 \pm 0.247308$  mV which could be considered neutral and was as expected.

#### 1.14.4 Stability of polymeric structures in buffer solutions at different pH over time

Pull-PTX-ALN conjugate solutions were prepared in water (pH6) and in buffers at different pH. The first pH selected was pH5.5 to mimic the acidic bone lacunae at the tumour site where the drug should be released, and pH7.4 to simulate the pH value prevalent in plasma.

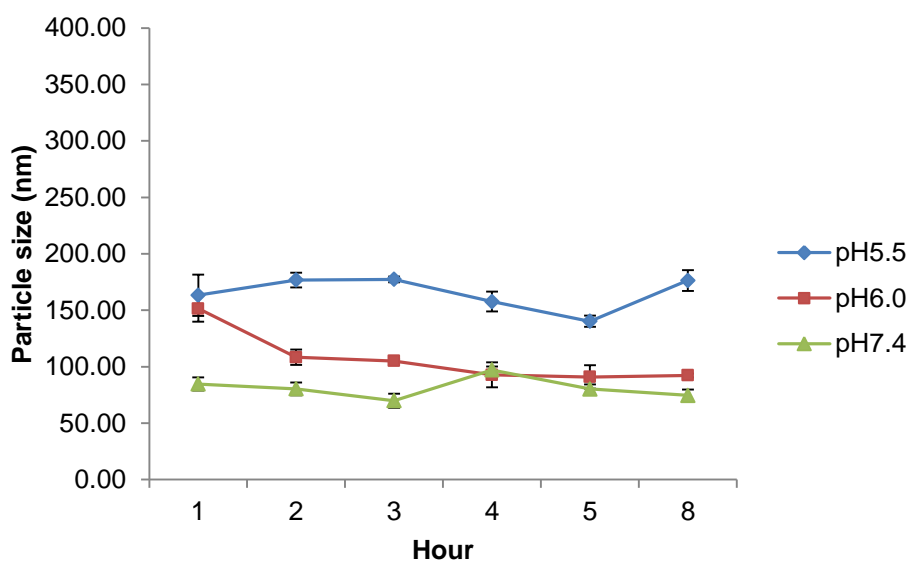


Figure 3-25 Size-time course profiles of Pull-PTX-ALN at 25°C at pH5.5(◆), 6.0(■)and 7.4(▲)

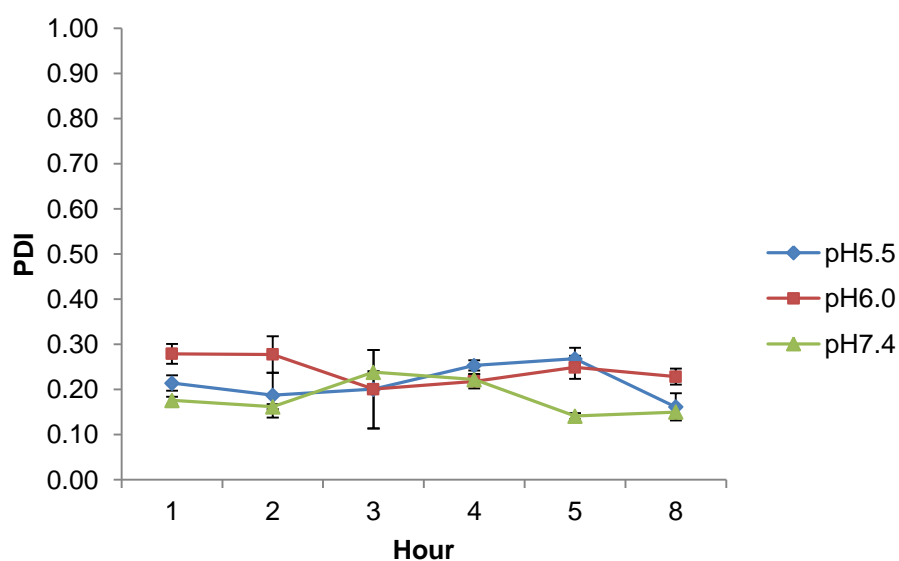
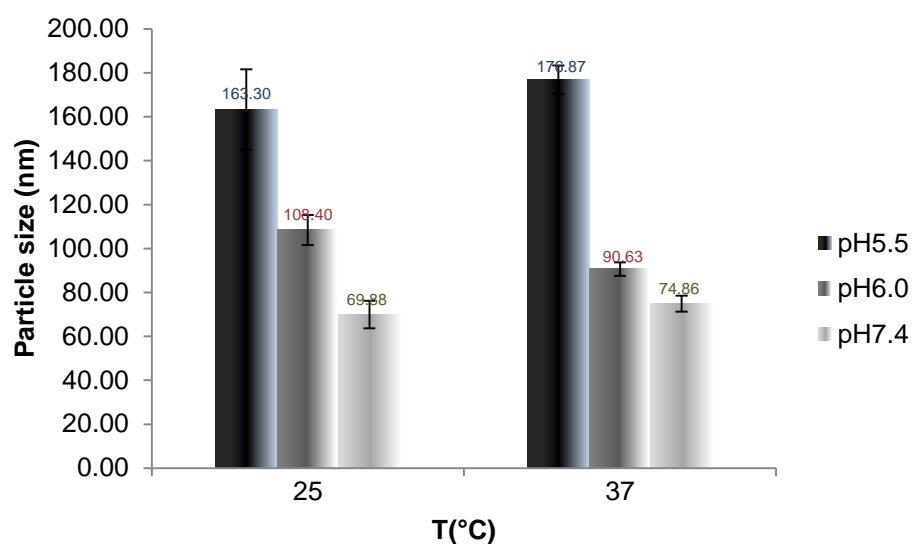


Figure 3-26 Polydispersity-time course profiles of Pull-PTX-ALN at 25°C at pH5.5(◆), 6.0(■) and 7.4(▲)

The size of self-assemblies and polydispersity index was monitored over time and showed that both at acidic and plasma pH, the nanoparticles were completely stable over 8h. This was expected as, on the assumption that paclitaxel remains on the polymeric carrier, the solubility of the overall colloid should not change. Indeed, as the equilibrium between hydrophilic and hydrophobic fragment is maintained, the assembly should be stable. This stability in time was important as the conjugate was designed to only release paclitaxel in the presence of Cathepsin K. after it travels to the target site was reached.

#### 1.14.5 Stability of polymeric structures in buffer solutions at different T°C

The stability of Pull-PTX-ALN at room temperature (25°C) and physiological temperature (37°C) was also examined by monitoring the size of the self-assemblies at these temperatures, using DLS.



**Figure 3-27** Size-temperature of Pull-PTX-ALN at 25°C and 37°C and at pH5.5, 6.0 and 7.4

The analysis confirmed that the particles were stable at both temperatures, independently of the pH of the solution.

#### 1.14.6 Critical micellar concentration

The Critical Micellar Concentration (CMC) is defined as the definite concentration above which polymeric micelles form in aqueous solution.



At the CMC, polymers containing a hydrophobic part and a hydrophilic fragment may assemble in an ordered manner in order to minimise the contact of the hydrophobic fragment with water molecules, leading to a core-shell micellar structure.

The fluorescent probe pyrene was chosen for the determination of the CMC. This non-polar poly-aromatic molecule preferably partitions from a hydrophilic to more hydrophobic environment which would be the core of the polymeric micelles, leading to a change in its fluorescent properties translated by a red shift in the excitation spectrum<sup>58</sup> (Figure 3-28).

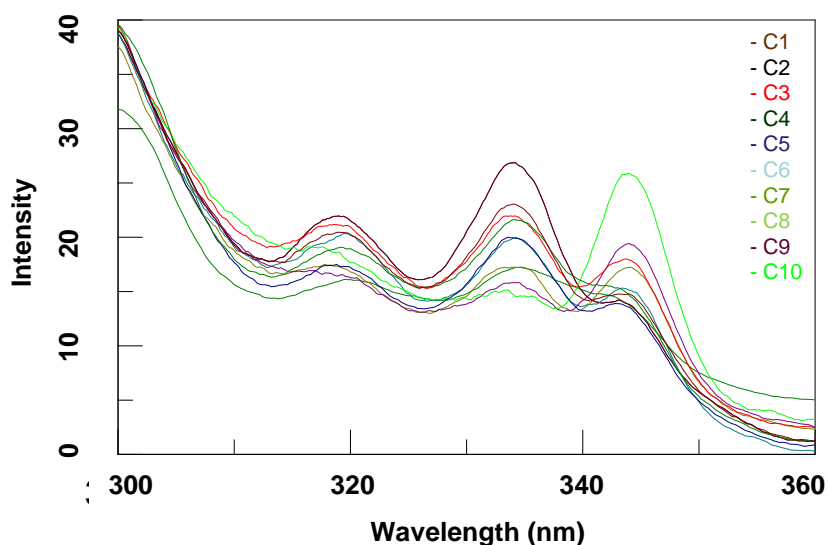


**Figure 3-28 Determination of CMC using a pyrene probe – Spectra at increasing concentration of polymer drug conjugate Pull-PTX-ALN**

The CMC of polymeric micelles can be described as the turning point of these modifications at the increase of polymer concentration.

The CMC of Pull-PTX-ALN was determined by way of the fluorescence intensity of pyrene as a function of the logarithm of the polymer concentration in PBS (20mM, pH7.4) (Figure 3-29).

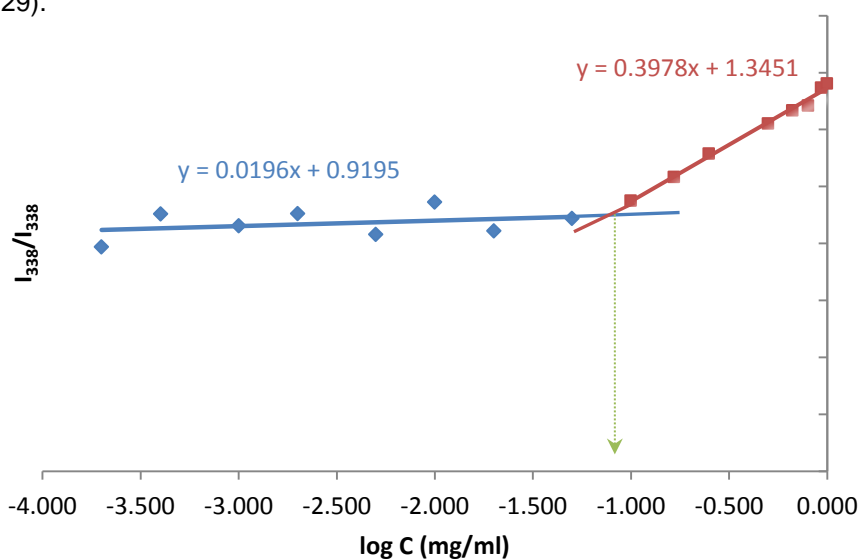


**Figure 3-29 critical micellar concentration of the Pull-PTX-ALN**

At low polymer concentration, low pyrene intensity was observed. Above a precise polymer concentration, a rapid rising in pyrene fluorescence intensity ratio was observed. The critical micellar concentration of the final polymer-drug conjugate Pull-PTX-ALN was obtained at 73.3 $\mu$ g/ml, considered as low CMC and suitable for drug delivery as to consider the dilution into plasma after injection of the drug.

#### 1.14.7 Transmission electron microscopy (TEM)

A Pull-PTX-ALN solution was prepared in water at a concentration of 1.5mg/ml, above the CMC, to confirm the presence of self-assemblies and determine their morphology.

The nanoparticles were visualised by TEM. Spherical structures with a narrow size distribution were observed, confirming the organisation of the polymer-drug in micellar structure.

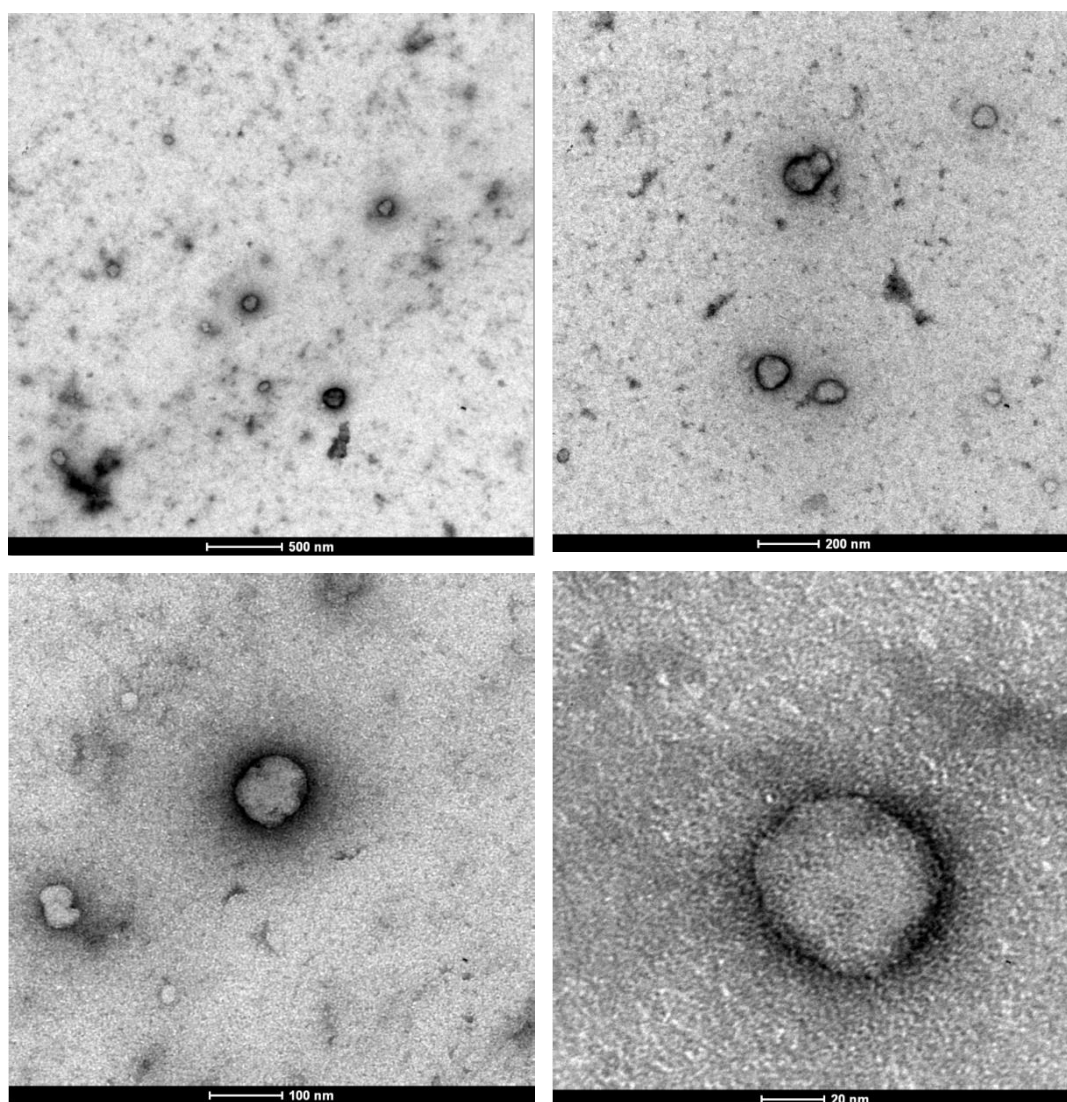


**Figure 3-30 TEM images of Pull-PTX-ALN micelles in water**

The average overall size of Pull-PTXALN micelles was approximately 90-135nm, which was in good agreement with the molecular size determined by DLS.

## 1.15 Pull-PTX-ALN: In-Vitro assays

### 1.15.1 Hydroxyapatite binding assay

Hydroxyapatite, main constituent of the bone, is particularly exposed in lysis sites when metastases reach bone tissues. Bisphosphonate show a strong affinity for the bone mineral as well-acknowledged in the literature. Alendronate, belonging to the bisphosphonate family and chosen in this project, has an especially strong affinity towards bone tissues. This characteristic is due to the presence of its phosphonate groups and hydroxyl groups.

The binding capacity of Pull-PTX-ALN and Pull-PTX polymer conjugate and free alendronate to bone mineral through ALN was assessed at the physiological temperature of 37°C. Hydroxyapatite was used as a model mineral simulating bone tissues.

The conjugates were incubated with the bone mineral HA for 0, 10, 30, 60, 120 and 180 and 480min.

Samples were taken at the specified time points and analysed by UV spectrophotometry by quantifying separately the alendronate concentration in the supernatant, after complexation with Fe(III) ions and paclitaxel by direct reading. Both analyses allowed the quantification of the non-bounded polymer in the supernatant. Results from both methods were confronted and gave same profiles. Pullulan bound to PTX (Pull-PTX) through the same peptidyl and self-immolative linkers as for Pull-PTX-ALN was synthesised, to use as reference for this test and following assays. The quantity of PTX on the polymer backbone was equivalent to the quantity used for the synthesis of Pull-PTX-ALN.

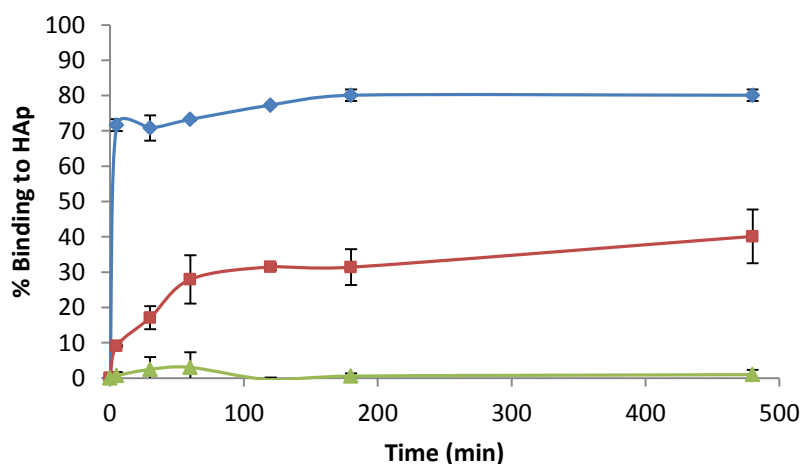


**Figure 3-31 Binding kinetics of ALN, (◆)Pull-PTX-ALN(■), Pull-PTX (▲) to the bone mineral hydroxyapatite at the temperature of 37°C and pH 7.4**

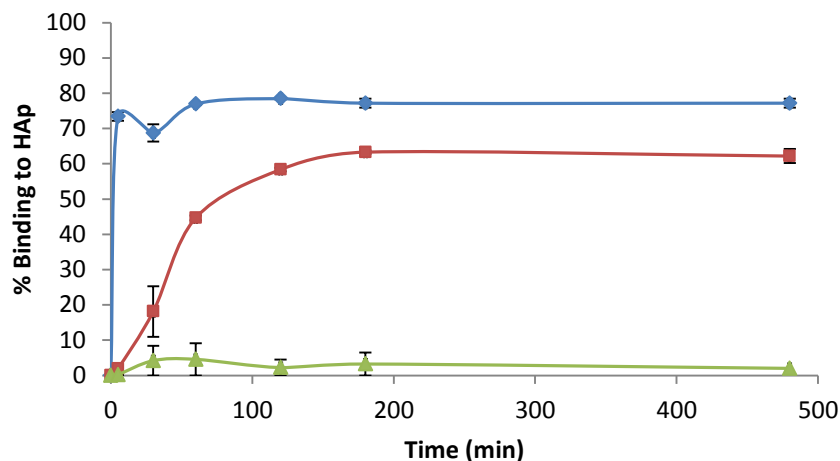


**Figure 3-32 Binding kinetics of ALN, (◆)Pull-PTX-ALN(■), Pull-PTX (▲) to the bone mineral hydroxyapatite at the temperature of 37°C and pH 5.5**

After 5 min of incubation, 80% of free alendronate was bound to HAp to reach a plateau between 75 and 80%. The pH of incubation did not affect the binding of free alendronate.

Pull-PTX-ALN was bound to hydroxyapatite at a different rate and ratio in respect to free alendronate. It was also noticed variations in the binding capacity of the polymer conjugate, depending on the pH of incubation. Indeed, after 30min at pH 7.4, 30% of polymer conjugate linked to the bone mineral and reached a plateau of around 40% binding. When decreasing the pH to 5.5, pH simulating tumour tissues, approximately 45% Pull-PTX-ALN was bound to hydroxyapatite after 30min, against 30% at pH 7.4, and a plateau was reached after around 65% binding.

The polymer conjugate Pull-PTX, exempt of alendronate, did not bind at all to hydroxyapatite as expected.

The results indicate that the Pull-PTX-ALN conjugate can accurately and rapidly target the bone tissue lysis sites.

### 1.15.2 Drug release in-vitro assay

In this project, the polymer-drug conjugate was designed so that it would release the unmodified form of the anti-tumour drug paclitaxel at the target site. The enzyme triggered release occurs in several consecutive steps (cascade reaction). Primarily, the peptide Gly-Gly-Pro-Nle should rearrange in the subsites of the active site of Cathepsin K; the amide bond between Gly and Pro would be cleaved. Consecutively, the amide bond between norleucine and 4-aminobenzyl alcohol moiety would break apart to finally free the unmodified paclitaxel after an 1,6-elimination.

The drug release assay was performed at 37°C and pH5.5, mimicking the physiological tumour environment. The HPLC traces showed a shift to the left of the polymer-drug conjugate from 18min to 15min at a flow rate of 0.7ml.min<sup>-1</sup>, demonstrating an increase of hydrophilicity due to the loss of paclitaxel. It was assumed that the paclitaxel peak should show at a retention time of 8min, however it was presumed to be in minute quantity at the limit of detection by the HPLC UV detector. Additionally, the peak of paclitaxel was probably covered by incubation materials and cleavage products. The available enzyme amount was not sufficient for increasing scales for the assay. It was decided to follow the kinetic of drug release indirectly by measuring the quantity of Pull-PTX-ALN remaining, surmising the loss of paclitaxel, i.e. the paclitaxel release.

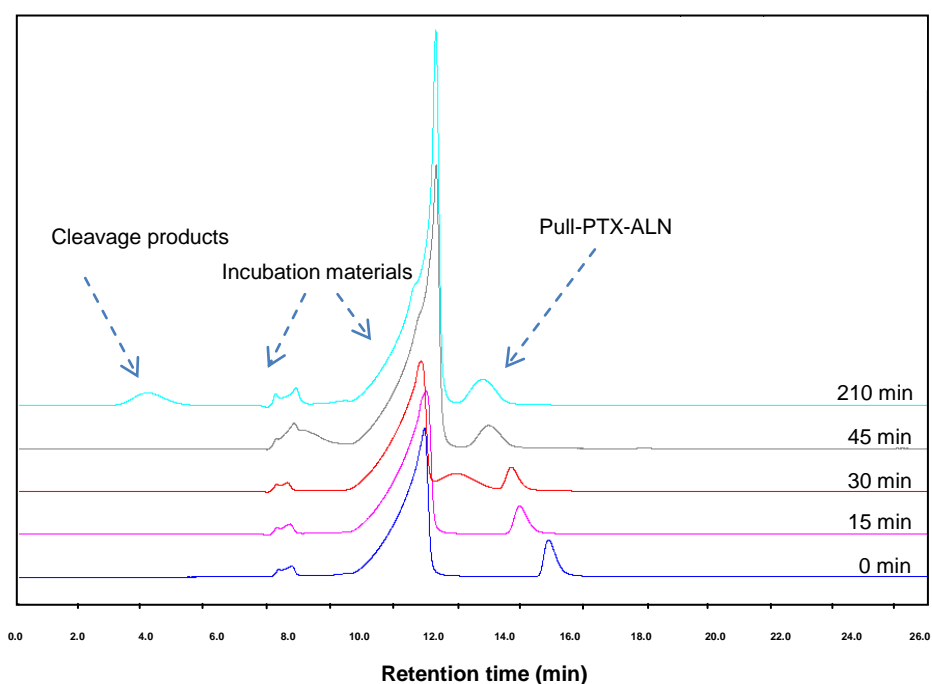


**Figure 3-33 HPLC traces of the drug release assay using Cathepsin K as trigger for the release of paclitaxel**

The % disappearance of Pull-PTX-ALN was plotted against the time of incubation in presence of Cathepsin K. A control was performed using identical conditions of incubation, excluding Cathepsin K.

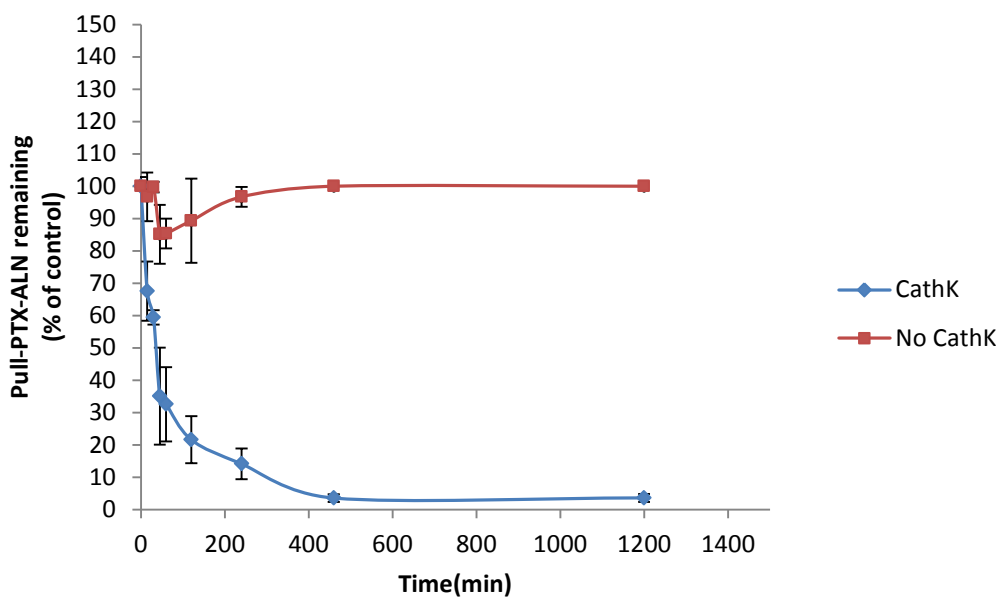


**Figure 3-34 Kinetics of the drug release assay using Cathepsin K as trigger for the release of paclitaxel**

The graph showed that after 45min, around 45% of Pull-PTX-ALN disappeared.

The enzyme degraded the spacer more slowly after that time and reached a plateau at approximately 96% disappearance of the polymer-drug conjugate peak after 8h incubation.

Over the same amount of time, results demonstrated that the control did not free PTX as the quantity of Pull-PTX-ALN remained equal all along the experiment.

The results from the drug release assay proved that the new Pull-PTX-ALN conjugate fulfilled with elementary requirements for efficient anticancer prodrugs by releasing the active drug PTX only in the environment mimicking conditions in case of breast cancer bone metastasis; i.e., the drug release of PTX was only triggered by the presence of Cathepsin K.

### 1.15.3 Red Blood Cell Lysis Assay

The biocompatibility of Pull-PTX-ALN was assessed using rat red blood cell (RBC) haemolysis assay. Rat RBC solution was incubated with serial concentrations of PTX (1:1:8 ethanol/Cremophor EL/saline), and Pull-PTX-ALN conjugate at equivalent PTX and ALN concentrations. Dextran, and poly(ethylene imine) (PEI) served respectively as negative and positive control for haemolysis.

Results are presented in Figure 3-35 as % of haemoglobin release produced by the various compounds

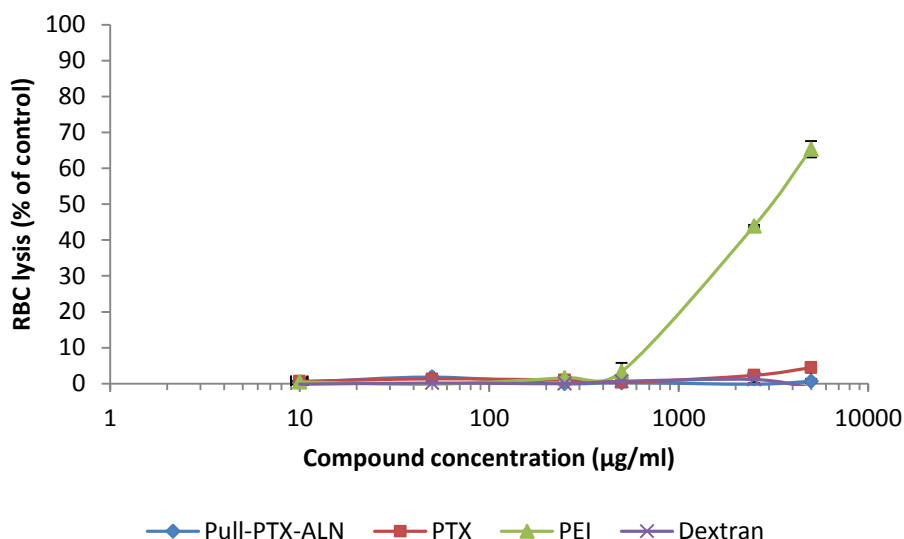


**Figure 3-35 Biocompatibility of PTX, Pull-PTX-ALN, Dextran and PEI in RBC.**

PTX-PEG-ALN conjugate did not exhibit detectable RBC haemolysis at any concentrations up to 5 mg/ml (the expected blood concentration after in vivo administrations is about 0.5 mg/ml) as shown in Figure 3-35. PTX vehicle cytotoxicity is known on normal non-proliferating cells and certainly, a slight RBC haemolysis of approximately 4% was observed in RBC incubated with PTX. The identified haemolysis was also possibly instigated by the Cremophor EL vehicle in which PTX was dissolved.

## 1.16 Cell Studies

### 1.16.1 Evaluation of the anti-tumour properties of Pull-PTX-ALN

#### 1.16.1.1 Cytotoxicity of Pull-PTX-ALN on MDA-MB231 cells, murine 4T1 cells and bone SAOS-2 cells

A further step in this project was to assess whether PTX retained its cytotoxic activity when covalently bound to the polymeric carrier pullulan. Consequently, cytotoxicity assays were performed on a range of cell lines. Cell toxicity on mammary adenocarcinoma cells sourced from bone metastasis MDA-MB231 BM, on murine mammary adenocarcinoma 4T1 and bone sarcoma cell lines SAOS-2 was evaluated.

Pullulan bound to ALN (Pull-ALN) through the same PEG spacer as for Pull-PTX-ALN was synthesised, to use as reference for this test and the following assays. The quantity of ALN on the polymer backbone was equivalent to the quantity used for the synthesis of Pull-PTX-ALN. The range of compounds tested was free PTX, free PTX in combination with free ALN, Pullulan, Pull-PTX, Pull-ALN and Pull-PTX-ALN at equivalent



concentration of PTX and ALN. Results are shown in Figure 3-38, Figure 3-39, and Figure 3-41.

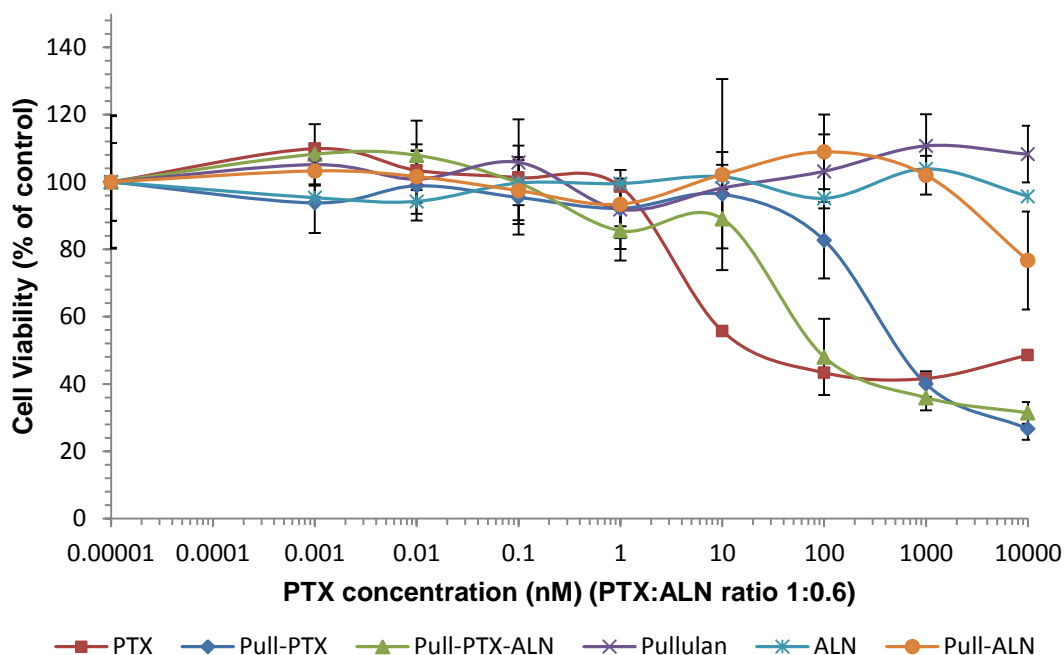


**Figure 3-36 3-37** Cell toxicity assay in MDA-MB231 BM mammary adenocarcinoma cells were incubated with free PTX, free ALN, Pullulan, Pull-PTX, Pull-ALN and Pull-PTX-ALN at equivalent concentration of PTX and ALN for 72 h. Data represent the mean  $\pm$ SD (standard deviation). The X-axis is presented as a logarithmic scale

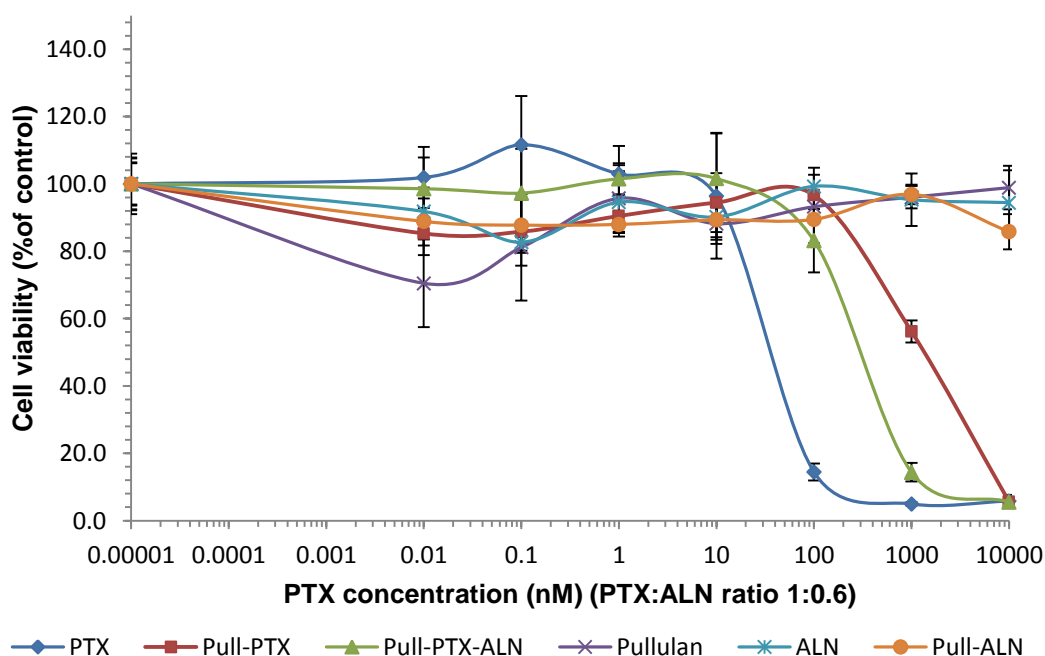


**Figure 3-38** Cell toxicity assay in murine 4T1 mammary adenocarcinoma cells. Cells were incubated with free PTX, free ALN, Pullulan, Pull-PTX, Pull-ALN and Pull-PTX-ALN at equivalent concentration of PTX and ALN for 72 h. Data represent the mean  $\pm$ SD (standard deviation). The X-axis is presented as a logarithmic scale



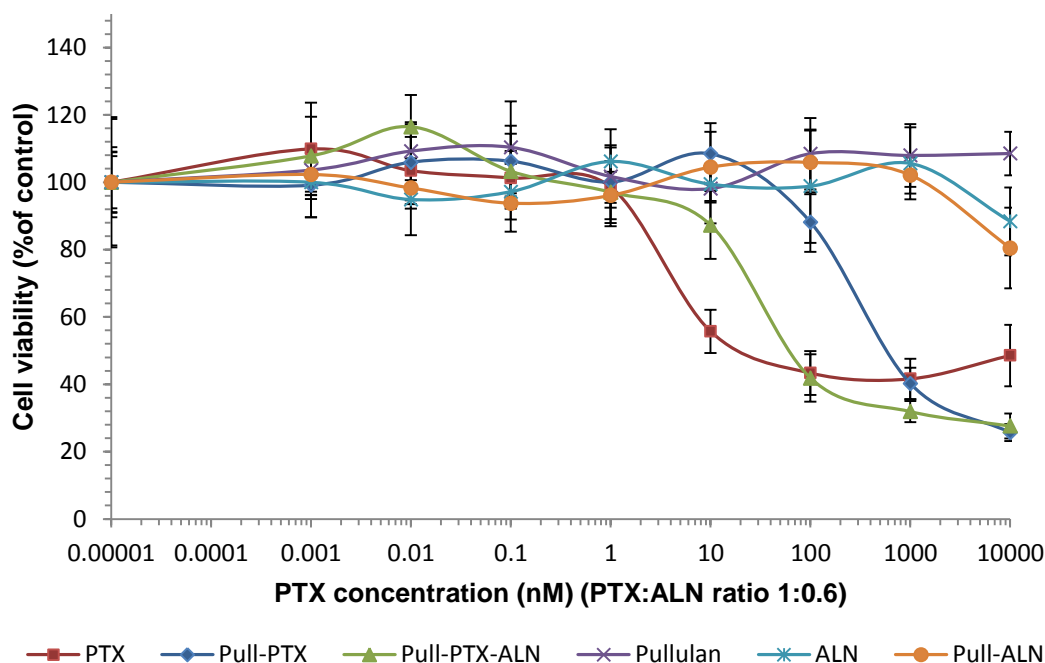


**Figure 3-39** Cell toxicity assay in human sarcoma SAOS-2 cells were incubated with free PTX, free ALN, Pullulan, Pull-PTX, Pull-ALN and Pull-PTX-ALN at equivalent concentration of PTX and ALN for 72 h. Data represent the mean  $\pm$ SD (standard deviation). The X-axis is presented as a logarithmic scale

Cells proliferation was inhibited by both Pull-PTX and Pull-PTX-ALN polymer-drug conjugates, exhibiting  $IC_{50}$  about 1-fold and two-fold higher respectively, than the  $IC_{50}$  of the free drug paclitaxel (PTX) for the three cell lines MDA-MB231 BM, 4T1 and SAOS-2 as reported in **Table 3-3**.

**Table 3-3** Cytotoxicity of PTX, Pull-PTX and Pull-PTX-ALN on MDA-MB231 BM, 4T1 and SAOS-2 cell lines

	MDA-MB231 BM	4T1	SAOS-2
$IC_{50}$ PTX (nM)	20	30	3
$IC_{50}$ PullPTX (nM)	500	1500	500
$IC_{50}$ PullPTXALN (nM)	90	300	60

For all cell lines verified, Pullulan served as the control and was non-toxic at any of the concentrations tested. Alendronate alone was found not to be toxic at any of the concentrations tested.

#### 1.16.1.2 Wound healing assay Pull-PTX-ALN on MDA-MB231 BM cells

Furthermore the influence of Pull-PTX-ALN on the ability of MDA-MB231 BM to migrate was assessed, modelling the phenomenon of metastasis in breast cancer. A wound healing assay was carried out (Figure 3-40) to check if cells would move in a defined direction to close the wound. MDA-MB231 BM cells were incubated with free PTX, free ALN, a combination of free ALN and free PTX, Pullulan, Pull-PTX, Pull-ALN and Pull-PTX-ALN at equivalent concentration of PTX and ALN for 24h.

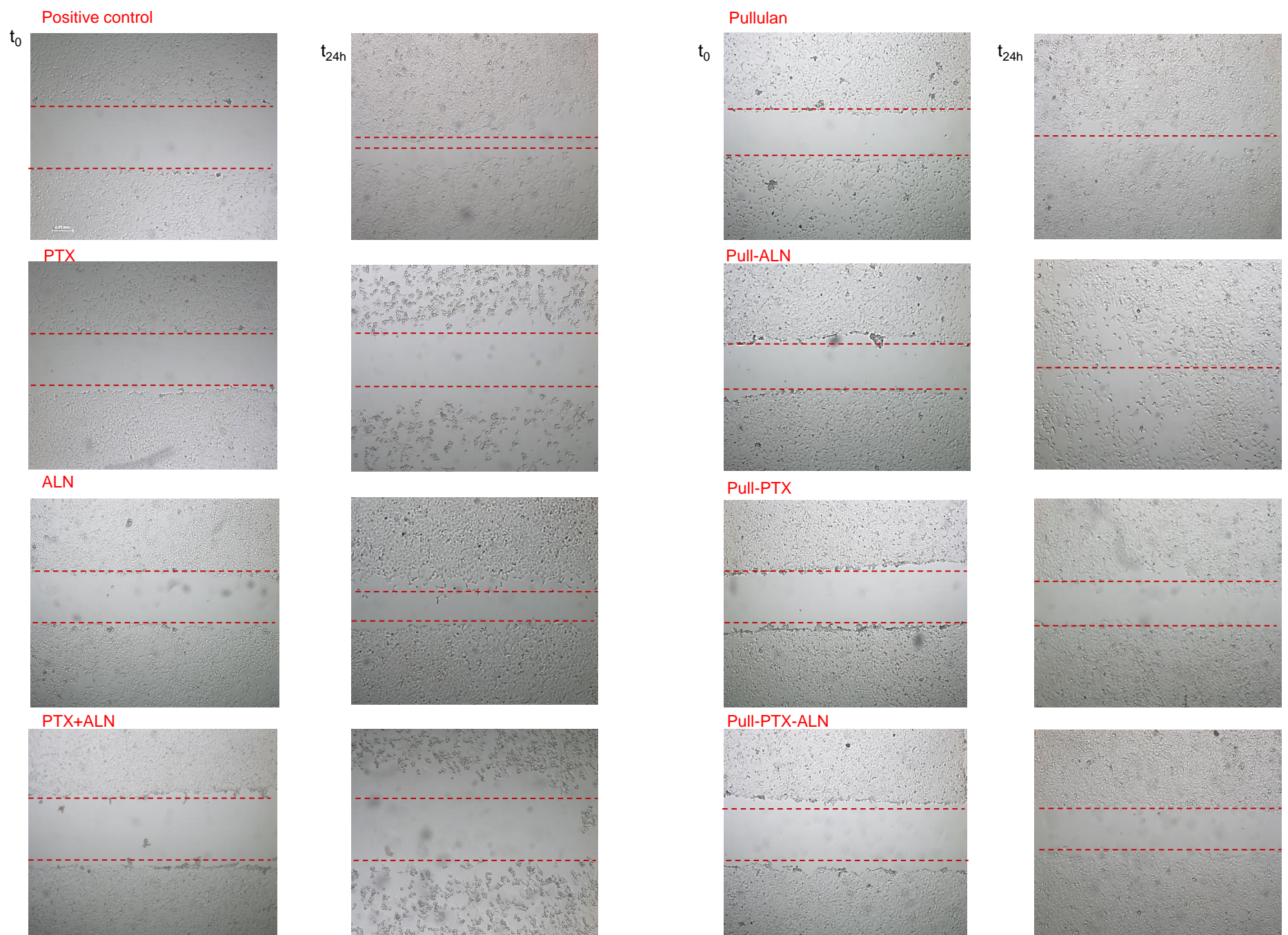


**Figure 3-40 Wound healing assay on MDA-MB231 BM cells incubated with free PTX, free ALN, Pullulan, Pull-PTX, Pull-ALN and Pull-PTX-ALN at equivalent concentration of PTX and for 24 h. (scale bar represents 100  $\mu$ m).**

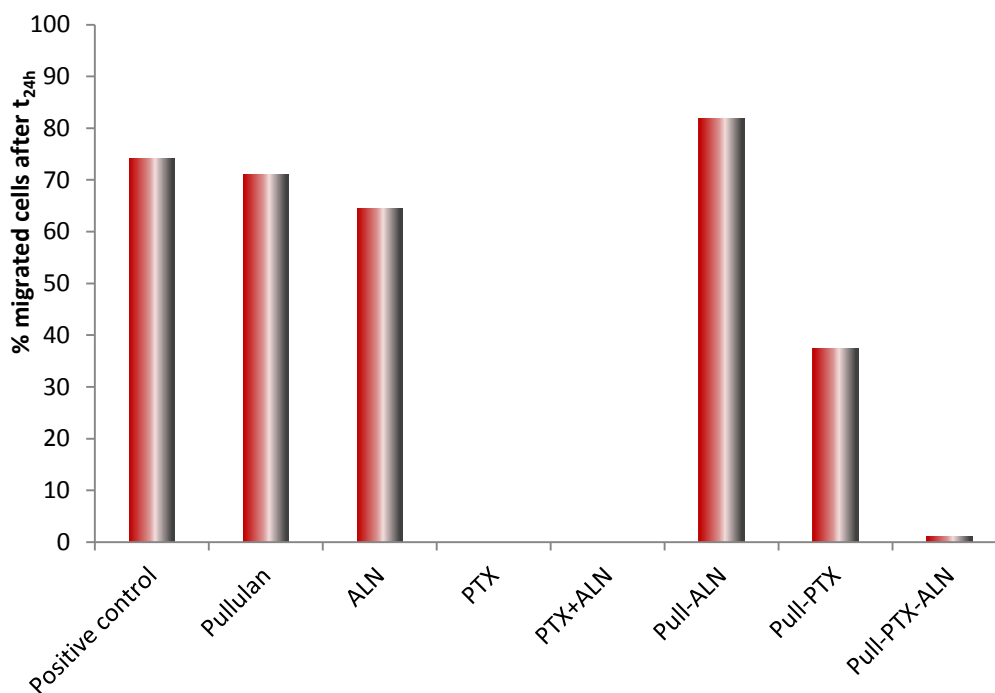


**Figure 3-41 % migrated cells in a wound healing assay performed on MDA-MB231 BM cells incubated with free PTX, free ALN, a combination of PTX and ALN, Pullulan, Pull-PTX, Pull-ALN and Pull-PTX-ALN at equivalent concentration of PTX and ALN for 24h-**

The migration of MDA-MB231 BM incubated with both Pull-PTX and Pull-PTX-ALN was inhibited by over 63 and 99% respectively (Figure 3-41). The previous cell proliferation assays demonstrated that the presence of ALN onto the polymer backbone might have a synergetic anti-tumour effect when in combination with PTX; this hypothesis was confirmed with the wound healing assays. Pull-PTX-ALN prevented mammary adenocarcinoma cells from migrating in the same fashion as PTX free drug.

### 1.16.2 Inhibition of angiogenic cascade

The anti-angiogenic properties of Pull-PTX-ALN were assessed by performing endothelial cell proliferation assays, capillary-like tube formation assay and migration assay so as to evaluate if the polymer-drug conjugate preserved the features of the free drug PTX.

### 1.16.2.1 Cytotoxicity of Pull-PTX-ALN on Human Vein Endothelial Cells (HUVEC)

Primarily, HUVEC were incubated with, Pullulan, Pull-PTX, Pull-ALN and Pull-PTX-ALN at equivalent concentration of PTX and ALN. The proliferation of HUVEC was inhibited similarly by free PTX and free PTX in combination with free ALN and Pull-PTX-ALN exhibiting an IC<sub>50</sub> of ~15nM. Pull-PTX inhibited HUVEC with a twofold higher IC<sub>50</sub> (~700nM) than Pull-PTX-ALN.

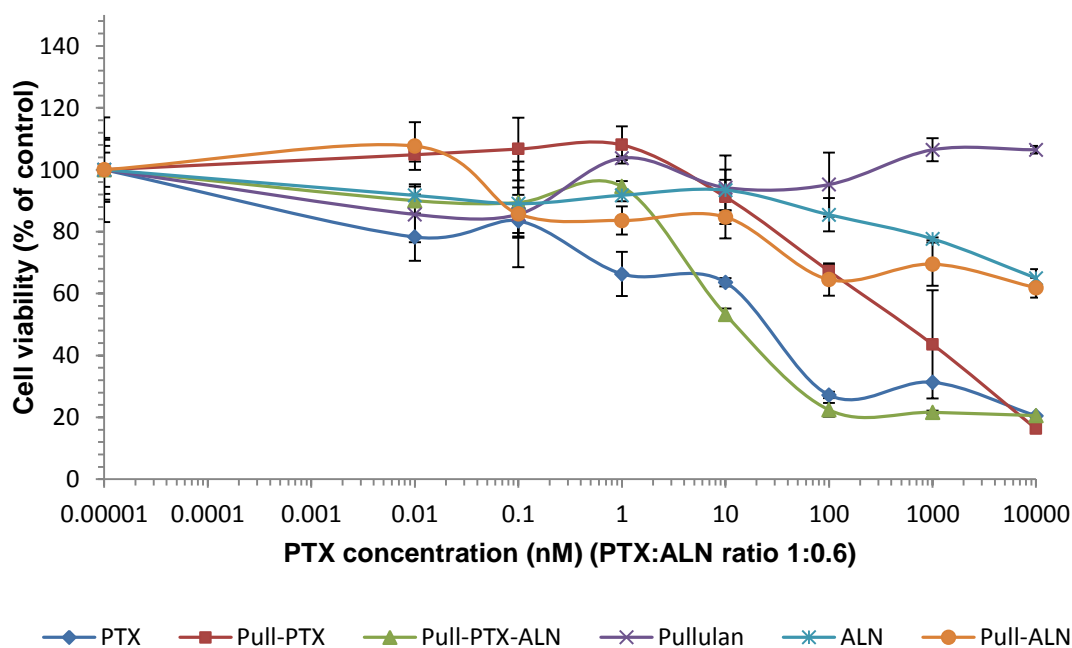


**Figure 3-42 Cell toxicity assay in human umbilical vein endothelial cell (HUVEC).** HUVEC were incubated with free PTX, free ALN, Pullulan, Pull-PTX, Pull-ALN and Pull-PTX-ALN at equivalent concentration of PTX and ALN for 72 h. Data represent the mean  $\pm$ SD (standard deviation). The X-axis is presented as logarithmic scale

### 1.16.2.2 Capillary-like tube formation assay on HUVEC

Finally, the anti-angiogenic activity of the polymer-drug conjugate Pull-PTX-ALN was evaluated by capillary-like tube formation assay. The test performed on Matrigel.



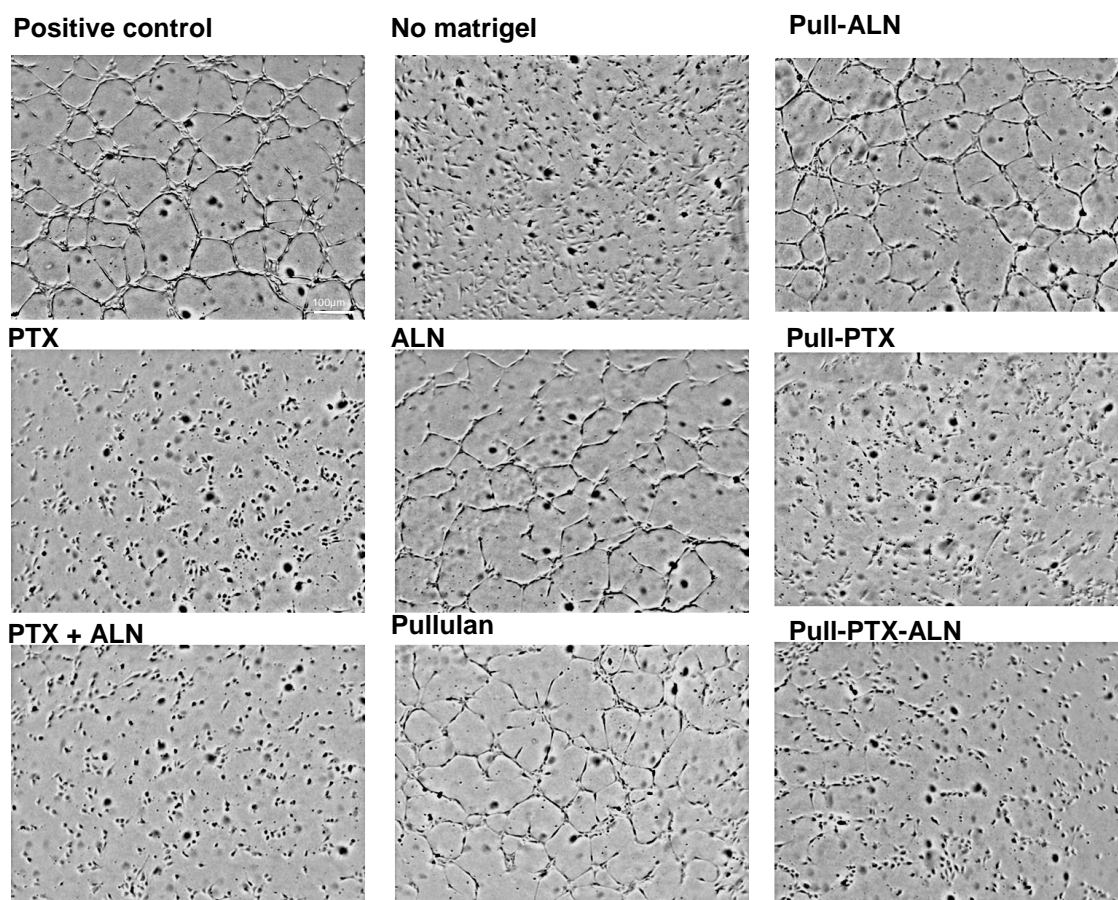


**Figure 3-43** Capillary like-tube formation assay : representative images of capillary-like tube structures of HUVEC seeded on Matrigel following treatment (scale bar represents 100  $\mu$ m).

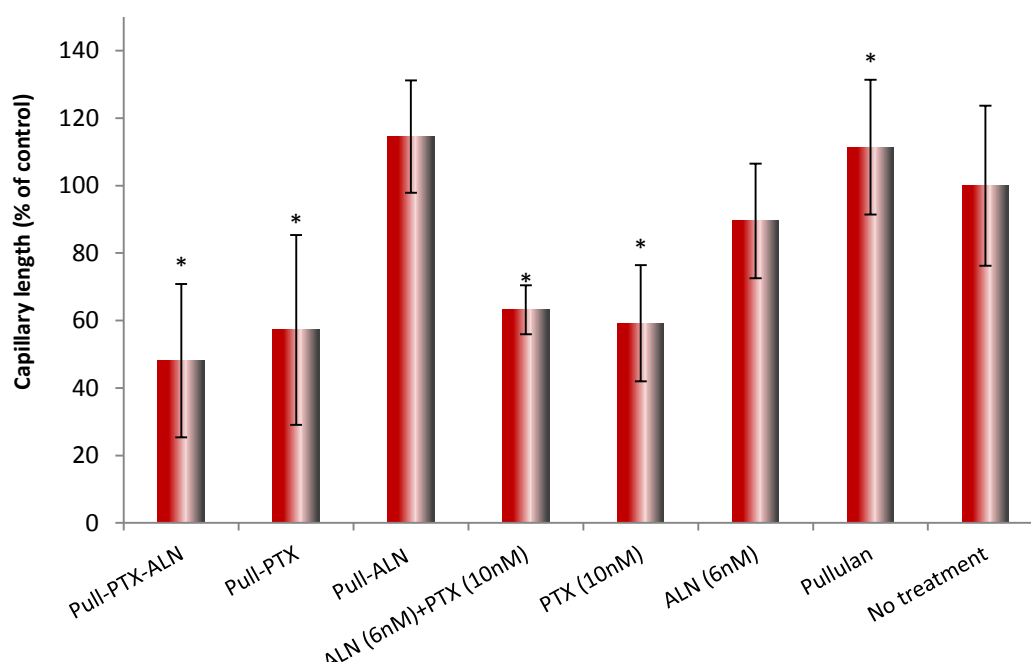


**Figure 3-44** Capillary like-tube formation assay: Quantitative analysis of the mean length of the tubes. Data represents mean  $\pm$  SD. \* $p < 0.05$

The assay was performed at non-cytotoxic concentration at the indicated incubation time and showed that Pull-PTX and Pull-PTX-ALN both demonstrated a significant anti-angiogenic potential. The conjugates inhibited the formation of tubular structures of HUVEC by ~60% as comparable with free PTX and PTX combined with ALN. However, the pullulan carrier and the targeting agent ALN did not prevent HUVEC from forming capillary-like tubes (Figure 3-44).

# DISCUSSION

---





## **4. Discussion**

The field of selective drug delivery refers to the development of systems in which drugs are directly delivered to a specific site of the organism according to particular mechanisms and kinetics, in order to optimise the targeting to the diseased tissue and improve the drug performance of the therapeutic effect.

To such purpose, in the past years, various supramolecular systems defined as "polymer therapeutics" have been developed. These "nano-medicines" are obtained by chemical conjugation or physical assembly of bioactive molecules with polymeric macromolecules and/or other functional molecules to endow nano-systems with specific biopharmaceutical or physico-chemical features. The polymeric part represents the basic structure, platform, on which molecules or chemical functions can be physically or chemically anchored. Consequently, the polymer must possess specific characteristics for pharmaceutical applications, including biocompatibility, solubility, ability to be eliminated and multifunctionality. The use of polymer therapeutics for drug delivery has opened new perspectives for the development of novel and efficient treatments of several pathologies. They are of particular interest in the field of anti-tumour therapy to overcome drawbacks related to the employment of chemotherapeutics, which, due to their poor selectivity towards tumour cells, often cause serious damage to normal tissues inducing strong side effects. They also are usually poorly soluble in water, instable and produce problematic pharmacokinetic profiles.

The structural particularity of the vascular endothelium, the micro-environmental characteristics (pH, temperature, redox potential and enzymatic composition) as well as the overexpression of specific receptors of tumour tissues can be exploited for the development of new passive or active targeting technologies for specific delivery of the medicine. For these reasons, polymeric drug delivery systems, bio-conjugates or physically assembled systems are becoming more important in the field of anti-tumour therapy.

Polymer-anti-tumour drug conjugates have been investigated for many years as improved therapies against cancer, aimed to address the relevant limitations of current therapies using low molecular weight drugs; it is well acknowledged that most of the chemotherapeutics are potent drugs. However, they generally lack of selectivity to direct the cytotoxicity to tumour cells, causing severe and serious side effects to normal healthy cells. The coupling of antineoplastic drugs with water-soluble polymers has been demonstrated to strongly improve both the safety profile and anti-tumour effectiveness of the overall drug conjugate, by playing on several aspects, such as:

- Increasing the solubility: many anti-tumour agents are poorly soluble in biological fluids, requiring an oil formulation for clinical administration,
- Improving the biodistribution and consequently reducing the concentration in sites of dose-limiting toxicity: conjugates have limited distribution due to their large sizes,
- Providing passive targeting to solid tumours; the enhanced permeability and retention (EPR) effect promotes the extravasation of macromolecules into tumours due to the abnormally leaky blood vessels in cancers with respect to healthy tissues
- By-passing P-glycoprotein-mediated drug resistance: due to alternative cellular entry and trafficking,
- Preventing drug inactivation and degradation.

The concept of utilising polymers in drug delivery has been explored in this project for improving the therapeutic performance of paclitaxel, an anti-tumoural drug used in the treatment of late stage breast cancer and more particularly, at its the metastases stage.

Metastases are defined as the delocalisation and propagation of tumour cells from the primary site to distant tissues or organs.

Metastases are directly connected to breast cancer-related mortality and occur in 25 to 50% of patient diagnosed with the disease. Only 25% of patients reach the average of 5 year survival rate. The actual common treatments are the use of traditional chemotherapy with its drawbacks, where anticancer drugs are often combined with other biomolecules.

Breast cancer metastases develop in bone at an advanced stage. Paclitaxel (PTX) is one of the main anticancer drugs currently utilised clinically for the treatment of solid tumours, and more particularly in advanced breast cancer. Paclitaxel promotes the stabilisation of microtubule assemblies and consequently discontinues mitosis and cellular division. Although being a potent anti-neoplastic agent, paclitaxel suffers from serious drawbacks, one of them being its poor selectivity towards tumour cells.

Since breast cancer metastases develop in bone at a final phase bisphosphonates, initially indicated for the treatment of osteoporosis or other bone related disease as anti-resorptive agents, have also been indicated for bone-related breast cancer metastases in breast cancer patients, and as they considerably improve breast cancer survival and reduce bone resorption induced by bone metastases. Additionally, recent studies demonstrated that bisphosphonates may also have direct anticancer activity and synergy with cytotoxic chemotherapy.

Although actual treatments exist, they suffer from serious drawbacks mentioned earlier. Therefore, there is a strong need for improving the actual therapeutics for the treatment of

breast cancer bone metastases, by developing innovative strategies for solubilising paclitaxel and targeting tumour tissues. One of these strategies is to use polymer based therapeutics.

In this framework, the present project was aimed at developing a new colloidal drug delivery system for disease site targeting and controlled release of anti-tumour drug and anti-resorptive agent. The simultaneous delivery, from a single polymeric carrier, of the two therapeutic agents that would act synergistically, would permit the administration of each drug at lower concentrations, increasing their combined anti-tumour efficiency and decreasing their toxicity.

Accordingly, a novel Pullulan based nano-system was designed to improve the biopharmaceutical and therapeutic properties of the anti-cancer drug paclitaxel, namely to increase the paclitaxel solubility in water and to promote its selective accumulation in the tumour. The novel polymer-drug conjugate would accomplish both synergistic inhibitory anti-tumour effect and dual active and passive targeting effect that would result in a fast tumour accumulation in bone-associated neoplasms.

In order to yield a bioconjugate with selective targeting properties, a few chemical approaches have been implemented in the construction of the supramolecular structure. Paclitaxel was conjugated to the polymer backbone through an enzyme sensitive peptide arm that provides for the drug release by action of enzymes that are overexpressed in the tumour tissue. Paclitaxel was associated with alendronate to endow a polymer therapeutic with selective recognition properties. Indeed, the bisphosphonate has high affinity toward the apatite structure of bone.

Similarly to other bone diseases, bone tumour causes local inflammation and results in the exposure of HAp to blood. These two characteristics can be exploited to deliver high drug contents distinctively to diseased tissue.

Accordingly, the alendronate was grafted to the polysaccharide backbone to provide a bioconjugate with enhanced selectivity for the bone metastasises. Therefore, active targeting properties conveyed by alendronate combined with selective drug release due to specific enzymes, associated with the colloidal properties of the overall construct that exploit the micro-environmental features of the bone metastases by the EPR effect, can ensure a selective accumulation and release of the anti-tumour drug at the desired site of action. Bisphosphonates bind strongly to HAp and retain much of the binding affinity after conjugation to other molecules or carriers.

Pullulan is a linear polysaccharide that presents only primary and secondary alcohol groups, which cannot easily exploited for conjugation.

Therefore, in a first stage, Pullulan was activated in order to produce a polymer with multipoint attachment sites that should be exploited for the multiple conjugations of the various modules, namely drug and targeting agent. One characteristic feature of Pullulan, is the presence of vicinal hydroxyl groups on its backbone. This advantage was utilised to form active aldehyde groups by oxidation. Periodate oxidation was selected as oxidising agent to achieve the ring-opening cleavage of the 1,2-diols at C-2 and C-3 of polysaccharides very efficiently, and accurately. Periodate allows the selective oxidation of vicinal diol groups of the polysaccharide backbone to form reactive aldehyde functions that can be used as anchoring groups. As compared to other activation methods, the oxidation offers an easy control of the amount of anchoring groups along the polymer chains. Furthermore, the aldehyde groups are stable until functionalization and can be derivatised with a variety of moieties.

The quantification of the formed aldehyde groups was performed by pH titration, exploiting the formation of HCl after the reaction of aldehydes with hydroxylamine hydrochloride. This quantification method uses a nucleophilic attack of the reagent onto the carbonyl carbon, but not all aldehydes are accessible, thus resulting in the detection of 2 out of 3 of the aldehydes generated by periodate reaction. A possible explanation of such phenomenon is the spontaneous formation of a hemiacetal (with recyclisation) in  $\alpha$ -1,4 of the glycosidic residue (Bruneel D., 1993)<sup>53</sup>.

Oxidised Pullulan was obtained with different degrees of oxidation using different molar ratios oxidant/glycosidic units. More precisely, the polysaccharide was prepared with a theoretical degree of oxidation of the glycosidic units of 30% and 95% which should correspond to 20% and 60% detectable aldehydes by hydroxylamine method. . The kinetic studies of aldehyde formation by periodate oxidation showed that after 30min, almost 90% of the maximum oxidation was obtained to reach plateau after 1h. The reaction yielded an oxidation degree of 23% and 63% respectively (Hydroxylamine titration), which corresponded to 34% and 95% of total aldehydes. These results indicate that the oxidation reaction was complete. Slightly higher oxidation values with respect to the theoretical values can be attributable to the analytical process that includes some inaccuracies.

As described in the literature, and according to previous studies<sup>22c</sup>, the periodate oxidation of Pullulan resulted in the reduction of the polysaccharide molecular weight<sup>53</sup>. The two pullulan derivatives presented a molecular weight of about 20kDa and 93kDa in the case of the 65% and the 23% oxidized pullulan correspondingly.

On the basis of these considerations, it was decided to use a 23% oxidised pullulan corresponding to a number of aldehyde functions sufficient to attached prodrugs. This choice allowed keeping a molecular weight close to native pullulan, which properties are well documented in literature; thus, avoiding possible alterations of pullulan properties

that might occur in the much lower molecular weight of the 65% oxidised pullulan. This option represented a reasonable compromise between degree of oxidation, molecular weight of the polymer backbone and preservation of polysaccharide structure.

Paclitaxel was conjugated to pullulan through an enzyme sensitive spacer in order to obtain an efficient and selective drug release and activation exclusively in the tumour site. This type of spacer has an advantage over other spacers as it must hydrolyse only in presence of specific enzymes at the target site, independently from temperature, pH or other environmental factors. Enzyme sensitive spacers are more stable compared to other spacers such as carbonates, esters or hydrazones. The use of this type of spacer also contributes to the targeting function and constitutes a further motivation of this choice.

The enzyme sensitive spacer chosen for the paclitaxel conjugate was a Cathepsin K sensitive tetrapeptide.

Cathepsin K is an enzyme expressed outside the cell, highly present at osteolytic lesions and site of active bone resorption, which makes Cathepsin K specific spacer a distinct and suitable choice for selective delivery to bone.

In order to achieve Cathepsin K selectivity a Gly-Gly-Pro-Nle tetrapeptide was synthesised. The oligopeptide sequence predisposed to cleavage by Cathepsin K was carefully chosen. This sequence was selected according to the work of Schechter and Berger, which showed that Cathepsin K had a distinctive predilection for proline in P2 position. The basic amino acids, lysine and arginine were preferred in P1 position. Nevertheless, it was chosen to use the neutral amino acid norleucine in P1 position to warrant the stability of the spacer in blood circulation. The cleavable Gly-Pro oligopeptide, in positions P3 and P2 respectively, were selected according to the literature (Rejmanová P et al). Finally, glycine was chosen for position P3. The same research group showed that the increase of the length of the spacer from three to four amino acid residues decreased the steric hindrance in an enzyme-substrate complex for chymotrypsin and Cathepsin B.

The tetrapeptide spacer was obtained by Solid Phase Peptide Synthesis using a hydroxymethyl-based Wang resin, which is known to be an unhindered resin, easing the formation of the amide linkage between amino acid residues. The resin beads were of 200-400 mesh in order to ensure a good penetration of the reagents inside the porous gel. Fmoc group was used as a protecting group of the amino function because it allows the final cleavage of the peptide from the resin under mild conditions, which avoids deleterious changes in the structural integrity of the oligopeptide.

The selected peptide sequence was built in a linear approach using a C>N strategy, from the C-terminus to the N-terminus to obtain, after cleavage from the resin, a final tetrapeptide bearing a protected amine and a free carboxylic group available for further conjugation.

The coupling of Proline to Norleucine was not complete, as revealed by a colorimetric test (Kaiser test) due to the aggregation of the hydrophobic amino acid proline; therefore, a double coupling was necessary for this amino acid residue to ensure a complete coupling between the two amino acid residues.

The last amino acid residue glycine was chosen to remain Fmoc protected so that further functionalization of the final tetrapeptide could be performed via its carboxylic group, exempting any reaction with the primary amine group. The latter was needed in the final step of synthesis of the polymer-drug conjugate.

The subsequent work focused on the anti-tumour function by creating a paclitaxel prodrug to ensure selective release at the tumour site via enzymatic catalysis.

Two methods to conjugate methods paclitaxel to the tetrapeptide spacer were carried out according to two approaches.

In a first attempt, Fmoc-Gly-Gly-Pro-Nle was conjugated to the hydroxyl bond of paclitaxel via direct binding after activation of the oligopeptide carboxylic acid. This simple approach would accomplish the function of liberating paclitaxel triggered by Gly-Pro Cathepsin K cleavage while Pro-Nle would remain attached to the anti-tumour drug since the enzyme hydrolyses the substrate on position P3-P2. The specific activity of paclitaxel-GlyPro would necessitate some investigations.

The first approach was initially chosen for its simplicity in terms of synthesis. Multiple coupling agents were used for the paclitaxel conjugation, including, N,N'-dicyclohexylcarbodiimide (DCC) coupling in presence of 4-(dimethylamino)pyridine (DMAP) catalyst, and 1-ethyl-3-(3-dimethylaminopropyl) carbodiimide (EDC) coupling in presence of DMAP. Also, numerous conditions were investigated, including the use of reagent excesses, solvents and temperature. However, in all cases, the synthesis resulted in very poor product yields. This could be explained by the poor accessibility of the paclitaxel hydroxyl group and the steric hindrance exerted by the large Fmoc protecting group born by the tetrapeptide.

In order to overcome these steric limitations and improve free drug release, a second approach using a 4-aminobenzyl alcohol based, self-immolative spacer was designed to create the paclitaxel prodrug. The fundamental process of self-immolation refers to a spontaneous and irreversible dissociation of compounds made of various modules into their constituent modules, through an intramolecular reaction. The 4-aminobenzyl alcohol

used in this synthesis was selected because it undergoes 1,6-elimination that yields the cleavage of the benzylic carbonate bond and release free paclitaxel as first reported in literature by Katzenellenbogen and co-workers in 1981<sup>59</sup> and later by Greenwald *et al.*<sup>54</sup>. This method may have another benefit as it would increase the distance between the conjugated drug paclitaxel and the active cleavage site. Paclitaxel is in fact a sterically bulky molecule and the enzymatic access to the substrate may be problematic and prevent the cleavage and release of the anti-tumoural drug. The introduction of the self-immolative spacer allows circumventing the risks of steric restrictions and favour drug release. In such a case free PTX is released, exempt of any amino-acid residues.

A shortcoming to this second method would be the longer synthesis due to the numerous steps necessary to obtain the final prodrug. Katzenellenbogen and co-workers reported the 4-aminobenzyl alcohol spacer functionalization with a lysine and conjugation to a 4-nitroaniline molecule through a carbamate linkage at the benzylic site<sup>59</sup>. Following enzymatic cleavage of the amino acid residue, the strongly electron-donating 4-aminobenzyl group initiates a 1,6-elimination reaction, followed by a spontaneous decarboxylation to release the 4-nitroaniline. Similarly, the synthesis of the prodrug containing the enzyme sensitive substrate Fmoc-Gly-Gly-Pro-Nle and the benzyl carbonate self-immolative spacer was successfully produced through a 5-step synthesis. In the final step the amine function of glycine in P4 position was deprotected, allowing for further conjugation to the pullulan polymeric carrier. The critical step in this synthesis was the second step where p-nitrophenyl chloroformate was introduced to the molecule. The reactant was highly unstable in handling conditions and deactivated rapidly by forming stable by-products. Increased precautions in handling were taken to ensure best yields to move on the subsequent steps.

With regard to the targeting module, a process similar to the one used for paclitaxel was originally designed. The Cathepsin K sensitive peptidyl-alendronate module would have fulfilled two functions; the targeting of the polymer-drug conjugate to the bone and the action of the bisphosphonate as anti-resorptive agent. Accordingly, alendronate could on one side, reduce bone metastases induced pain and bone resorption induced fracture, and on the other side, kill the tumour at the selected site.

Various strategies were considered for the synthesis of the peptidyl-alendronate, including, N,N'-dicyclohexylcarbodiimide (DCC) coupling in presence of 4-(dimethylamino)pyridine (DMAP) catalyst, and 1-ethyl-3-(3-dimethylaminopropyl) carbodiimide (EDC) coupling in presence of DMAP, solution phase O-Benzotriazole-N,N,N',N'-tetramethyl-uronium-hexafluoro-phosphate / Hydroxybenzotriazole (HBTU/HOBt) coupling, EDC in presence of N-hydroxysuccinimide (NHS) coupling, 4,5-dihydrothiazole-2-thiol (TT) in presence of DCC coupling, pH were varied from 7 to above 11. None of the synthesis described above succeeded, probably because of the divergent



solubility of reagents. Alendronate is in fact soluble only in aqueous medium while, Fmoc-Gly-Gly-Pro-Nle was only soluble in organic solvents. Additionally, the pKa of the alendronate amino group is 11.4. At pH above this pKa the peptidyl spacer degraded, as observed by the mass spectra obtained with the reaction mixture. As reported in the literature by Uludag *et al*<sup>55</sup>, below this pKa, coupling was not favoured. Indeed, very low coupling was obtained. Therefore, a new approach, which replaces the tetrapeptide with a relatively low molecular weight poly(ethylene glycol) (PEG) was designed. This second approach does not allow for the alendronate release. Therefore, alendronate retains only the targeting function while the anti-resorptive function that requires the bisphosphonate release is probably lost. The 3kDa PEG plays the role of spacer between Pullulan conveying flexibility and free movement of the targeting agent to reach its target; hydroxyapatite. In order to produce a conjugate with a free amino group for Pullulan conjugation, tBoc-NH-PEG-NHS was first covalently bond to alendronate through its NHS activated carboxylic acid and then deprotected by TFA to free the primary amine.

In order to optimise the rate of conjugation of ALN to PEG, several attempts were performed at pH ranging from 7 to 11.4. As reported above, as the pH increases the alendronate reactivity increases. Nevertheless, the inactivation of t-Boc-PEG-NHS by NHS hydrolysis also increases thus, competing with conjugation process. The results obtained in the pH range of 7-9, well acknowledged pH range for optimum NHS reactivity, showed that all conditions generated equivalent results of approximately 24%mol conjugation of ALN, while at higher pH the conjugation was negligible. Moreover, NHS is a hydrolysis sensitive molecule and conjugations completed in water would necessarily compete with the rate of hydrolysis, hence the low binding rate attained.

Other conditions adopted to enhance the reaction yield included the use of a mixture of solvents DMSO/H<sub>2</sub>O at different ratios. Nonetheless, also in such a case no improvements were obtained.

Even the re-activation of PEG by NHS/DCC, prior to coupling with alendronate, did not resulted in an improvement of the reaction yield.

In conclusion the maximal alendronate conjugation yield was 24%mol. The final product was a mixture of tBoc-PEG-ALN and tBoc-PEG-COOH, formed by hydrolysis of NHS by water. The two species were not separated since tBoc-PEG-COOH could have two advantages; allowing binding of a fluorophore for later investigations and improving the overall solubility of the final bio-conjugate. This deprotected product obtained by treatment with trifluoroacetic acid was used for conjugation to the oxidized pullulan.

The preparation of the final bioconjugate pullulan derivatised with NH<sub>2</sub>-GlyGlyProNle $\phi$ paclitaxel and NH<sub>2</sub>-PEG-alendronate Pull-PTX-ALN was performed according to a multi-step protocol in order to obtain a suitable composition of all modules.



Aimed at obtaining the maximal drug payload, NH<sub>2</sub>-GlyGlyProNle- $\phi$ -PTX was first conjugated to the aldehyde-pullulan under reductive amination followed by the conjugation of NH<sub>2</sub>-PEG-Alendronate. This sequence was followed to prevent the steric hindrance of PEG-Alendronate that could limit the conjugation of the drug. The reduction process was set up in order to selectively stabilize the Schiff base formed by NH<sub>2</sub>-GlyGlyProNle- $\phi$ -PTX or NH<sub>2</sub>-PEG-alendronate conjugation to the aldehydes of pullulan. within the first step, when NH<sub>2</sub>-GlyGlyProNle $\phi$ PTX was conjugated, triacetoxyborohydride was used as selectively allowed the reduction of the Schiff bases to secondary amino groups in organic solvent without reducing the unreacted free aldehydes remaining that are then used for the NH<sub>2</sub>-PEG-alendronate conjugation.. In the last step, when NH<sub>2</sub>-PEG-alendronate was added, sodium borohydride was used. This less selective reductive agent was employed to ensure the complete reduction of Schiff bases and likewise, the reduction of unreacted aldehydes to alcohol functions. The complete reduction of the aldehyde groups was necessary to obtain a safe product for pharmaceutical use; indeed several studies show that molecules bearing aldehyde functional groups have a distinct cellular toxicity.

To evaluate the drug payload in the bioconjugate, the NH<sub>2</sub>-GlyGlyProNle $\phi$ PTX conjugation was carried out by using a range of NH<sub>2</sub>-GlyGlyProNle $\phi$ PTX: oxidised Pullulan weight ratios (2:100, 5:100, 10:100 and 20:100). The results obtained by spectroscopic analysis of the bioconjugates showed that even using high NH<sub>2</sub>-GlyGlyProNle $\phi$ PTX: oxidised Pullulan ratios, maximal 7.8% drug loading was obtained It should be noted that the synthesis was performed in DMSO where all reagents are freely soluble.. Possible explanations to this behaviour are the hindrance of the reagents as both of them have high molecular weight, or to the change of the polymer structure when the NH<sub>2</sub>-GlyGlyProNle $\phi$ PTX derivatives are conjugated, preventing further conjugation The conjugation of 7.8% <sub>w/w</sub> of paclitaxel was in line with the drug loading reported with similar polymer therapeutics<sup>60</sup> and can be considered suitable for pharmaceutical purposes. Moreover, the solubility of the conjugate in physiological solution is strictly affected by the paclitaxel content that is a poorly soluble molecule. PTX is a drug poorly soluble in water (water solubility of 0.3 $\mu$ g/ml and is used clinically, solubilised in a substantial amount of Cremophor EL in Taxol® formulation (Bristol–Myers Squibb). It is therefore expected that too high paclitaxel payloads would result in products with low solubility that have no biopharmaceutical prerequisites for in vivo applications.

In the case of alendronate the conjugation was found to be 1.2%<sub>w/w</sub>; value compatible with literature to ensure bone targeting and anti-tumour activity. In order to perform these in-vitro studies, Pull-PTX and Pull-ALN were synthesised at equivalent amounts of ALN and PTX as for Pull-PTX-ALN.

The polymer-drug conjugate Pull-PTX-ALN, was fully soluble at a concentration of 513µg/ml paclitaxel equivalent whereas the equivalent amount of paclitaxel in its free form was completely insoluble; this result demonstrated a first advantage in binding PTX to the polysaccharide carrier pullulan.

The dimensions of Pull-PTX-ALN in solution were assessed by both Gel permeation chromatography and Dynamic Light Scattering that allowed for determination of apparent molecular size and colloidal size, respectively. The molecular weight of the final product was of 89kDa and the polydispersity index (PDI) was 1.88. These values indicate that the final product has a size above the threshold value of estimated glomerular filtration, which is commonly accepted to be 68kDa for proteins (albumin molecular weight) and 30k to 50Da for polymers. Therefore, the system is expected to circulate for prolonged time in the bloodstream thus displaying high systemic bioavailability. On the other hand, the size of the bioconjugate can allow for passive deposition in the tumours according to the EPR effect. It is in fact reported in the literature that EPR effect takes place in case of macromolecules with size over the threshold value of 50kDa.

The Dynamic Light Scattering analysis showed that Pull-PTX-ALN has a mean average hydrodynamic diameter of 163.30±18.25nm, 100.20±7.3nm and 69.88±6027nm at pH5.5, 6.0 (water) and, pH7.4 respectively whereas native Pullulan alone had a particle size of around 10nm at all pH. The higher size of the bioconjugates as compared to native pullulan is ascribable to supramolecular physical associations due to the presence of hydrophobic segments of PTX along the polysaccharide backbone. On the other hand, the different size at the various pH indicates the pH sensitivity of this derivative. This may be due to the presence of carboxyl groups deriving from PEG-COOH and the phosphate group of alendronate along the polymer backbone. As the pH decreases, the percentage of unionized groups increases. The reduction of negative charge repulsion and the increase of unionised hydrophobic groups can result in increased interchain associations.

The Critical micellar concentration (CMC) of the Pull-PTX-ALN was 73.3µg/ml which confirmed the self-assembling attitude of the bioconjugate already described above. The CMC; this value was compatible with requirement for drug delivery applications. Indeed, a low CMC was necessary to ensure that the nano-assembly would retain its structure upon intravenous injection. Micelles must stay intact upon injection to prevent the premature release the anti-tumoural drug paclitaxel from the polymeric vehicle before reaching the target cells.

The micellar shape of Pull-PTX-ALN was confirmed by Transmission electron microscopy (TEM), which showed that above the CMC the bioconjugate formed circular shape nano-assemblies of approximately 100nm, size.

According to the structural data obtained by DLS and TEM it was hypothesised that the bioconjugate forms structures where the paclitaxel mainly inside the supramolecular assembly is engaged into hydrophobic bonds that stabilize the colloidal system while the alendronate is externally exposed on the colloidal surface where is available for the target recognition.

Interestingly, the DLS analysis showed a single colloidal population at all pH over more than 8h either at room or physiological temperature, demonstrating that the bioconjugate was pretty stable as no aggregates were formed during storage. Finally, the size of the polymer-drug conjugate in solution was much below the threshold of 600nm for accumulating in tumour masses; Pull-PTX-ALN was a good candidate to benefit from the passive accumulation in tumours by EPR effect.

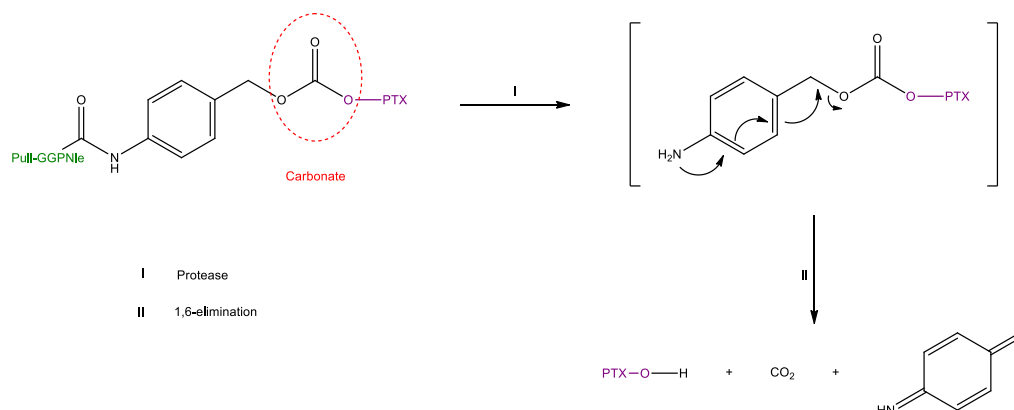
In order to confirm the stability of the polymer-drug conjugate in solution, release studies of PTX and ALN were conducted in buffers at pH 7.4 and pH 5.5 at 37°C, which simulate osteoclast lysosomal and physiological pH, respectively. The results showed that over 24h no drug release was observed indicating that in the absence of Cathepsin K the bioconjugate is chemically stable and no drug is released.

In vitro studies showed that the polymer-drug conjugate displayed a pronounced affinity for the bone mineral model hydroxyapatite employed to simulate bone tissues. After 60min incubation at pH 7.4 and 5.5, which simulate the physiological and Howship's lacunae pH, respectively, 40% and 65% of Pull-PTX-ALN were bound to hydroxyapatite. The difference of binding observed between the two pH tested cannot be easily explained. Probably, the different conformation of the supramolecular association, together with the different size and the altered overall charge have role in the interaction of the bioconjugate with the substrate of the bioconjugate. Indeed, as reported above, as the pH decreases, the polymer hydrodynamic diameter increases. .

The paclitaxel release in the presence of Cathepsin K showed that the novel bioconjugate has suitable biopharmaceutical properties for in vivo application.

While in the absence of Cathepsin K no drug release was observed, in the presence of the enzyme, a fast release of the anti-neoplastic agent PTX (96% of control) from the polymer-drug conjugate was obtained within 8h at 37°C. The study was carried out under conditions simulating lysosomes of target cells, i.e. conditions of pH and enzyme present in the osteoclast lacunae. This indicated that Pull-PTX-ALN was a good substrate for the enzyme and steric hindrance did not appear to be an issue for the drug release. According to the bioconjugate structure, the release mechanism includes a two-step cleavage: the cleavage of the amide bond between norleucine residue and the 4-aminobenzyl alcohol would occur first, followed by the quasi-spontaneous 1,6-elimination

of the self-immolative spacer and final release of free paclitaxel, exempt of any amino acid residues (Scheme 4 1).



#### **Scheme 4-1 Proposed mechanism for Cathepsin K triggered drug release**

In conclusion, the controlled release of paclitaxel triggered by Cathepsin K was successfully achieved.

Another essential aspect in nano-systems used for therapeutic applications is to ensure that they will not cause toxicity to blood elements after injection into a patient.

The presence of haemolytic substances in contact with blood may cause loss of, or damage to, red blood cells. Consequently, an increased level of free plasma haemoglobin may be produced, inducing toxic effects or other effects which could strain the kidneys or other organs. Haemolysis (i.e., damage to red blood cells) can lead to life-threatening disorders such as anaemia, hypertension, arrhythmia, and renal failure.

Haemolytic properties were evaluated and showed that Pull-PTX-ALN was non-toxic therefore blood compatible, as revealed by the in vitro RBC lysis assay, whereas the commercial vehicle for PTX that contains Cremophor EL has significant haemolytic activity.

The toxicity and biological activity of Pull-PTX-ALN was assessed by in vitro in cell cultures, namely. Human mammary adenocarcinoma cells sourced from bone metastasis MDA-MB231 BM, murine mammary adenocarcinoma 4T1 and bone sarcoma cell lines SAOS-2 were used as model.

The MDA-MB231 BM cell line was chosen to simulate the early invasive phase of breast cancer that forms bone metastases. The 4T1 cell line was selected as it mimics a stage IV human breast cancer with similar kinetics to human breast cancer metastatisation; when injected in mice these breast cancer cells spontaneously disseminate tumour cells from the primary tumour to the bone thus making them a good model in breast cancer

bone metastasis targeting. The SAOS-2 cell line was elected as being an appropriate cell model of the bone tissue.

The studies performed by using the MTT and Coulter counter assays showed that Pullulan used as control and alendronate were non-cytotoxic at any of the concentrations tested while the cells proliferation was inhibited by both Pull-PTX and Pull-PTX-ALN polymer-drug conjugates, as well as by PTX free drug. The tumour cell killing efficacy or IC<sub>50</sub> of Pull-PTX-ALN and Pull-PTX were approximately one fold and two-fold higher than for PTX alone respectively, at equivalent drug concentration. The different IC<sub>50</sub> of Pull-PTX-ALN and free PTX is due to a combination of effect: different free drug availability and different cell up-take-systems. The difference of IC<sub>50</sub> of Pull-PTX-ALN and Pull-PTX suggested a synergism between PTX and ALN in inhibiting the tumour cell proliferation. Indeed, according with the literature, the efficacy of the polymer-drug conjugate bearing alendronate was higher as compared to the alendronate free counterpart.

It is worth to note that the lower biological efficacy obtained with the bioconjugate as compared to the free drug can be compensated in vivo, by a favourable pharmacokinetic profile of the former as compared to the latter. The combination of EPR effect for passive accumulation in the tumour and active targeting by the use of the bisphosphonate alendronate can increase the drug deposition in the tumour.

A wound healing assay performed using MDA-MB231 BM cells allowed to evaluate of the bioconjugate on cell migration. This assay was intended to simulate the process of tumour cell invasion and metastasis; indeed, tumour dissemination is usually assumed as the migration of single cells that disconnect from the primary tumour, enter lymphatic vessels or the blood circulation, and seed in distant organs.

The migration of MDA-MB231 BM incubated with both Pull-PTX and Pull-PTX-ALN was inhibited by over 63% and 99%, respectively. These results suggest once again that the presence of ALN onto the polymer backbone has a synergetic anti-tumoural effect with PTX.

Finally, the anti-angiogenic activity of Pull-PTX-ALN was assessed.

Angiogenesis can be defined as the creation of new blood vessels from an existing vasculature. This expansion involves endothelial cells which reorganise to form a three-dimensional vessel structure. Angiogenesis is a fundamental process in the development of cancerous tumours and dissemination of malignant tumour or metastasis; therefore, it was an important parameter to investigate for the purpose of this project.

Anti-angiogenic properties of Pull-PTX-ALN were appraised by two different assays completed on Human Vein Endothelial Cells (HUVEC), namely a cell proliferation assay and a capillary-like tube assay.

The results from these investigations indicated that Pull-PTX-ALN retained anti-angiogenic properties by inhibiting cell proliferation and was analogous to free PTX. In comparison, Pull-PTX showed a two-fold higher IC<sub>50</sub>, confirming the synergistic effect of ALN in inhibiting cell proliferation.

Angiogenesis can be defined as the creation of new blood vessels from an existing vasculature. This expansion involves endothelial cells which reorganise to form a three-dimensional vessel structure. Angiogenesis is a fundamental process in the development of cancerous tumours and dissemination of malignant tumour or metastasis; therefore, it was an important parameter to investigate for the purpose of this project.

The ability of HUVEC to form capillaries, simulating the angiogenesis, showed that Pull-PTX-ALN and Pull-PTX are as potent as the combination of free ALN plus PTX at equivalent concentrations, impeding the formation of the network. On the other hand, Pullulan alone and Pull-ALN did not significantly reduce the tube formation, demonstrating the essential presence of PTX for inhibiting tube formation.

Therefore, the overall results on cells suggest that Pull-PTX-ALN has a double role by preventing angiogenesis and causing tumour cell death.

# CONCLUSION

---





## 5. Conclusion

The development of new carriers for the delivery of anti-tumour drugs represents an important step in the creation of new efficient and selective therapeutic systems. These systems allow to improve the chemico-physical and pharmacological characteristics of this class of molecules by increasing their solubility and stability, and conferring new biopharmaceutical properties of biodegradability and biocompatibility.

This study was aimed at creating a new drug-delivery system for the treatment of breast cancer bone metastases, system based on a natural polysaccharide, Pullulan.

Pullulan has proven to be a versatile scaffold for the creation of promising polymer therapeutics for bioconjugation chemistry of the drug to obtain a supra-molecular structure. Pullulan was efficiently able of organising in self-assembly of adequate size for parenteral administration. The backbone of pullulan has proven to be well suited for the attachment of polymeric prodrugs for the controlled release of active molecules. Paclitaxel was conjugated to the polymer via a Cathepsin K sensitive spacer, which ensured adequate stability in plasma (pH 7.4 ), while allowing a drug release exclusively in the Howship's lacunae in osteoclasts, as a result of hydrolysis of the spacer in the osteoclast's pit where Cathepsin K is located (pH 5.5 ), followed by instantaneous self-immolation of a second short spacer. The conjugation of the alendronate, through a PEG flexible spacer, allowed to obtain an active targeting, using a process of high affinity of the bisphosphonate for the mineral bone hydroxyapatite, particularly exposed around bone metastases. The molecular weight and hydrodynamic volume determined are appropriate in order to take advantage of the EPR effect and reduce the renal clearance of the drug. Polymer-paclitaxel conjugates are presumed to prolong their plasma half-life and to have superior tumour accumulation as a result of their slow excretion from kidney and the enhanced permeation and retention effects, correspondingly.

Pull-PTX-ALN was found as a promising bone targeted drug delivery system able to act as anti-tumour and anti-angiogenic agent in-vitro. The overall results of this thesis work are promising and showed the polymer-paclitaxel conjugate is suitable in-vitro; therefore, the area of future research would go towards in-vivo investigations.

The studies discussed above supported that there is an added benefit by the inclusion of the alendronate to the polymeric carrier, contributing to the ability of the bisphosphonate to reduce tumour growth in bone as strongly demonstrated an increased anti-tumour effects when combined with paclitaxel, result of a synergism between the two drugs.

The reduce cytotoxicity of the polymer-paclitaxel conjugates might be a strategic property to improve their paclitaxel-equivalent dose, while preserving a reasonable toxicity profile for in-vivo animal models and clinical developments of chemotherapy, versus the Cremophor EL formulation of paclitaxel.



# REFERENCES

---



## 6. References

1. Brown, J. M.; Giaccia, A. J., The unique physiology of solid tumors: opportunities (and problems) for cancer therapy. *Cancer research* **1998**, *58* (7), 1408-16.
2. (a) 2013, N. o. N. M. A., Nobel lectures ,Physiology or Medicine 1901-1921, "Paul Ehrlich - Biographical". *Elsevier Publishing Company* **1967**; (b) Fitzgerald J. G., Ehrlich-Hata Remedy for Syphilis. *Cancer Medicine Association Journal* **1911** 1.
3. (a) Uludag, H., Bisphosphonates as a foundation of drug delivery to bone. *Current pharmaceutical design* **2002**, *8* (21), 1929-44; (b) Warr, D. G.; Hesketh, P. J.; Gralla, R. J.; Muss, H. B.; Herrstedt, J.; Eisenberg, P. D.; Raftopoulos, H.; Grunberg, S. M.; Gabriel, M.; Rodgers, A.; Bohidar, N.; Klinger, G.; Hustad, C. M.; Horgan, K. J.; Skobieranda, F., Efficacy and tolerability of aprepitant for the prevention of chemotherapy-induced nausea and vomiting in patients with breast cancer after moderately emetogenic chemotherapy. *Journal of clinical oncology : official journal of the American Society of Clinical Oncology* **2005**, *23* (12), 2822-30.
4. Weibel, H.; Nielsen, L. S.; Larsen, C.; Bundgaard, H., Macromolecular prodrugs. IXX. Kinetics of hydrolysis of benzyl dextran carbonate ester conjugates in aqueous buffer solutions and human plasma. *Acta pharmaceutica Nordica* **1991**, *3* (3), 159-62.
5. (a) Dando, T. M.; Perry, C. M., Aprepitant: a review of its use in the prevention of chemotherapy-induced nausea and vomiting. *Drugs* **2004**, *64* (7), 777-94; (b) Aapro, M. S.; Schmoll, H. J.; Jahn, F.; Carides, A. D.; Webb, R. T., Review of the efficacy of aprepitant for the prevention of chemotherapy-induced nausea and vomiting in a range of tumor types. *Cancer treatment reviews* **2013**, *39* (1), 113-7.
6. Erez, R.; Ebner, S.; Attali, B.; Shabat, D., Chemotherapeutic bone-targeted bisphosphonate prodrugs with hydrolytic mode of activation. *Bioorganic & medicinal chemistry letters* **2008**, *18* (2), 816-20.
7. (a) Herrstedt, J., New perspectives in antiemetic treatment. *Supportive care in cancer : official journal of the Multinational Association of Supportive Care in Cancer* **1996**, *4* (6), 416-9; (b) Curran, M. P.; Robinson, D. M., Aprepitant: a review of its use in the prevention of nausea and vomiting. *Drugs* **2009**, *69* (13), 1853-78; (c) Hernandez, S. L.; Sheyner, I.; Stover, K. T.; Stewart, J. T., Dronabinol Treatment of Refractory Nausea and Vomiting Related to Peritoneal Carcinomatosis. *The American journal of hospice & palliative care* **2013**.

8. Weidner, N.; Folkman, J.; Pozza, F.; Bevilacqua, P.; Allred, E. N.; Moore, D. H.; Meli, S.; Gasparini, G., Tumor angiogenesis: a new significant and independent prognostic indicator in early-stage breast carcinoma. *Journal of the National Cancer Institute* **1992**, *84* (24), 1875-87.
9. Folkman, J.; Shing, Y., Angiogenesis. *The Journal of biological chemistry* **1992**, *267* (16), 10931-4.
10. Holleb, A. I.; Folkman, J., Tumor angiogenesis. *CA: a cancer journal for clinicians* **1972**, *22* (4), 226-9.
11. (a) Folkman, J., Tumor angiogenesis: therapeutic implications. *The New England journal of medicine* **1971**, *285* (21), 1182-6; (b) Wike-Hooley, J. L.; Haveman, J.; Reinhold, H. S., The relevance of tumour pH to the treatment of malignant disease. *Radiotherapy and oncology : journal of the European Society for Therapeutic Radiology and Oncology* **1984**, *2* (4), 343-66; (c) Tannock, I. F.; Rotin, D., Acid pH in tumors and its potential for therapeutic exploitation. *Cancer research* **1989**, *49* (16), 4373-84; (d) Rofstad, E. K.; Sundfor, K.; Lyng, H.; Trope, C. G., Hypoxia-induced treatment failure in advanced squamous cell carcinoma of the uterine cervix is primarily due to hypoxia-induced radiation resistance rather than hypoxia-induced metastasis. *British journal of cancer* **2000**, *83* (3), 354-9.
12. (a) Rofstad, E. K., Microenvironment-induced cancer metastasis. *International journal of radiation biology* **2000**, *76* (5), 589-605; (b) Luanpitpong, S.; Chanvorachote, P.; Nimmannit, U.; Leonard, S. S.; Stehlik, C.; Wang, L.; Rojanasakul, Y., Mitochondrial superoxide mediates doxorubicin-induced keratinocyte apoptosis through oxidative modification of ERK and Bcl-2 ubiquitination. *Biochemical pharmacology* **2012**, *83* (12), 1643-54.
13. Lammers, T.; Hennink, W. E.; Storm, G., Tumour-targeted nanomedicines: principles and practice. *British journal of cancer* **2008**, *99* (3), 392-7.
14. Schroeder, A.; Heller, D. A.; Winslow, M. M.; Dahlman, J. E.; Pratt, G. W.; Langer, R.; Jacks, T.; Anderson, D. G., Treating metastatic cancer with nanotechnology. *Nature reviews. Cancer* **2012**, *12* (1), 39-50.
15. Sanborn R., An Emerging Potential Therapy for Bone Health: Denosumab. <http://cancergrace.org/cancer-101/tag/bone-density/> **2009**.

16. Yoo, H. S.; Lee, K. H.; Oh, J. E.; Park, T. G., In vitro and in vivo anti-tumor activities of nanoparticles based on doxorubicin–PLGA conjugates. *Journal of Controlled Release* **2000**, *68* (3), 419-431.
17. (a) Wang, R.; Billone, P. S.; Mullett, W. M., Nanomedicine in Action: An Overview of Cancer Nanomedicine on the Market and in Clinical Trials. *Journal of Nanomaterials* **2013**, *2013*, 12; (b) Ventola, C. L., The nanomedicine revolution: part 2: current and future clinical applications. *P & T : a peer-reviewed journal for formulary management* **2012**, *37* (10), 582-91; (c) Immordino, M. L.; Dosio, F.; Cattel, L., Stealth liposomes: review of the basic science, rationale, and clinical applications, existing and potential. *International journal of nanomedicine* **2006**, *1* (3), 297-315.
18. Hiroshi, M., The enhanced permeability and retention (EPR) effect in tumor vasculature: the key role of tumor-selective macromolecular drug targeting. *Advances in Enzyme Regulation* **2001**, *41* (1), 189-207.
19. Eldon et, a., NKTR-102, a novel PEGylated irinotecan conjugate, results in sustained tumour growth inhibition in mouse models of human colorectal and lung tumours that is associated with increased and sustained SN38 exposure. **2007**.
20. (a) Haag, R.; Kratz, F., Polymer Therapeutics: Concepts and Applications. *Angewandte Chemie International Edition* **2006**, *45* (8), 1198-1215; (b) Fox, M. E.; Szoka, F. C.; Fréchet, J. M. J., Soluble Polymer Carriers for the Treatment of Cancer: The Importance of Molecular Architecture. *Accounts of Chemical Research* **2009**, *42* (8), 1141-1151.
21. Wu, J.; Nantz, M. H.; Zern, M. A., Targeting hepatocytes for drug and gene delivery: emerging novel approaches and applications. *Frontiers in bioscience : a journal and virtual library* **2002**, *7*, d717-25.
22. (a) Yoo, H. S.; Park, T. G., Folate-receptor-targeted delivery of doxorubicin nano-aggregates stabilized by doxorubicin-PEG-folate conjugate. *Journal of controlled release : official journal of the Controlled Release Society* **2004**, *100* (2), 247-56; (b) Salmaso, S.; Bersani, S.; Semenzato, A.; Caliceti, P., New cyclodextrin bioconjugates for active tumour targeting. *Journal of drug targeting* **2007**, *15* (6), 379-90; (c) Scomparin, A.; Salmaso, S.; Bersani, S.; Satchi-Fainaro, R.; Caliceti, P., Novel folated and non-folated pullulan bioconjugates for anticancer drug delivery. *European journal of pharmaceutical sciences : official journal of the European Federation for Pharmaceutical Sciences* **2011**, *42* (5), 547-58.

23. (a) Kolhatkar, R.; Lote, A.; Khambati, H., Active tumor targeting of nanomaterials using folic acid, transferrin and integrin receptors. *Current drug discovery technologies* **2011**, *8* (3), 197-206; (b) Dufes, C.; Al Robaian, M.; Somani, S., Transferrin and the transferrin receptor for the targeted delivery of therapeutic agents to the brain and cancer cells. *Therapeutic delivery* **2013**, *4* (5), 629-40.
24. Park, K., Polysaccharide-based near-infrared fluorescence nanoprobes for cancer diagnosis. *Quantitative Imaging in Medicine and Surgery* **2012**, *2* (2), 106-113.
25. Albert, A., Avidity of terramycin and aureomycin for metallic cations. *Nature* **1953**, *172* (4370), 201.
26. Albert A, R. C. W., Avidity of the Tetracyclines for the Cations of Metals. *Nature* **1956**, *177*, 433.
27. Testa, B.; Mayer, J. M., *Hydrolysis in drug and prodrug metabolism*. John Wiley & Sons: 2003.
28. (a) Rogers, J. D.; Lindberg, R. D.; Hill, C. S.; Gehan, E., Spindle and giant cell carcinoma of the thyroid: A different therapeutic approach. *Cancer* **1974**, *34* (4), 1328-1332; (b) Dubowchik, G. M.; Firestone, R. A., Cathepsin B-sensitive dipeptide prodrugs. 1. A model study of structural requirements for efficient release of doxorubicin. *Bioorganic & medicinal chemistry letters* **1998**, *8* (23), 3341-3346.
29. Ringsdorf, H., Structure and properties of pharmacologically active polymers. *Journal of Polymer Science: Polymer Symposia* **1975**, *51* (1), 135-153.
30. Duncan, R., Drug-polymer conjugates: Potential for improved chemotherapy. *Anti-Cancer Drugs* **1992**, *3* (3), 175-210.
31. Vasey, P. A.; Kaye, S. B.; Morrison, R.; Twelves, C.; Wilson, P.; Duncan, R.; Thomson, A. H.; Murray, L. S.; Hilditch, T. E.; Murray, T.; Burtles, S.; Fraier, D.; Frigerio, E.; Cassidy, J., Phase I clinical and pharmacokinetic study of PK1 [N-(2-hydroxypropyl)methacrylamide copolymer doxorubicin]: first member of a new class of chemotherapeutic agents-drug-polymer conjugates. Cancer Research Campaign Phase I/II Committee. *Clinical cancer research : an official journal of the American Association for Cancer Research* **1999**, *5* (1), 83-94.
32. Seymour, L. W.; Ferry, D. R.; Anderson, D.; Hesslewood, S.; Julyan, P. J.; Poyner, R.; Doran, J.; Young, A. M.; Burtles, S.; Kerr, D. J., Hepatic drug targeting: phase



I evaluation of polymer-bound doxorubicin. *Journal of clinical oncology : official journal of the American Society of Clinical Oncology* **2002**, 20 (6), 1668-76.

33. Meerum Terwoegt, J. M.; ten Bokkel Huinink, W. W.; Schellens, J. H.; Schot, M.; Mandjes, I. A.; Zurlo, M. G.; Rocchetti, M.; Rosing, H.; Koopman, F. J.; Beijnen, J. H., Phase I clinical and pharmacokinetic study of PNU166945, a novel water-soluble polymer-conjugated prodrug of paclitaxel. *Anticancer Drugs* **2001**, 12 (4), 315-23.

34. Bauer R., Physiology of *Dematium pullulans* (de Bary). *Zentralblatt fur Bakteriologie, Parasitenkunde, Infektionskrankheiten und Hygiene* **1938**, 98.

35. Leathers, T. D., Biotechnological production and applications of pullulan. *Applied microbiology and biotechnology* **2003**, 62 (5-6), 468-73.

36. Gupta, M.; Gupta, A. K., In vitro cytotoxicity studies of hydrogel pullulan nanoparticles prepared by AOT/N-hexane micellar system. *Journal of pharmacy & pharmaceutical sciences : a publication of the Canadian Society for Pharmaceutical Sciences, Societe canadienne des sciences pharmaceutiques* **2004**, 7 (1), 38-46.

37. (a) Tanaka, T.; Fujishima, Y.; Hanano, S.; Kaneo, Y., Intracellular disposition of polysaccharides in rat liver parenchymal and nonparenchymal cells. *Int J Pharm* **2004**, 286 (1-2), 9-17; (b) Kaneo, Y.; Tanaka, T.; Nakano, T.; Yamaguchi, Y., Evidence for receptor-mediated hepatic uptake of pullulan in rats. *Journal of controlled release : official journal of the Controlled Release Society* **2001**, 70 (3), 365-73.

38. (a) Suginoshita, Y.; Tabata, Y.; Moriyasu, F.; Ikada, Y.; Chiba, T., Liver targeting of interferon-beta with a liver-affinity polysaccharide based on metal coordination in mice. *The Journal of pharmacology and experimental therapeutics* **2001**, 298 (2), 805-11; (b) Suginoshita, Y.; Tabata, Y.; Matsumura, T.; Toda, Y.; Nabeshima, M.; Moriyasu, F.; Ikada, Y.; Chiba, T., Liver targeting of human interferon-beta with pullulan based on metal coordination. *Journal of controlled release : official journal of the Controlled Release Society* **2002**, 83 (1), 75-88.

39. Nogusa, H.; Yano, T.; Okuno, S.; Hamana, H.; Inoue, K., Synthesis of carboxymethylpullulan-peptide-doxorubicin conjugates and their properties. *Chemical & pharmaceutical bulletin* **1995**, 43 (11), 1931-6.

40. (a) Veronese, F. M.; Sacca, B.; Polverino de Laureto, P.; Sergi, M.; Caliceti, P.; Schiavon, O.; Orsolini, P., New PEGs for peptide and protein modification, suitable for identification of the PEGylation site. *Bioconjugate chemistry* **2001**, *12* (1), 62-70; (b) Veronese, F. M., Peptide and protein PEGylation: a review of problems and solutions. *Biomaterials* **2001**, *22* (5), 405-17.
41. (a) Rowinsky, E. K.; Rizzo, J.; Ochoa, L.; Takimoto, C. H.; Forouzes, B.; Schwartz, G.; Hammond, L. A.; Patnaik, A.; Kwiatek, J.; Goetz, A.; Denis, L.; McGuire, J.; Tolcher, A. W., A phase I and pharmacokinetic study of pegylated camptothecin as a 1-hour infusion every 3 weeks in patients with advanced solid malignancies. *Journal of clinical oncology : official journal of the American Society of Clinical Oncology* **2003**, *21* (1), 148-57; (b) Conover, C. D.; Greenwald, R. B.; Pendri, A.; Gilbert, C. W.; Shum, K. L., Camptothecin delivery systems: enhanced efficacy and tumor accumulation of camptothecin following its conjugation to polyethylene glycol via a glycine linker. *Cancer chemotherapy and pharmacology* **1998**, *42* (5), 407-14.
42. Liggins, R. T.; Hunter, W. L.; Burt, H. M., Solid-state characterization of paclitaxel. *Journal of Pharmaceutical Sciences* **1997**, *86* (12), 1458-1463.
43. Venkatraman, S. S.; Jie, P.; Min, F.; Freddy, B. Y. C.; Leong-Huat, G., Micelle-like nanoparticles of PLA-PEG-PLA triblock copolymer as chemotherapeutic carrier. *International Journal of Pharmaceutics* **2005**, *298* (1), 219-232.
44. Shim, W. S.; Kim, S. W.; Choi, E. K.; Park, H. J.; Kim, J. S.; Lee, D. S., Novel pH sensitive block copolymer micelles for solvent free drug loading. *Macromolecular bioscience* **2006**, *6* (2), 179-86.
45. Torchilin, V. P.; Trubetskoy, V. S.; Whiteman, K. R.; Caliceti, P.; Ferruti, P.; Veronese, F. M., New synthetic amphiphilic polymers for steric protection of liposomes in vivo. *J Pharm Sci* **1995**, *84* (9), 1049-53.
46. Jin, X.; Mo, R.; Ding, Y.; Zheng, W.; Zhang, C., Paclitaxel-Loaded N-Octyl-O-sulfate Chitosan Micelles for Superior Cancer Therapeutic Efficacy and Overcoming Drug Resistance. *Molecular pharmaceutics* **2014**, *11* (1), 145-57.
47. Miwa, A.; Ishibe, A.; Nakano, M.; Yamahira, T.; Itai, S.; Jinno, S.; Kawahara, H., Development of novel chitosan derivatives as micellar carriers of taxol. *Pharmaceutical research* **1998**, *15* (12), 1844-50.

48. Kim, J. H.; Kim, Y. S.; Kim, S.; Park, J. H.; Kim, K.; Choi, K.; Chung, H.; Jeong, S. Y.; Park, R. W.; Kim, I. S.; Kwon, I. C., Hydrophobically modified glycol chitosan nanoparticles as carriers for paclitaxel. *Journal of controlled release : official journal of the Controlled Release Society* **2006**, *111* (1-2), 228-34.
49. Dominguez, L. J.; Di Bella, G.; Belvedere, M.; Barbagallo, M., Physiology of the aging bone and mechanisms of action of bisphosphonates. *Biogerontology* **2011**.
50. Ross J.R., S. Y., Edmonds P.M., Patel S., Wonderling D., Normand C. and Broadley K., A systematic review of the role of bisphosphonates in metastatic disease. *Health Technology Assessment* **2004**, *8*.
51. Bromme, D., Papain-like cysteine proteases. *Current protocols in protein science / editorial board, John E. Coligan ... [et al.]* **2001**, Chapter 21, Unit 21 2.
52. Lecaille, F.; Choe, Y.; Brandt, W.; Li, Z.; Craik, C. S.; Brömme, D., Selective inhibition of the collagenolytic activity of human cathepsin K by altering its S2 subsite specificity. *Biochemistry* **2002**, *41* (26), 8447-8454.
53. Bruneel, D.; Schacht, E., Chemical modification of pullulan: 1. Periodate oxidation. *Polymer* **1993**, *34* (12), 2628-2632.
54. Greenwald, R. B.; Pendri, A.; Conover, C. D.; Zhao, H.; Choe, Y. H.; Martinez, A.; Shum, K.; Guan, S., Drug Delivery Systems Employing 1,4- or 1,6-Elimination: Poly(ethylene glycol) Prodrugs of Amine-Containing Compounds. *Journal of Medicinal Chemistry* **1999**, *42* (18), 3657-3667.
55. Uludag, H.; Kousinioris, N.; Gao, T.; Kantoci, D., Bisphosphonate Conjugation to Proteins as a Means To Impart Bone Affinity. *Biotechnology Progress* **2000**, *16* (2), 258-267.
56. Abdel-Magid, A. F.; Carson, K. G.; Harris, B. D.; Maryanoff, C. A.; Shah, R. D., Reductive Amination of Aldehydes and Ketones with Sodium Triacetoxyborohydride. Studies on Direct and Indirect Reductive Amination Procedures<sup>1</sup>. *The Journal of Organic Chemistry* **1996**, *61* (11), 3849-3862.
57. Douroumis D., F. A., Drug Delivery Strategies for Poorly Water-Soluble Drugs. *John Wiley & Sons* **2012**.
58. (a) Wilhelm, M.; Zhao, C.-L.; Wang, Y.; Xu, R.; Winnik, M. A.; Mura, J.-L.; Riess, G.; Croucher, M. D., Poly(styrene-ethylene oxide) block copolymer micelle formation in

water. A fluorescence probe study. *Macromolecules* **1991**, *24* (5), 1033-1040; (b) Kwon, G.; Naito, M.; Yokoyama, M.; Okano, T.; Sakurai, Y.; Kataoka, K., Micelles based on AB block copolymers of poly(ethylene oxide) and poly(<sup>-2</sup>-benzyl L-aspartate). *Langmuir* **1993**, *9* (4), 945-949.

59. Carl, P. L. C., P. K.; Katzenellenbogen,, *Med. Chem.* **1981**, *24*.

60. Miller, K.; Eldar-Boock, A.; Polyak, D.; Segal, E.; Benayoun, L.; Shaked, Y.; Satchi-Fainaro, R., Antiangiogenic antitumor activity of HPMA copolymer-paclitaxel-alendronate conjugate on breast cancer bone metastasis mouse model. *Molecular pharmaceutics* **2011**, *8* (4), 1052-62.